STUDIES TOWARD THE ASYMMETRIC SYNTHESIS OF ESTER FUNCTIONALIZED NOVEL 1,4-OXAZEPINE-5-ONE DERIVATIVES

A Thesis Submitted to
the Graduate School of
Izmir Institute of Technology
in Partial Fulfilment of the Requirements for the Degree of

MASTER OF SCIENCE

in Chemistry

by

Hülya BOZOĞLU

July 2021

İZMİR

ACKNOWLEDGEMENTS

First of all I would like to express my appreciation to Prof. Dr. Ali ÇAĞIR for giving me the great opportunity to carry out my graduate study in his research laboratory, for his encouragement, patient, endless attention, and scientific guidance throughout this study. It was an invaluable experience for me to work with him.

I would also like to thank to Scientific and Technical Research Council of Turkey for financial support for this project (116-Z-591). Next, I would like to thank my labmates Tuğçe Kanbur and, Fikrican Dilek, Ezgi Vural and Bora Akman for their help and kind mess in the laboratory.

Besides I would like to thank all friends of me in IYTE especially C-301 officemates for their unfailing encouragement, and never ending friendship and enjoyable memories. I must add that, Can Berk Kandemir, thank you for support throughout this long process.

Finally, I am also grateful to my parents for their endless support, motivation, patience and limitless love. I dedicate my thesis to my mother Sevinç Bozoğlu my father İsmail Bozoğlu.

ABSTRACT

STUDIES TOWARD THE ASYMMETRIC SYNTHESIS OF ESTER FUNCTIONALIZED NOVEL 1, 4-OXAZEPINE-5-ONE DERIVATIVES

The MDM2/p53 is one of the most widely studied protein-protein interaction because of being a valuable target for the development of novel anticancer agents. MDM2 protein is the natural inhibitor of p53 protein which act as a tumor suppressor. When MDM2 is overexpressed, damaged DNA is allowed to replicate and therefore cancerous cells can be generated because p53 has lost of its activity. For this reason; maintaining the activity of wild-type p53 through inhibition of MDM2 can stop the proliferation of cancer cells. New drugs that inhibit this interaction are important for the treatment of cancer.

The aim of the study is synthesize chiral 1,4-oxazepine-5-one derivatives. *(R)*-2-amino-2-(4-chlorophenyl)acetic acid was used as starting material for the synthesis. The first step was a trityl protection of amine with trityl chloride. Trityl protected amino acid was reduced to N-Trt amino alcohol with $LiAlH_4$ then oxidized to aldehyde by using Dess-Martin periodinane. The resulting aldehyde was reacted with 3-chlorophenylmagnesium bromide. Up to this part of the synthesis, reactions were performed successfully. Then trityl group was removed by TFA and amino alcohol was obtained. Then addition of several α,β-unsaturated carbonyls to the deprotected amino alcohol was studied by coupling reagents such as HATU. Afterwards we performed some intramolecular cyclization attempts but all cyclization attempts were failed.

ÖZET

ESTER FONKSİYONELLENDİRİLMİŞ YENİ 1,4-OKSAZEPİN-5-ON TÜREVLERİNİN SENTEZİNE YÖNELİK ÇALIŞMALAR

p53/ MDM2 protein-protein etkileşimi, yeni antikanser ajanlarının keşfi için değerli hedefler olduğundan, son on yılda en yaygın şekildeçalışılmışlardır. MDM2 proteini, bir tümör baskılayıcı olarak işlev gören p53 proteininin doğal inhibitörüdür. MDM2 aşırı eksprese edildiğinde, hasarlı DNA'nın replikasyonuna izin verilir ve bu nedenle p53 aktivitesini kaybettiği için kanserli hücreler üretilebilir. Bu yüzden; MDM2'nin inhibisyonu yoluyla vahşi tip p53'ün aktivitesinin sürdürülmesi, kanser hücrelerinin çoğalmasını durdurabilir. Bu etkileşimi engelleyen yeni ilaçlar kanser tedavisi için önemlidir.

Bu çalışmada yeni kiral 1,4-oksazepin-5-on türevlerinin sentezlenmesi amaçlanmıştır. Sentez için başlangıç maddesi olarak *(R)*-2-Amino-2-(4-klorofenil) asetik asit kullanılmıştır. İlk adım, tritil klorür ile aminin tepkimesinden N-Trt korunmuş amin eldesidir. Tritil korumalı amino asit daha sonra $LiAlH_4$ kullanılarak N-Trt amino alkolüne indirgenmiş, ardından ve Dess-Martin periodinan reaktifi kullanılarak aldehite yükseltgenmiştir. Elde edilen aldehit, 3-klorofenilmagnezyum bromür ile reaksiyona sokulur. Sentezin bu kısmı tekrarlı olarak başarıyla gerçekleştirilmiştir. Daha sonra tritil grubu TFA ile uzaklaştırılır ve amino alkol elde edilir. Daha sonra koruması kaldırılmış amino alkole farklı α-β doymamış karbonil grubunun eklenmesi, HATU gibi bir birleştirme reaktifi ile gerçekleştirilmiştir. Son olarak bu yapıların molekül içi halkalaşma reaksiyonlarına çalışılmış fakat tüm denemeler başarısız olmuştur.

TABLE OF CONTENTS

LIST OF FIGURES

Figure **Page**

Figure **Page**

LIST OF TABLES

Table **Page**

LIST OF ABBREVIATIONS

d	Doublet
dd	Doublet of doublets
dt	Doublet of triplets
ddd	Doublet of doublet of doublets
DMP	Dess-Martin Periodinane
DCM	Dichloromethane
DMF	Dimethylformamide
Et_3N	Triethylamine
Eq.	Equivalent
m	Multiplet
mL	Milliliter
TMSCI	Trimethylsilylchloride
THF	Tetrahydrofuran

CHAPTER 1

INTRODUCTION

1.1. p53 and MDM2 in Cells

1.1.1. p53 in Cells

Cancer cells go to cell division indefinitely and offensive, unlike normal cells. At the same time, the behaviors of normal cells have a orderly cell division and limitations. In a healthy tissue, damaged cells have control path for damaged cells. This control is usually referred to as cell death (apoptosis), yet when this process terminates; it causes to uncontrollable cell division and leads to development of cancer. However, cancer cells pass the apoptotic cell death mechanism and continue to grow and divide. Tumor suppressor genes are normally a group of genes that regulate the proper cell division. Loss of normal function in both alleles may cause uncontrolled cell division and tumor growth. Tumor suppressor gene loss leads to the proliferation of normal cells in the body and disruption of the cell cycle. Mutation is one of the reasons of the cancer. p53 is the of one the genes that protect cell cycle and function as a tumor suppresor.[1]

Normal cells express wild type p53 tumor suppressor gene which is the most frequently inactivated gene in human malignancies. p53 was discovered in 1979. In mouse cells transformed with the SV40 DNA virus, a protein with a weight of 53-54 KDa that precipitated with the LT-antigen and was also found in transformed cells and this protein was called p53.[2] This protein has been found to be cellular, not viral. Later, the presence of the same protein was detected in cells exposed to the chemical carcinogen. At the first, assumed that p53 was the product of the oncogene which leads to the cancer but at the end 1980's realized that act as a tumor suppressor gene and generally mutated in a human cancer.[1] 53 in p53 shows the apparent molecular mass (in kDa) but is only 43.7 k Da. The reason for the low 9.3 kDA is due to the high number of proline residues in the protein.

Human p53 is encoded by a gene containing 11 exons and 10 introns, and this is chromosome no.17.[3,4] p53 protein is a phospho protein consisting of 393 amino acids and four units, one domain of which activates transcription factors. Other domain is core domain which is liable for the recognizing specific DNA sequences. Tetramerization of protein and damage of DNA controlled by the other two domains. This gene has 3 regions consisting of N-terminal region, central core region and C-terminal region.[5]

The p53 protein consists of two terminal domains which are N terminal and C terminal region. N terminal region has transactivation domain an amino-terminal, central core domain conserved the proline rich region. C terminal region is transcriptional domains includes localization signals and an oligomerization domain which is a strongly basic carboxyl terminal regulatory domain besides that nuclear localization signal sequence and 3 nuclear export signal sequence. p53 has diverse mechanisms for its both transcription dependent and independent anticancer activity.. The p53 cell located at the chromosome 17p location is involved in the functioning of important roles such as DNA repair, gene transcription, regulating metabolism cell cycle arrest, genomic stability, chromosome segregation and inhibiting cell migration and invasion aging and apoptosis [6] (Figure 1.1).

The well-known functions of p53 are the ability to promote apoptosis and cell cycle-arrest. Cell division, (called the cell cycle), follows a regular pathway required for cell proliferation and regeneration. There are several checkpoints for the prevent excessive cell growth.[7] The 53 kD mass nuclear phosphoprotein (p53) encoded by TP53, act as the transcription activator. During the mitosis the cell cycle is arrested at G1 and G2 checkpoints it helps the DNA repair mechanism by the prevents to mutagenic lesions.[8,9] In cases where DNA damage is too severe to be repaired, it fulfills the role of “genomic guardian” by triggering apoptosis. In the presence of mutated p53, normal p53 function is suppressed and cell proliferation progresses with genomic instability.[10,11,12]

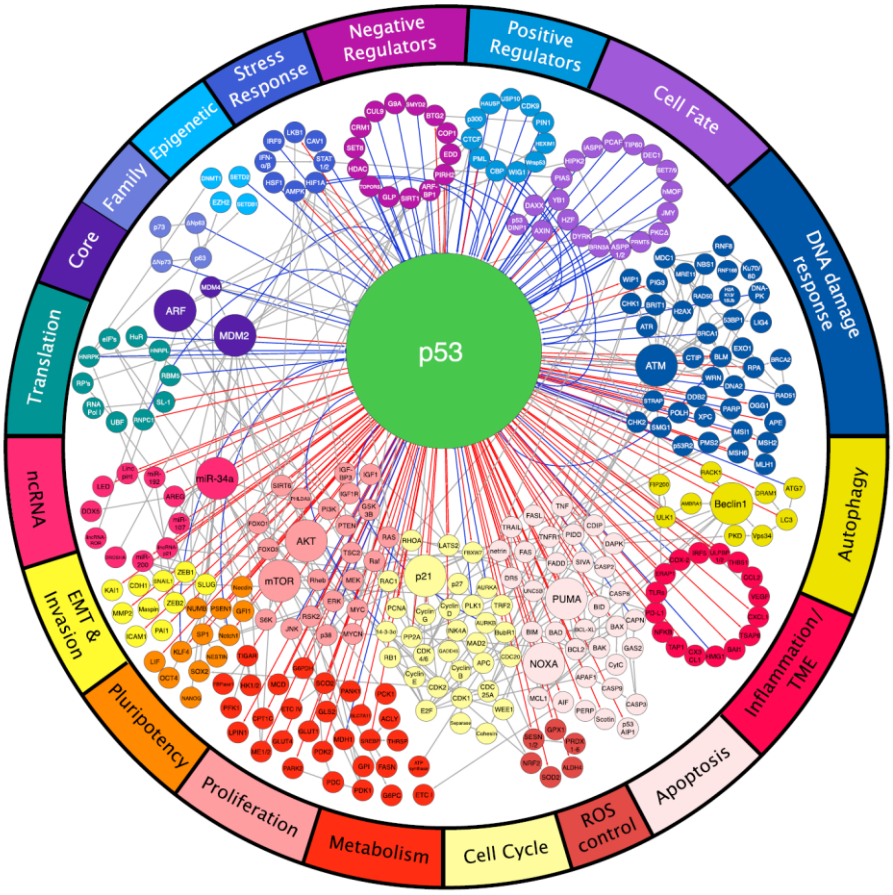

Figure 1.1.1 A wide variety of regulators govern the activity of p53 [13]

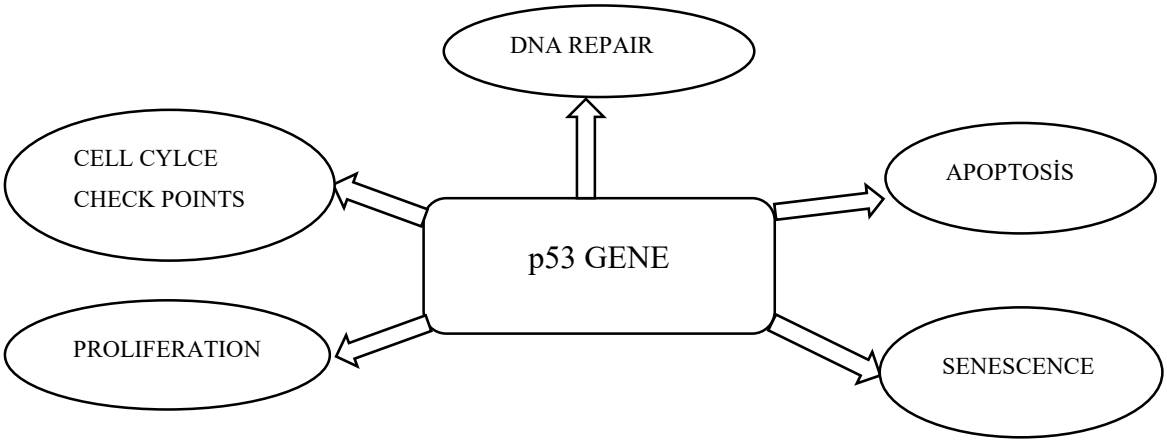

Figure 1.2. p53 controls many distinct biological processes [13]

The well-known functions of p53 are the ability to promote apoptosis and cell cycle-arrest. Cell division, (called the cell cycle), follows a regular pathway required for cell proliferation and regeneration. There are several checkpoints for the prevent excessive cell growth.[7] The 53 kD mass nuclear phosphoprotein (p53) encoded by TP53, act as the transcription activator. During the mitosis the cell cycle is arrested at G1 and G2 checkpoints it helps the DNA repair mechanism by the prevents to mutagenic lesions.[8,9] In cases where DNA damage is too severe to be repaired, it fulfills the role of "genomic guardian" by triggering apoptosis. In the presence of mutated p53, normal p53 function is suppressed and cell proliferation progresses with genomic instability.[10,11,12]

The importance of p53 in cell death was first confirmed in 1991 by M. Oren and co-workers using murine myeloid leukemia cell lines lacking the p53 gene. p53-induced apoptosis consists on transcriptional activation of proapoptotic target gene[14], classified as a two main pathway; "instrinc" (mitochondrial) pathway and "extrinsic" (death receptor) pathway. Under unstressed conditions high p53 levels can be detrimental to the growth and development of normal cells. Hence intracellular p53 levels are regulated by rapid proteasomal degradation.[15]

1.1.2. MDM2 in Cells

MDM2 (murine double minute 2) gene, originally cloned by Donna George and colleagues from first spontaneously transformed mouse "double minute" in cell lines (small chromatin without centromere particles) derived from chromosomes,1-2 mega bases (Mb) in size.

MDM2 is an E3 ubiquitin ligase consisting of 491 amino acids.[16] In 1991, three genes from 3T3DM cells isolated.[17] 10q of chromosome in MDM1 and MDM2 mice. HDM2 (Human double minute 2), which is the homologue of MDM2 in humans; it is mapped to the 12q region of the chromosome. Complex two consists of chained antiparallel α-layers and 5 β-helices MDM2 protein, able to form complex with p53 tumor suppressor protein.[18]The region located between amino acids 19-102, which is the beginning of the amino terminus, is the p53 binding site. Classification of the MDM2 gene, reported as an oncogene when experimentally overexpressed.

This overexpression can be due to increased transcription or translation. Overexpression of MDM2 prevents p53-mediated activation of apoptosis has been determined.[19] The most important known task of MDM2 gene is to bind p53 and block its functions.[20] MDM2 structurally consists of several domains; a central acidic domain, a zinc-finger domain, a nuclear localization signal (NLS), a p53-binding domain, a nuclear export signal (NES), a RING finger domain containing a nuclear localization signal sequence (Figure 1.3.). N-terminal domain of MDM2 critical for binding of p53.[21]

In particularly, MDM2 binds the transactivation domain of p53 and abolishes its transcription capability.[22] MDM2 also formed the ubiquitination of p53 protein for proteasomal degradation, upon binding.[23] Although the MDM2 protein is primarily nuclear, it oscillates between the nucleus and the cytoplasm. MDM2 is localized in the nucleus when cells are under unstressed condition for the catalyze mono- and polyubiquitination of p53 to limit its activity. Polyubiquitination of p53 causes degradation in the proteosome, while the monoubiquitinion of p53 promotes nuclear export MDM2.[24] MDM2 is not only responsible for p53 ubiquitination but also binds to the N-terminal transactivation domain of p53, disrupting p53 activity. The presence of p53 protein in low density in the cell is provided by the MDM2 protein, which is its negative regulator. MDM2 protein executes this regulation after binding to the amino end of the p53 protein, both by suppressing the transcriptional activity of the p53 protein and by providing proteasome-mediated degradation.[25] Nuclear cytoplasmic transfer of MDM2 is regulated by NLS and NES. Acidic domain of the MDM2 interacts with tumor suppressor. RING finger domain required E3 ubiquitin ligase activity of the MDM2 and also interact with the ring finger domain of the MDM4 (also known as MDMX in mice and HDMX in human).[26]

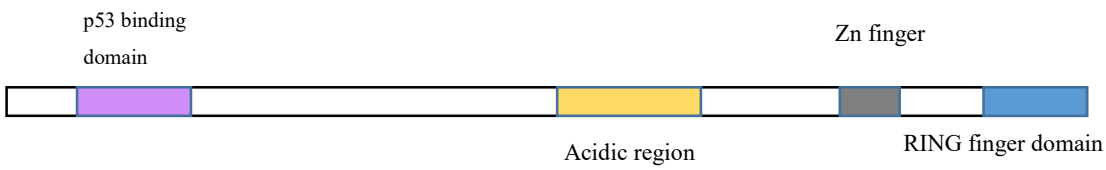

Figure 1.3. General representation of MDM2's regions

MDM4-MDM2 heterodimers act a crucial assignment in preventing lethal p53 activation during embryogenesis, deficiency of this heterodimerization causes embryonic lethality in mice. Mouse genetic studies indicate that for the suppressing p53 activity during the embryogenesis required MDM4-MDM2 heterodimer instead of MDM2 E3 ligase activity.[27] MDM2 has a short protein half-life thus regulated at the level of protein cycle and its activity regulated by several mechanisms.[28] One of them is MDM2-binding proteins, like as ribosomal proteins and ARF. Expression of ARF is induced in response to oncogenic stimulus activation. ARF not only stimulated p53 activation by suppressing MDM2 but also inhibit MDM2's catalytic activity directly through binding. Stability and activation of p53 in the nucleus is ensured by direct binding of ribosomal proteins to the MDM2 but mutant MDM2's cannot bind to ribosomal proteins.[29] The other mechanism of MDM2 regulation is Phosphorylation. MDM2 can be phosphorylated at multiple sites, especially in response genotoxic stress hence target of several kinases (Figure 1.4).[30]

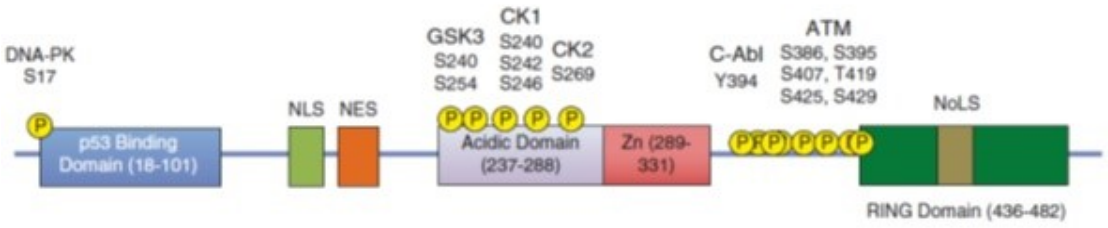

Figure 1.4 Schematic diagram of MDM2 protein. NLS nuclear localization signal, NES Nuclear export signal, NoLS Nucleolar localization, RING highly interesting new gene [30]

Additional information on the relationships determined between MDM2 and cancer has been obtained by defining the cancer-prone "Li-Fraumeni" syndrome, in which normal tissues express MDM2 in excess. The overabundant expression of MDM2 in normal tissues of individuals with "Li-Fraumeni" syndrome indicate that MDM2 can directly affect the high tumor incidence.[20]

1.1.3. MDM2 and p53 in Cells

The crystal structure of MDM2 and p53 complex was reported in 1996.[31] In later studies, Phe19, Trp23, Leu26 amino acid residues of p53 can bind into the hydrophobic pocket of the MDM2 protein.[32] It shows activity by binding as shown in the figure (Figure 1.5) below which is illuminated.

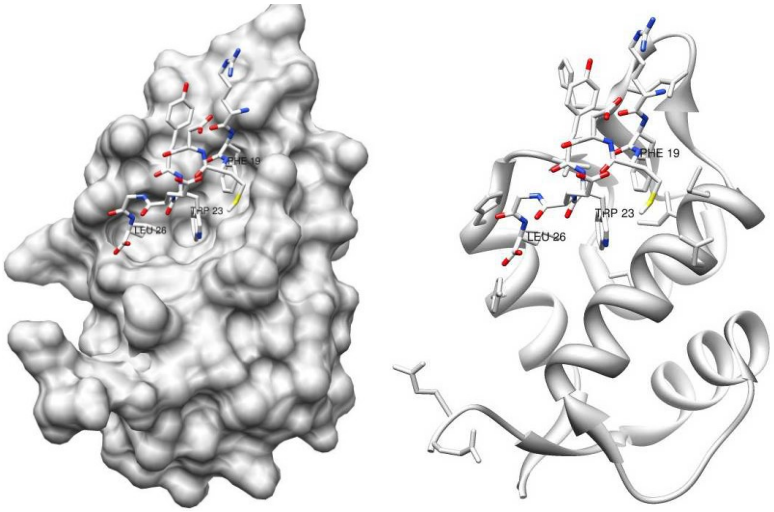

Figure 1.5. (Left) Surface representation of MDM2 in MDM2/p53 complex, (Right) It is a ribbon representation of MDM2 in the MDM2/p53 complex[32].

The MDM2 protein plays a fundamental role in controlling the functions of the p53 protein.[33] In normal cells, concentration of the MDM2 and p53 is balanced by each other. The MDM2 protein negatively regulates the functions of the p53 protein, both proteins act through a pathway called the "auto-regulatory feedback loop". In this pathway, p53 protein first binds to the MDM2 protein and activates it. MDM2 protein which is then activated inhibits the p53 protein.[34] It has been proven in transfection studies in mammalian cell culture and studies in mice that MDM2 has the ability to inhibit the functions of p53 in stopping the cell cycle in the G1 phase and inducing apoptosis.[18] In studies with mouse embryos, it has been observed that embryos without MDM2 gene activity die in the early stages of their development.[35] Inhibition of p53 functions by MDM2 is a necessary circumstance in the early stages of embryonic

development in mice. That means it shows that in order to ensure the normal development of the cells, they need the p53 and MDM2 relationship

1.2. Mutation of p53 in Cancer Cells and Inhibition of MDM2 as Anticancer Strategy

Mutations in the p53 gene are among the most common genetic alterations in different malignant tumor cells in humans. Normally, the protein is active in the tetramer structure and can be suppressed by the dominant-negative mix of p53, which becomes oncogenic with missense mutation. Mutation of p53 almost %80 is missense mutation.[36] Dominant-negative mutations do not entirely suppress native p53 function. Nevertheless, they mediate the reproduction of the population of null cells. Mutations in the p53 gene are concentrated in four regions (hot spots): in 129-146, 171-179, 234-260 and 270-287 triplets. These hot spots have been evolutionarily conserved, indicating their functional significance. Normally, p53, which binds with DNA-specific sequence, shows reduced affinity for DNA when mutated.[37] When the mutant p53 fails to bind to DNA, it also fails to activate genes linked to it.

Numerous genomic research results in indicated that; TP53 is the most frequently mutated gene, the spectrum of cancer types demonstrates a 50% mutation rate among all tumors.[38,39] Mutations in TP53 are both somatic contexts and germ-line, including sporadic tumors.[39,40] Mutations of TP53 may be the primary etiological status in some cancers and therefore occur in the early period of oncogenesis and leads to the initiation of the cellular transformation process. Significant rate of mutations also affect other domains of p53, the transactivation domains which include amino terminal (AT) region and the proline-rich domain, also the carboxyl-terminal domain containing the oligomerization domain (OD) and the negative regulator domain.

The classification of p53 mutations, particularly common DBD (DNA binding domain) mutations, can be divided into two main groups. First one is ‘DNA-contact mutations’, hotspot mutations, affecting DNA binding ability of mutant p53 and the amino acid residues which interact with DNA. The other one is ‘conformational mutations’ which indirectly affecting the DNA binding of the mutant protein and changing the folding and structure of the p53.[41] Mutant p53 proteins are thought to be unable to adjust the transcription of WT p53 target genes (loss of function (LOF)). Remarkably, many mutant p53 proteins have been detected in malignant cells at high

levels. Hence, mutant p53 proteins can enforce dominant negative effects (DNEs) while forming mixed tetramers with WT p53.[42] Besides that, some p53 mutants utilize gain-of-function (GOF) effects by binding to other tumor suppressors and transcription regulators, thus modulate their functions. Mutant p53 protein which is highly expressed can initiate tumorigenesis in three ways: 1- loss of the WT TP53 allele, 2- loss of the WT p53 activity and 3- interactions of mutant p53 protein with other transcription factors and tumour suppressors (Figure 1.6).[42] All these considered; the results of the p53 function and its regulation have provided an extensive assessment of the inactivation studies that can be performed in human cancers, as well as providing intensive information flow for therapeutic interventions.

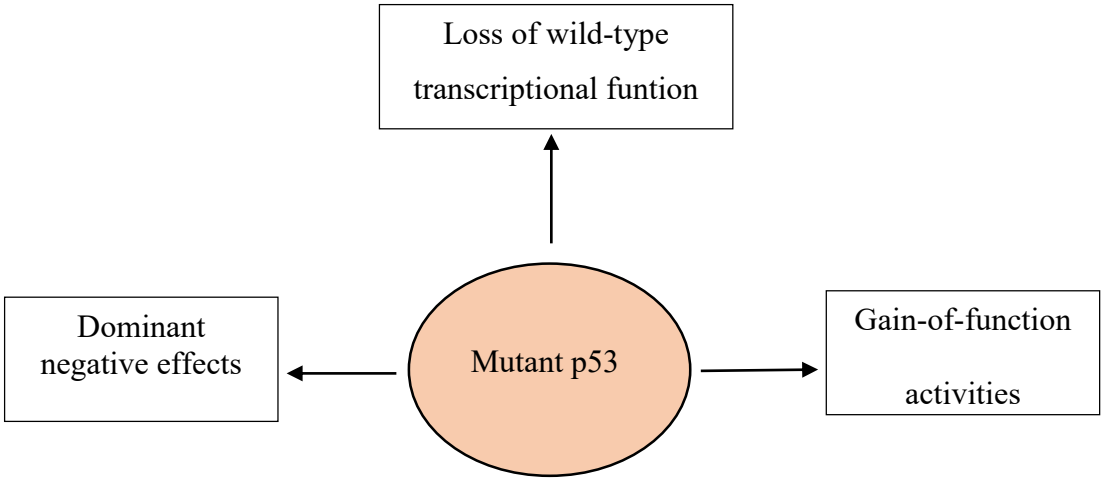

Figure.1.6. Effect of mutant p53 proteins on tumour development.

P53 activity includes many positive and negative feedback loops, the most important of which is the negative regulator MDM2 inhibitor. The general functioning of MDM2 is to control p53 activity, mainly by keeping p53 levels low in stress-free cells and turning off p53 after a stress-induced activation. On the other hand, overexpression of MDM2 leads to rapid degradation of wild type p53.[43,44] In this process, p53 also transcribes MDM2, for the prevent p53 from overworking and causing high levels of apoptosis then p53 is triggered for ubiquitinylation and degradation by MDM2. Thereby, prevention the action of p53 in the nucleus.[43] In turn, MDM2 protein binds to p53 protein and inhibits it through multiple mechanisms:

1- MDM2 functions as an E3 ligase and ubiquitinates p53 which leads to proteasomal degradation of p53.

2- MDM2 binds to the N-terminal transactivation domain of p53 and prevents p53 from direct binding to DNA and hence to work as a transcription factor.

3- MDM2 promotes export of p53 out from the cell nucleus. (Figure 1.7.)

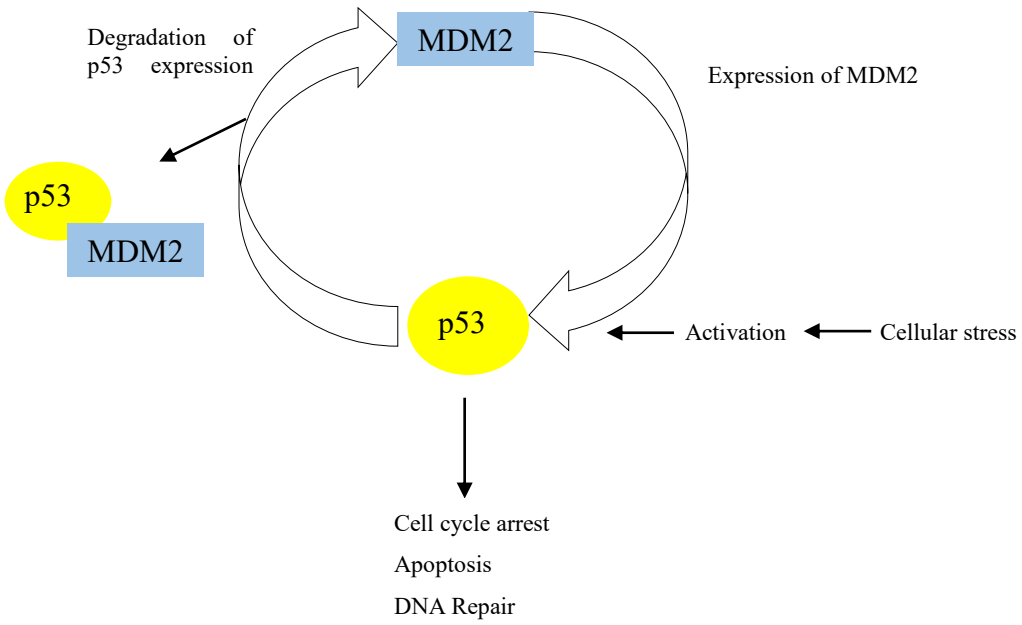

Figure 1.7. p53 negative and positive feed-back loops

According to the research results, a new potential treatment for human cancers is possible by inhibiting the MDM2-p53 interaction. Mutant p53 is generally resist to MDM2 for degradation promoted thus, there would have no therapeutic effect to the inhibition of the MDM2-p53 interaction.[42] There are 393 amino acids in the p53 structure, each of which has different functional importance and is organized according to their functions. The N-terminal domain includes amino acids 1 through 70 which includes residues involved in transcriptional activation. Among these residues, 1 through 52 ones the residues which involved in the first and crucial contact with the MDM2 protein[21]. p53 increases the function of MDM2 by binding to MDM2 at its binding site.[45]

MDM2 not only prevents its functions as a tumor suppressor protein by binding to p53, but also contributes to tumor formation by functioning independent of p53. According to the researches, it has been found that both MDM2 gene function increase excessively, and individuals with tumors carrying mutations in the p53 gene have an offensive prognosis than individuals carrying only one of these changes.[46]

The p53-MDM2 interaction is defined as a protein-protein interaction. Before the effect of the nature of the p53-MDM2 interaction was seen, it was thought that protein-protein interactions could not be effectively inhibited by drug-like small molecules. In drug discovery processes, smaller molecules are preferential to enhance absorption, distribution, metabolism, and excretion characteristics. Many contacts between proteins occur with the help of a pocket that generates most of the binding energy from several amino acids and has been termed "hot spot".[47] In 1996, the determination of the high resolution crystal structure of MDM2 complexed with residues 15-29 of a p53 peptide provided atomic details of their interactions, and it was suggested that non-peptide, drug-like, small molecule inhibitors could block the MDM2- p53 interaction.[31] The co-crystal structure demonstrated that the p53 has an α-helical conformation and interacts with MDM2 through three hydrophobic residues, Leu26, Phe19, Trp23 and which bind into a well-defined hydrophobic pocket in MDM2.[48] Three hydrophobic amino acids fit in three shapes and the electrostatic complement hydrophobic pocket, and the indole nitrogen of Trp23 of p53 forms a hydrogen bond with Leu54 of MDM2

1.3. Examples of MDM2 Inhibitors

In recent studies, several small molecules have been discovered that used as a MDM2 inhibitors. There is a number of listed MDM2 inhibitor in this section of the thesis.

1.3.1. Imidazole Derivatives

The first small molecule for the p53-MDM2 interaction was identified as an antagonist which both in vitro and in vivo result showed that potent and selective. These molecules referred cis-imidazodolines nutlins. 2,4,5 imidazoline compound defined as a

nutlins.[49,50,51,52] Nutlin-3's active enantiomer inhibited cell proliferation with more than 10-fold potency in p53 wild-type cancer cell lines, while the inactive enantiomer did not have distinct specificity suggesting off-target effects. Enantiomers were separated by supercritical chiral HLPC and then X-ray view of MDM2-Nutlin-3a crystal complex structure was obtained (Figure 1.8.).[52]

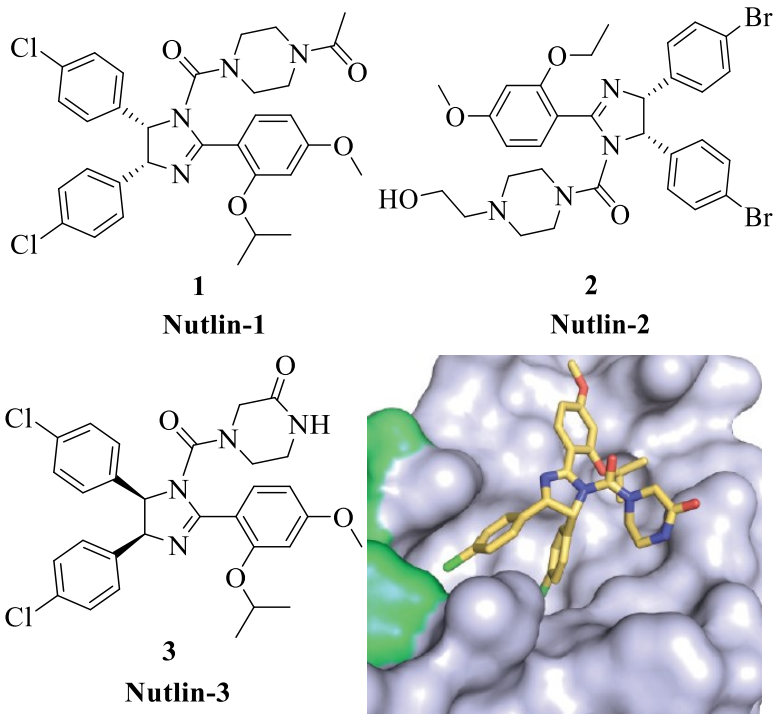

Figure 1.8. Structure of potent nutlin inhibitors of MDM2 and co-crystal structure of complex human MDM2 with nutlin 3a [53]

Cell line made with nutlins in their experiments, it was determined that they increase the accumulation of p53 because they have showed good cell permeability. It has also been shown that the increased p53 level is achieved through a posttranslational mechanism, not by increased p53 expression. Cell based studies demonstrated that wild-type p53 cell lines are sensitive to these compounds, and this was confirmed through cellular proliferation experiments yielding IC_{50} values of 1.4–1.8 μM for wild-type p53 cells.[51,52]

1.3.2. Oxindoles and Spiro-Oxindoles Derivatives

Spiro-oxindole fragments form the core of an alkaloid family and have bioactive properties and compatibility of the spiro-oxindole scaffold with synthetic chemistry has increased the interest in its production as a medical agent.[54] The Trp23 of the p53 pharmacophore model was replaced by a 6-halo-oxindole moiety characterized by the presence of an -NH group capable of binding MDM2 through H bond and an externally water-facing oxo- group. These derivatives showed p53-MDM2 agnostic activity.[55] Spiro-pyrrolidine system which substituted hydrophobic mimics the side chain Phe19 and Leu26. Onwards the studies demonstrated that appeared that the 3-chloro substituent fit perfectly in the MDM2 binding pocket. Chemical optimization of this compound led to the strongest compound **4** which is showed a high selectivity of action against cancerous cells with wild type p53 (Figure 1.9.). The p53- MDM2 crystal structure analysis showed that the Leu22 residue is also critical for binding, further optimization require for the compound **4** to conserve. This interaction by substituting the secondary amide with an amino ethyl morpholine moiety and co-incorporating a fluorine atom at position 2- of the phenyl ring provided a stronger inhibitor **5** (also known as MI-63) but it has weaker activity (IC_{50}= 18 μM) in p53-null tumor cells.[56] In subsequent studies, an improved derivative of the spiro-oxindole group **6** (MI-219) has been reported (Figure 1.9). Substitution of the 3,4-dihydroxy butyl amide moiety resulted in a higher binding affinity to MDM2 as well as improved pharmacokinetic properties.

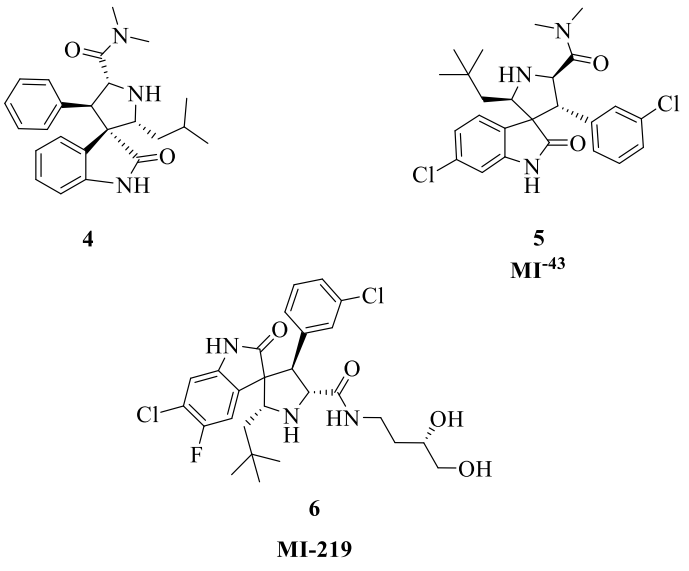

4 **5** **MI-43** **6** **MI-219**

Figure 1.9. Structure of spiro-oxindole derivatives that inhibit MDM2

1.3.3. Chalcone Derivatives

One of the earliest defined classifications of MDM2-p53 inhibitors is based on chalcone structures. Chalcones (1,3-diphenyl-2-propen-1-one) act as a MDM2 antagonists. They bound to the Mdm2 through binding pocket but the bound is weak.[57](Figure 1.10)

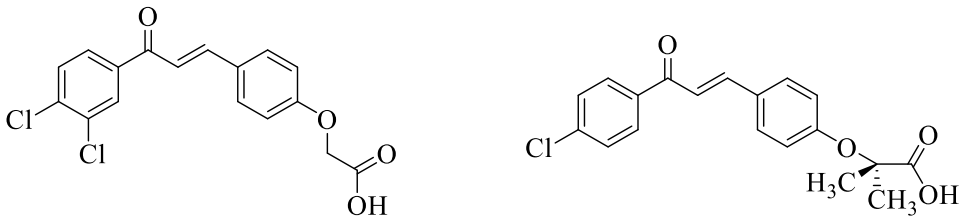

7 **8**

Figure 1.10. Structure of chalcone derivatives as p53-MDM2 inhibitors

1.3.4. 1,4-Benzodiazepine-2,5-diones

p53-MDM2 inhibitors based on a 1,4-benzodiazepine-2,5-dione skeleton, small molecule that mimic Phe19, Trp23 and Leu26 residues of the p53 peptide, were developed by the company Jonson & Jonson.[58] The compounds have been optimized to improve binding to MDM2. The result of this optimization, compound TDP222669 shown in Figure 1.11.(compound **9**) was found and the compound binds to MDM2 at the same binding site as the p53 peptide.[59] Chlorophenyl moieties are located in the Trp23 and Leu26 binding pockets iodobenzene goes into the Phe19 binding pocket.

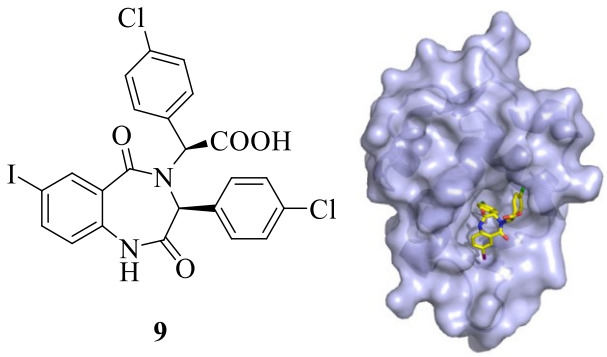

9

Figure 1.11 Structure of 1,4-benzodiazepine-2,5-dione as an MDM2 inhibitor TDP222669 and crystal structure of 1,4-benzodiazepine-2,5-dione co-crystalized with the MDM2 protein.[59]

Although depending on the compound carboxyl group ionization; showed low solubility and does not penetrate cell membranes well, and it was found to have poor bioavailability. Therefore, the carboxylic group was replaced with methyl to improve molecular properties.[58]

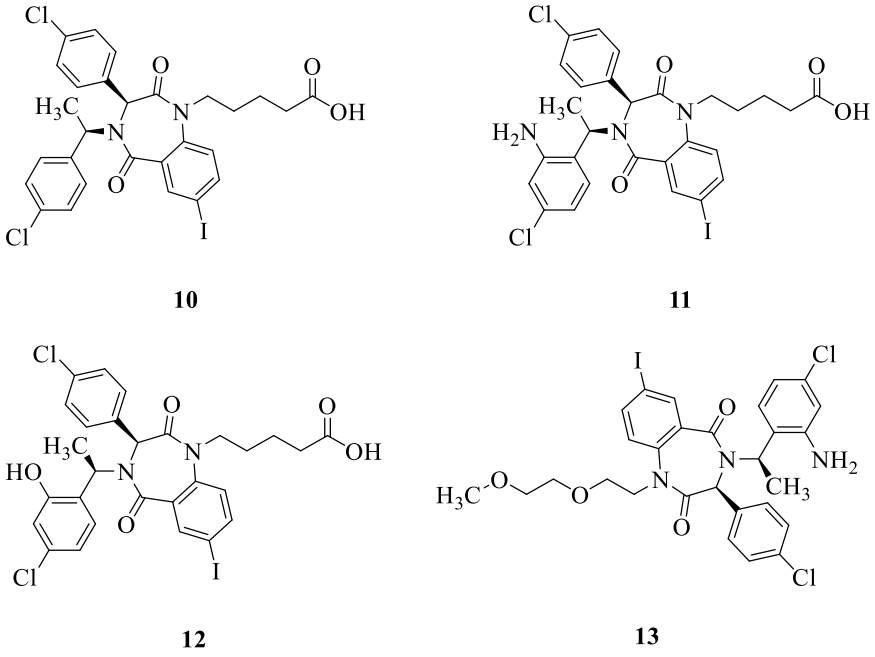

Figure 1.12 Structure of 1,4-benzodiazepine-2,5-dione derivatives as MDM2 inhibitors

1.3.5. Sulfonamides

Compound **14** developed as a pharmacophoric model for MDM2 binding, which can potentially mimic the essential parts of p53 that allow it to bind to MDM2, and its use in the discovery of non-peptidic agents. These compound discovered 3D pharmacophore research by the National Cancer Institute and having IC_{50} = 31.8 μM.[60](Figure 1.13)

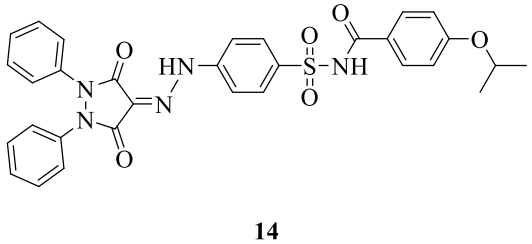

Figure 1.13 Structure of sulfonamide compound NSC 279287

1.3.6. Piperidinone Derivatives

Another p53-MDM2 inhibitor models were found by Amgen scientist who was determined through high throughput screening. They have synthesized the AMG-232 molecule as MDM2 inhibitors. It acts as a potent and selective inhibitor of MDM2- p53 interaction with remarkable pharmacokinetic properties and in vivo antitumor activity in xenograft models.[61] For the improvement halogenated phenyl rings were retained for attachment to pockets of tryptophan and leucine, but different halogens and substitution patterns were studied. Furthermore to improve the water solubility of the molecule, a carboxylic acid group was placed adjacent to the piperidone and various N-alkyl side chains were investigated it was also determined that cyclopropyl subtituted derivative is quite potent with IC_{50} values of 340 nM. (Figure 1.14)

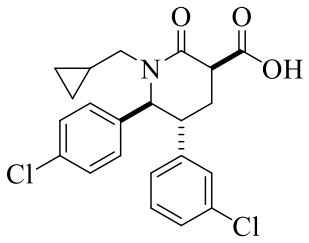

15

Figure 1.14 Structure of the initial Amgen lead piperidinone.

1.3.7. Morpholinone Derivatives

Morpholinone derivatives discovered as a MDM2 inhibitors by the Amgen researches at 2014. In the first studies of morpholinone compounds, it was seen that this scaffold would be a convenient template for the design of MDM2- p53 inhibitors.[62] AM- 8735 is a potent and selective MDM2 inhibitor with significant biochemical potency and cellular potency (SJSA-1, EdU IC_{50} = 25 nM). Further indicated unique antitumor activity in SJSA-1 osteosarcoma xenograft model (ED_{50} = 41 mg/kg).[63](Figure 1.15)

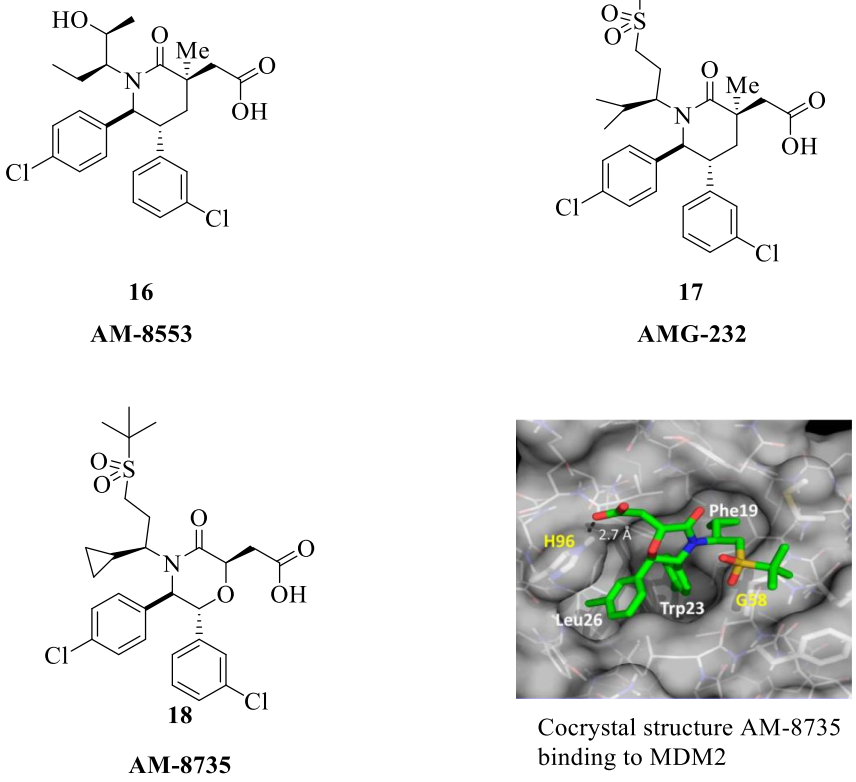

Figure 1.15. Potent morpholinone and piperidinone inhibitors of the MDM2−p53 interaction.[62]

1.4. Action Modes of AMG 232 and AMG 8735

According to previous studies by Amgen researchers; the biochemical and cellular improvement of the AM 8553 component has led to the discovery of sulfone analogues. The sulfone added component was observed to be the strongest component among the piperidone sulfone derivatives. This observation has been used to stabilize the core and substituent conformation in the piperidone class of inhibitors and found AMG-232.[61] The piperidinone sequence was thought to be stable by making additional contact with the MDM2 protein, but the gauche conformation for phenyl rings was observed to be the main factor.[64] Herewith, studies on piperidinone have been applied in morpholinone derivatives and compared. First studies with morpholinone compounds observed that it has a strong scaffold that can be designed for MDM2-p53 inhibitors.[65] (Figure 1.16.)

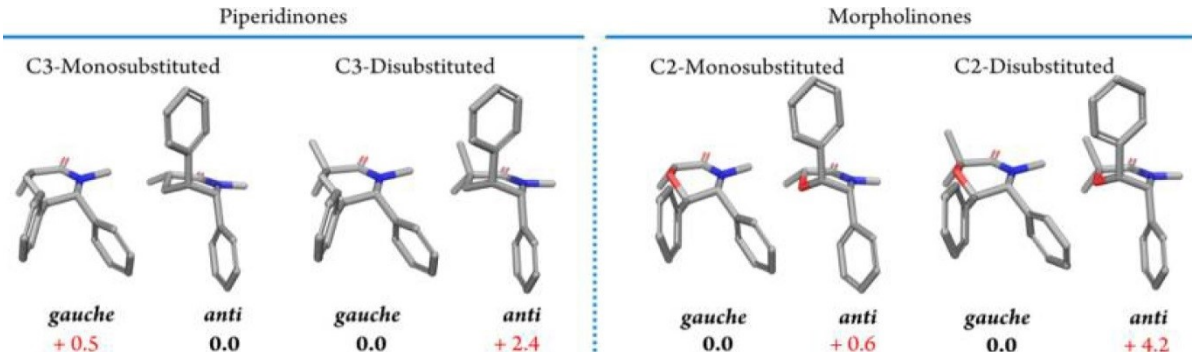

Figure 1.16. Structure and energies of the mono, di-substituted piperidinone and morpholinone inhibitors.[65]

Additionally morpholinone has been observed to be more stable in hepocytes than piperidinones, confirming that this is consistent between preclinical species and humans. Conversely, similar quantum mechanics calculations on the morpholinone nucleus suggest that the MDM2-binding gauche conformer is preferred even in the absence of a stabilizing methyl substituent, while the piperidinone inhibitor needs the methyl substituent to achieve conformational equilibrium.[64] Morpholinone inhibitors are less effective but have improved hepatocyte stability and potency over piperidinone inhibitors. Based on these improvements, the AM 8735 (Figure 1.18.) inhibitor was discovered by Amgen scientists with improved pharmacokinetic properties.

The synthesis pathway of AM-8735 discovered by Amgen contains important points for our study. Gonzalez and co-workers starting from the (*R*)-4-chlorophenylglycine and obtained (*R,R*) amino alcohol (**25**) by enantioselective synthesis. Firstly reduced to amino alcohol **(20)** by $LiAlH_4$ then protected amino group by Boc group. After this part, alcohol was oxidized to aldehyde by Dess Martin Periodinanone (DMP), for the stereoselective addition to aldehyde used 3-chlorophenyl magnesium bromide as a Grignard reagent and turned protected N-Boc amino alcohols (**23**). Deprotection reaction occured with using acid and neutralized the product (**25**). The amino alcohol reacted with chloroacetyl chloride under basic condition to give compound (**26**) as a morpholinone.[65] (Figure 1.17) Then N-alkylation performed from morpholinone to compound **29** by using ethyl 2-bromo-2-cyclopropylacetate because of the chiral amino alcohol obtained diastereomers **29 a** and **29 b**. Compound **29 a** could

be reduced to primary alcohol with superhyride. In the next step alcohol converted to tioether by using Mitsunobu reaction to give compound **18** which is AM-8735.(Figure 1.18.)

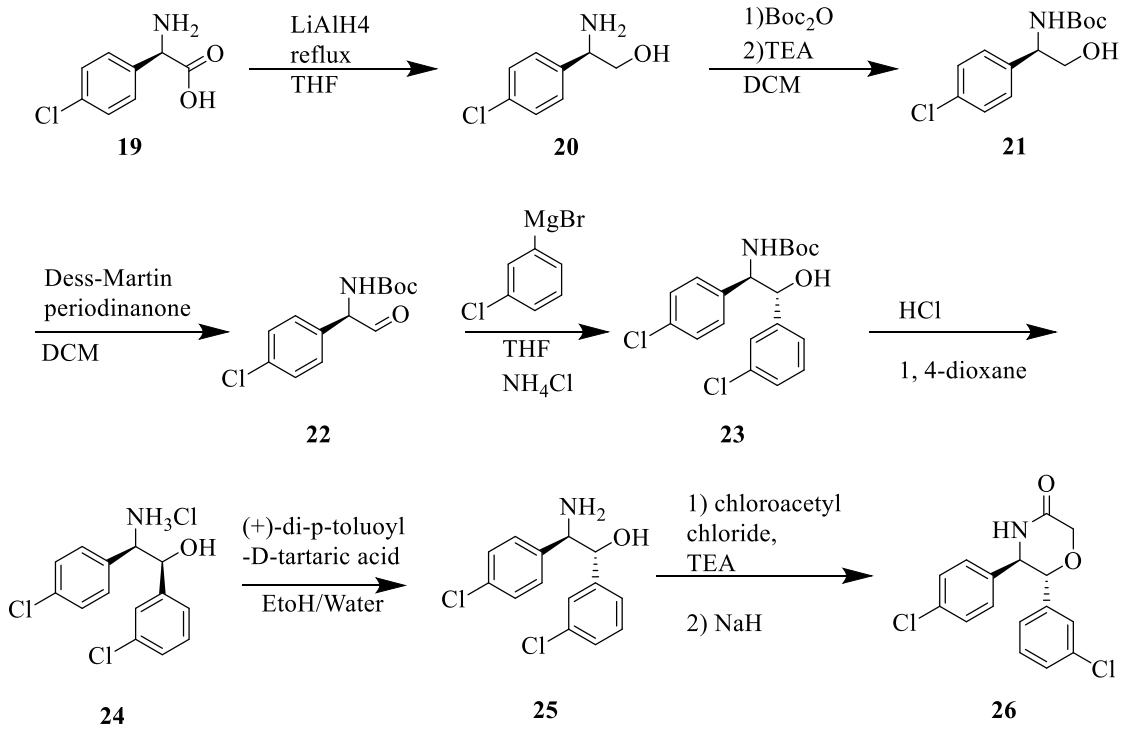

Figure 1.17. Preparation of (5*R*,6*R*)-6-(3-chlorophenyl)-5-(4-chlorophenyl)morpholin-3-one reported by Gonzales and co-work

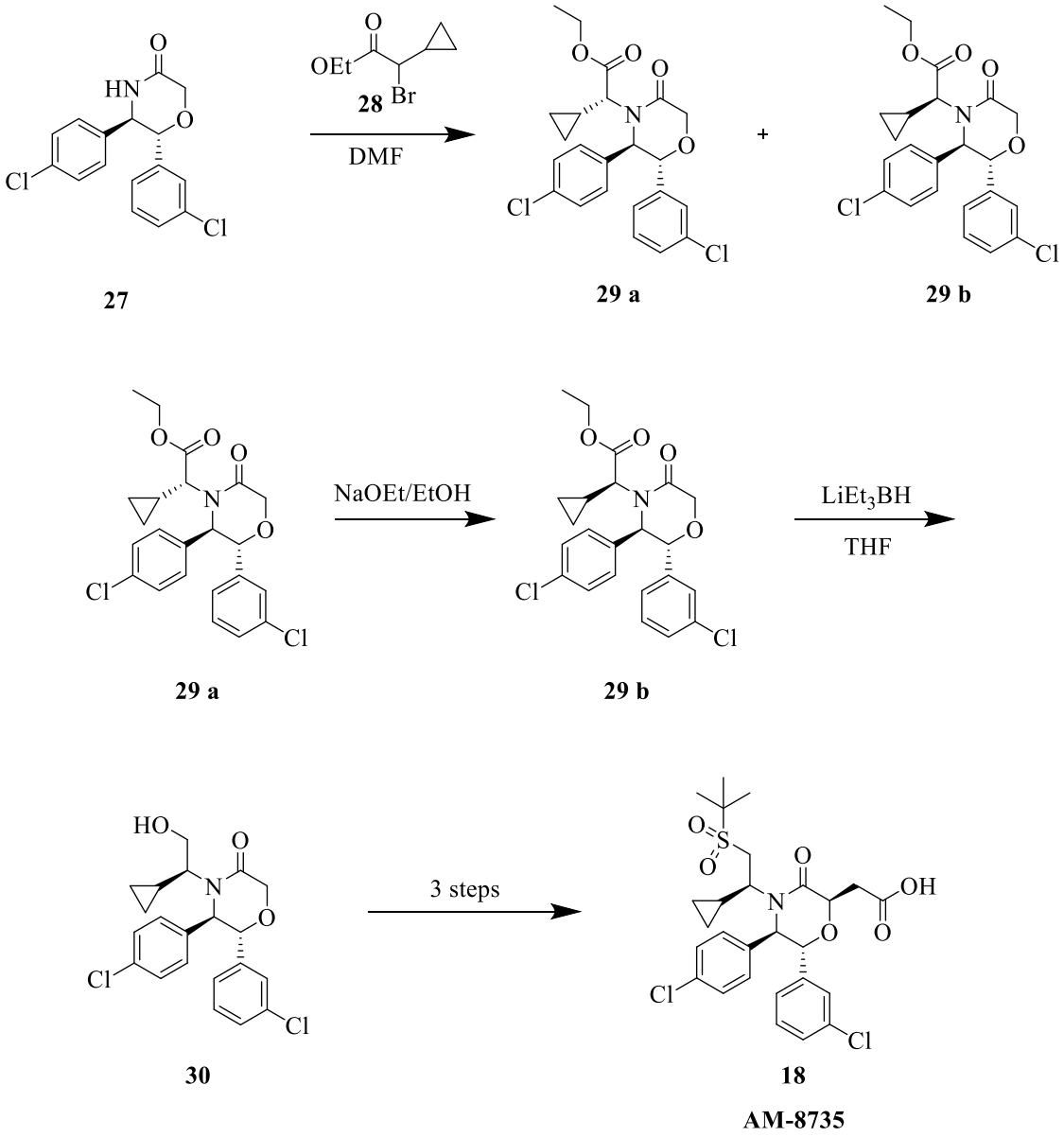

Figure 1.18. Synthesis of AM-8735 which is the best morpholinone derived MDM2 inhibitor.[65]

1.5. Aim of the Study

In this study conversion of (R)-4-chlorophenyl glycine to chiral 1,4-oxazepine-5-one derivatives as potential MDM2 inhibitors. For this reason, required a preparation of chiral aminoalcohol (**25**) is essential. In the calculations made in this study, a similar path was followed in the synthesis of morpholinone [65] derivatives since phenyl groups are more stable in the gauch position and are similar to morpholinone derivatives.(Figure 1.19)

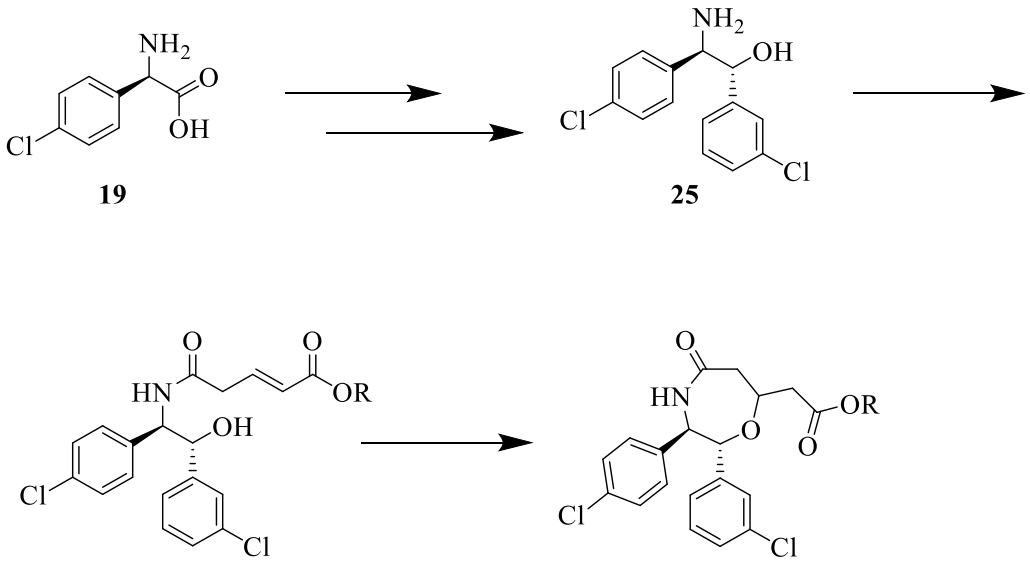

Figure 1.19 Proposed synthesis of novel oxazepinone derivatives as potential MDM2 inhibitors

CHAPTER 2

RESULT AND DISCUSSION

2.1. Trityl Protection of (*R*)-2-Amino-2-(4-chlorophenyl)acetic acid

Synthesis was started with protection of (*R*)-2-amino-2-(4-chlorophenyl) acetic acid **(19)** by using trimethylsilyl chloride (TMSCl) and then followed with tritylchloride addition and Et_3N. Product was used in the next step without purification (Figure 2.1)

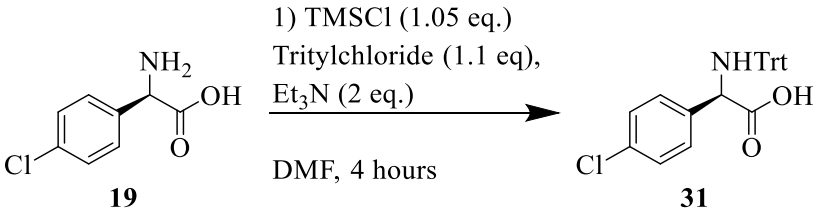

Figure 2.1. N-Trt protection of (*R*)-2-amino-2-(4-chlorophenyl)acetic acid

2.2. Reduction of (R)-2-Amino-2-(4-chlorophenyl)acetic acid

In this part of synthesis *(R)*-2-(4-chlorophenyl)-2-(tritylamino)acetic acid was reduced by 2 eq. of $LiAlH_4$ in anhydrous THF. The reaction was completed in 4 hours and the product (*R*)-2-(4-chlorophenyl)-2-(tritylamino)ethanol was purified by SiO_2 column chromotography and isolated yields were between 43-84% as shown in Figure 2.2

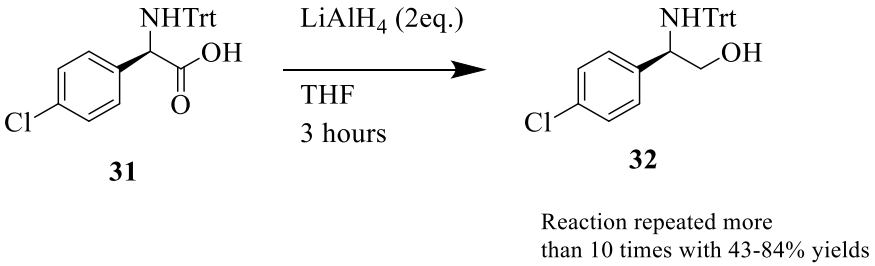

Figure 2.2. Reduction of *(R)*-2-(4-chlorophenyl)-2-(tritylamino)acetic acid with $LiAlH_4$

2.3. Oxidation of (*R*)-2-(4-chlorophenyl)-2-(tritylamino)ethanol with Dess Martin Periodinane

Formed N-Trt protected aminoalcohol (**32**) was oxidized to aldehyde by using Dess Martin Periodinone (DMP) in wet DCM which was prepared by washing of DCM with equal amounts of distilled water. The reaction was monitored by TLC and reactions were quenched with saturated $NaHCO_3$ solution at the end of 1 hour. This reaction generally gave high yields in all trials. Aldehyde was used without any purification because the possibility of the racemization for the chiral center of the compound **33**. (Figure 2.2)

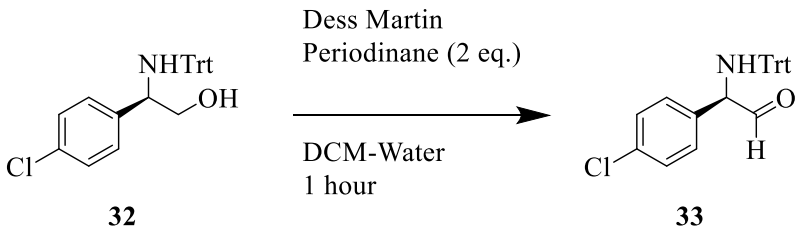

Figure 2.3. Oxidation of (*R*)-2-(4-chlorophenyl)-2-(tritylamino)ethan-1-ol with Dess Martin Periodinane

2.4. Reaction of (*R*)-2-(4-Chlorophenyl)-2-(tritylamino)acetaldehyde with Grignard Reagent

In the next step, obtained aldehyde **33** was converted to the corresponding chiral amino alcohol (**34**) by using Grignard reagent. Grignard reaction was performed by addition of 0.5 M 3-chlorophenylmagnesium bromide to the aldehyde in dry THF solution. During the reaction nucleophilic addition of Grignard reagent can be performed on both faces of aldehyde. This will form a mixture of two diastereomers and the amounts of the (*R*,*R*)-diastereomer is more than the amount of (*R*,*S*)-diastereomer because of the chiral center next to aldehyde. All of the attempts to purify these mixtures of diastereomers were not completely successful and varying amount of the mixtures of diasteromers were obtained from column chromatography. (Table 2.1.)

Table 2.1. Diastereomer formed from the reaction of (R)-2-(4-chlorophenyl)-2-(tritylamino)acetaldehyde with Grignard reagent

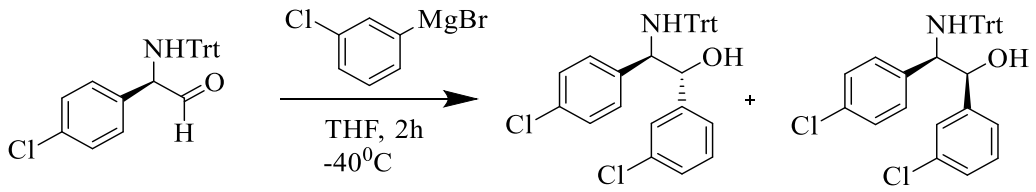

33 **34** **35**

Entry	**Grignard reagent (eq.)**	**Yield (%)**	**Diastereomer Ratios (34:35)**
1	1.5	58	1.00:0.17
2	1.75	34	1.00:0.22
3	1.75	42	1.00:0.24
4	1.75	47	1.00:0.15
6	1.75	50	1.00:0.30
8	1.75	32	1.00:0.14
10	1.5	30	1.00:0.80
11	1.5	31	1.00:0.25
12	1.5	50	1.00:0.60
13	1.5	56	1.00:0.38
14	1.5	55	1.00:0.82
15	1.5	40	1.00:0.78

2.5. Deprotection of (*R*)-2-(4-Chlorophenyl)-2-(tritylamino)acetaldehyde by using TFA

Deprotection of N-Trt protected aminoalcohol was performed by using TFA in wet DCM at room temperature. Wet DCM was prepared by washing of DCM with equal amounts of distilled water. The reaction was monitored by TLC and reactions were quenched at the end of the 45-180 minutes. The isolated yields of the product (**25**) were 28-62%. However better yields were obtained at the end of the 45 minutes. (Figure 2.4.)

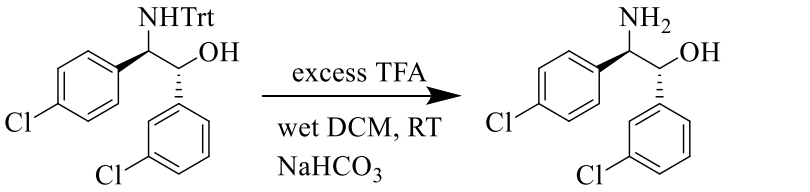

34 **25**

with 28-62% yields
for more than 10 repeats

Figure 2.4. Deprotection of N-protected aminoalcohols with TFA

2.6. Coupling Reaction of (*1R,2R*)-2-amino-1-(3-chlorophenyl)-2-(4-chlorophenyl)ethan-1-ol with (*E*)-5-methoxy-5-oxopent-3-enoic acid

In the next step, coupling of the chiral amino alcohol to α-β-unsaturated carbonyl was aimed. glutaconic acid **36** was converted to monoester **38** by addition of methanol in the presence of DEAD and PPh_3 in DCM as shown in Table 2.2. Reaction was monitored by TLC and finalized at the end of the 24 hours, and a product was purified with 28-32% yield. And then, addition of compound **38** to chiral aminoalcohol **25** to produce compound **39** was attempted by using HATU and DIPEA in DMF at room temperature, however all attempts were failed at this step (Figure 2.5).

Table 2.2. Conversation of Glutaconic acid (**36**) to (E)-5-methoxy-5-oxopent-3-enoic acid (**38**)

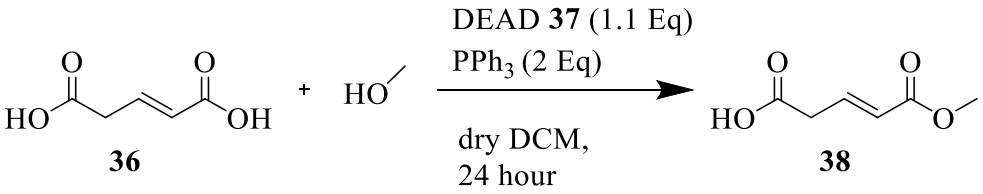

36 **38**

Entry	Time	Yield %
1	overnight	28
2	24 hours	32

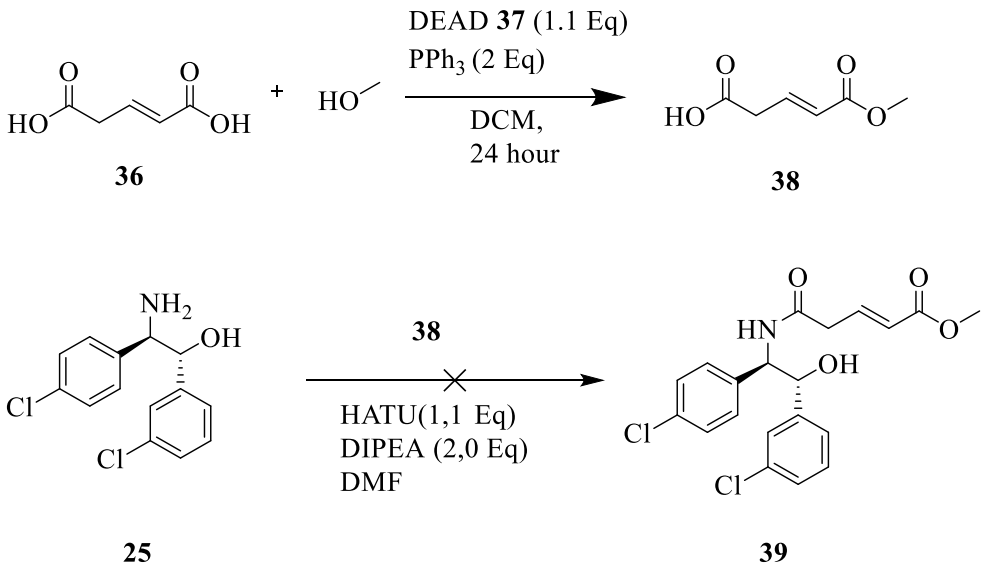

Figure 2.5. Preparation of methyl (*E*)-5-(((1*R*,2*R*)-2-(3-chlorophenyl)-1-(4-chlorophenyl)-2-hydroxyethyl)amino)-5-oxopent-2-enoate

2.7. Michael Addition of (*1R,2R*)-1-(3-chlorophenyl)-2-(4-chlorophenyl)-2-(tritylamino)ethan-1-ol with dibenzyl (*E*)-pent-2-enedioate

Because of the coupling of compound **25** to monoester **38** was failed, synthesis strategy have been changed. In here, it was aimed to perform the Michael addition in the first step and cyclization would be the second step. For this purpose glutaconic acid **36** was transferred to diester **41** by adding benzyl alcohol **40** by using catalytic amount of TsOH and these trials was successful in DCM as 46% yield. (Figure 2.6) Synthesized compound **41** was reacted with compound **34** in the presence of different bases in t-BuOH. These trials were not successful. Expected product **42** could not be synthesized. (Table 2.3.)

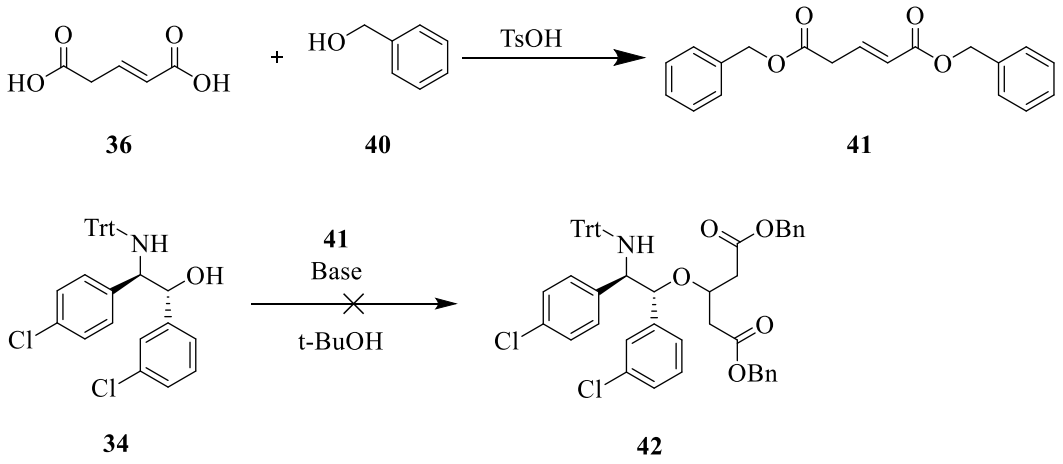

Figure 2.6. Synthesis of dibenzyl 3-((1*R*,2*R*)-1-(3-chlorophenyl)-2-(4-chlorophenyl)-2-(tritylamino)ethoxy)pentanedioate

Table 2.3. Michael addition of compounds **34** to compound **41**

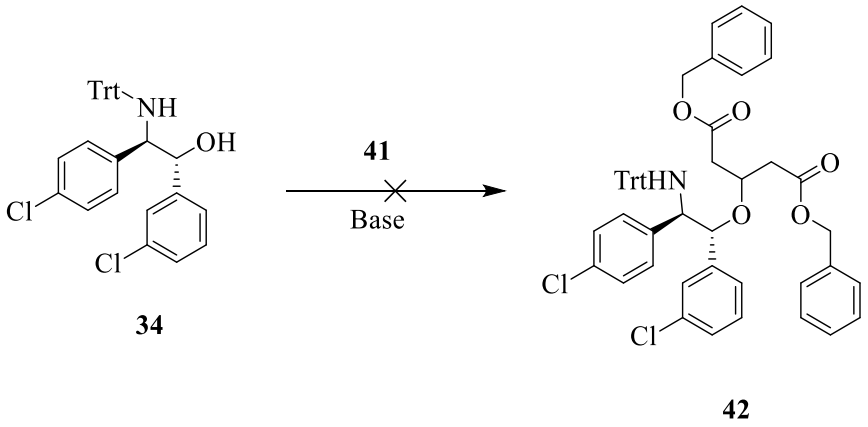

Entry	Solvent	Base (Eq)	Compound 41 (Eq)	Yield %
1	THF	NaH (3)	1	No Reaction
		Na_2CO_3(4)		
2	DMF	Cs_2CO_3(2.5)	1.5	No Reaction

2.8. Synthesis of (*E*)-5-((tert-butyldimetylsilyl)oxy)pent-2-enoic acid

Because the addition of the glutaconic acid to chiral amine was failed, addition of another α,β-unsaturated carbonyl derivative was aimed in this part of the thesis in. Firstly synthesis of TBDMSO protected carboxylic acid **46** was planned.(Figure 2.7)

Alcohol was oxidized to aldehyde (**43**) with the help of PCC (Table 2.4) but boiling point of aldehyde is too low to concentrate under reduced pressure. Compound **43** was used without purification in next step. Formed aldehyde was converted to compound **45** with the help of the Witting reaction 19-41% yields. (Figure 2.8) Finally conversion of ester **45** into corresponding carboxylic acid **46** (Table 2.5.) was tried but all attempts were failed.

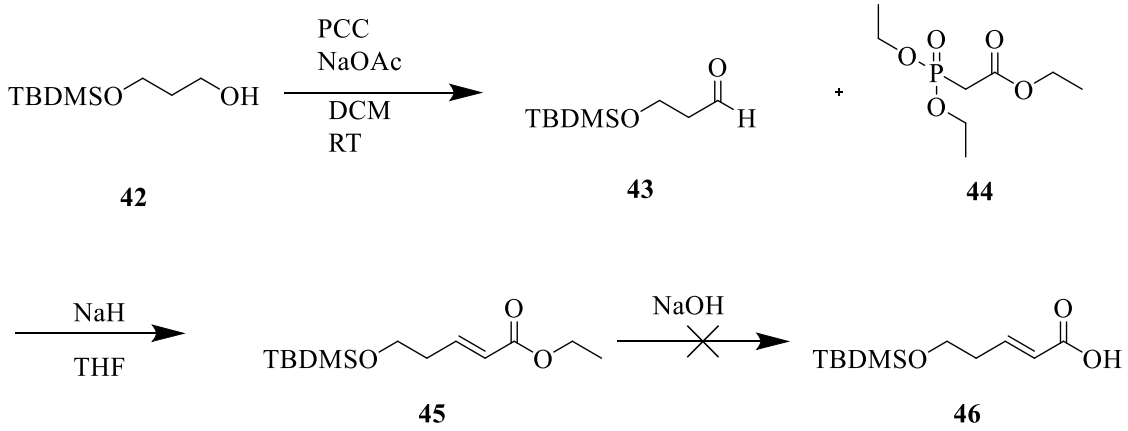

Figure 2.7. Proposed route for the synthesis of (*E*)-5-((tert-butyldimethylsilyl)oxy)pent-2-enoic acid

Table 2.4. Oxidation of 3-((tert-butyldimethylsilyl)oxy)propan-1-ol with PCC

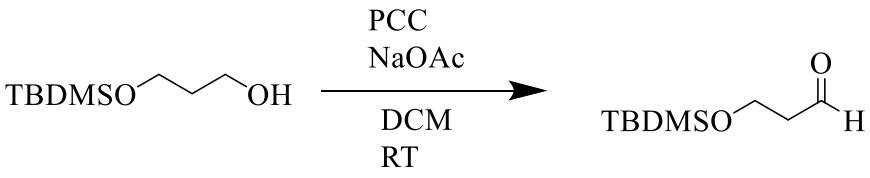

42 **43**

Entry	NaOAc (Eq)	PCC (Eq)	Time (Hour)	Yield %
1	-	1.5	1.5	Aldehyde could not be isolated
2	-	1.5	5	Aldehyde could not be isolated
3	0.9	1.1	1.5	Aldehyde could not be isolated

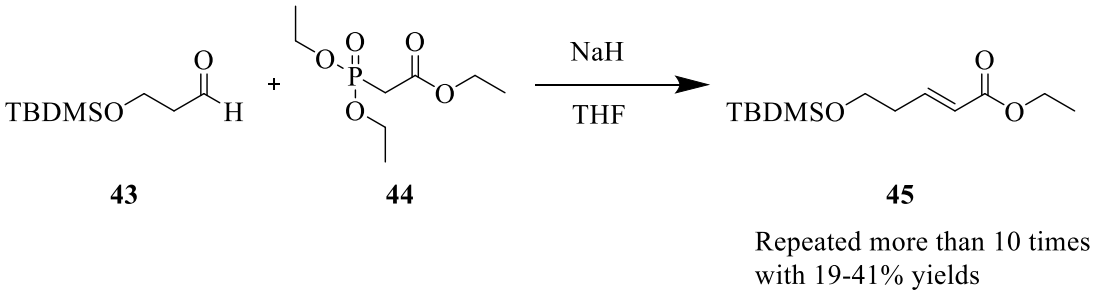

Figure 2.8. Witting Reaction of 3-((tert-butyldimethylsilyl)oxy)propanal with ethyl 2-(diethoxyphosphoryl)acetate

Table 2.5. Hydrolysis of ethyl (E)-5-((tert-butyldimethylsilyl)oxy)pent-2-enoate to carboxylic acid by using NaOH.

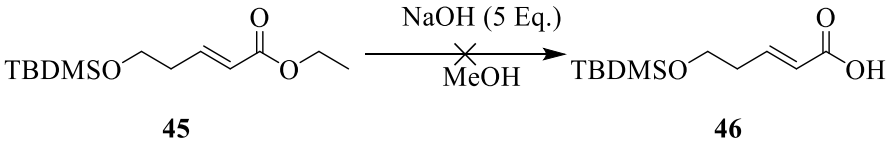

Entry	Temp. (ºC)	Time (h)	Yield % 46
1	0	2	Trans esterification
2	0	1.5	Trans esterification
3	RT	0.5	Not expected product
4	RT	6	Trans esterification

2.9. Preparation of (*E*)-5-(benzyloxy)pent-2-enoic acid

Hence, TBDMS protected α,β-unsaturated carboxylic acid **45** could not be isolated, similar reactions was tried with benzyl group protection instead of TBDMS because benzyl group was more stable than TBDMS group. At the beginning propane-1,3-diol was reacted with benzyl bromide **48**. Compound **49** was synthesized in 39% yield then it was oxidized to aldehyde by using PCC. Aldehyde **50** was used without purified in next step. Compound **51** was prepared by addition of ethyl 2-(diethoxyphosphoryl)acetate as a ylide for Witting reaction and overall yield of the last two step was calculated as 29%. These monoester **51** was converted to carboxylic acid **52** with NaOH in 1,4-dioxane in 57% yield. (Figure 2.9.)

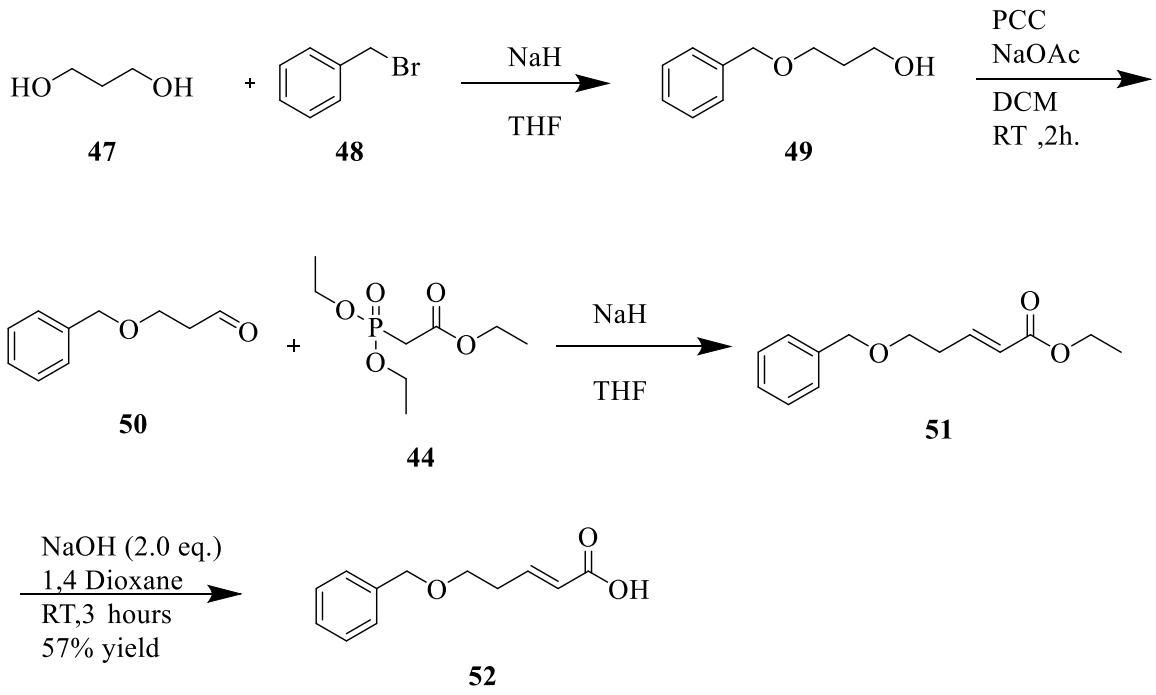

Figure 2.9. Synthesis of (*E*)-5-(benzyloxy)pent-2-enoic acid

2.10. Coupling Reaction of (*1R,2R*)-2-amino-1-(3-chlorophenyl)-2-(4-chlorophenyl)ethan-1-ol with (*E*)-5-(benzyloxy)pent-2-enoic acid

Benzyl protected α,β-unsaturated carboxylic acid **52** was reacted with compound **34** in the presence of HATU and DIPEA. Reaction was stirred overnight and monitored with TLC then quenched. The product was purified with SiO_2 column chromatography by using 100: 4 Chloroform: MeOH solvent system. The compound **53** obtained 45% yield. (Figure 2.10.)

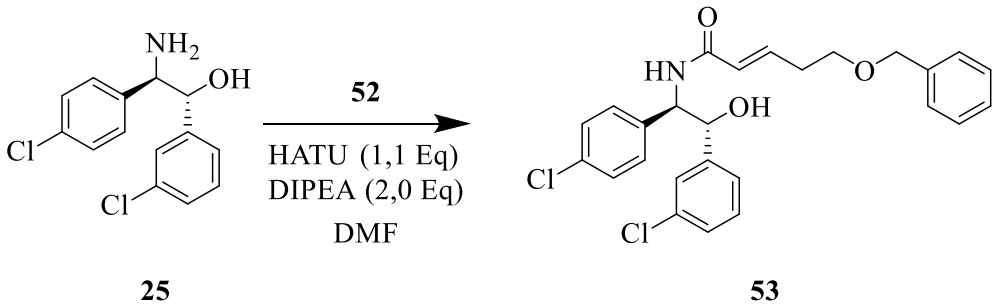

Figure 2.10. Addition of amino alcohol to (*E*)-5-(benzyloxy)pent-2-enoic acid

2.11. Trials for the cyclization Reaction of (*E*)-5-(benzyloxy)-N-((1*R*, 2*R*)-2-(3-chlorophenyl)-1-(4-chlorophenyl)-2-hydroxyethyl)pent-2-enamide

In this step, cyclization reaction was carried out with (*E*)-5-(benzyloxy)-N-((1*R*, 2*R*)-2-(3-chlorophenyl)-1-(4-chlorophenyl)-2-hydroxyethyl)pent-2-enamide and different catalysts. However, ^{1}H NMR studies of the crude products indicated that cyclization reaction was failed. It seems that hydroxyl group of chiral amino alcohol is too far away from the β-carbon of Michael acceptor group due to the planarity of the α,β-unsaturated carbonyl in 3-dimension.(Table 2.6.) This distance can be the main reason for the lack of cyclization reaction.

Table 2.6. Attempts for the synthesis of (2*R*,3*R*)-7-(2-(benzyloxy)ethyl)-2-(3-chlorophenyl)-3-(4-chlorophenyl)-1,4-oxazepan-5-one

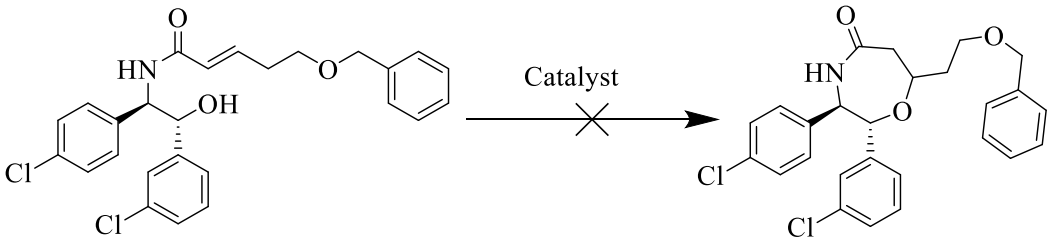

53 **54**

Entry	Catalyst	Solvent	Temp. (ºC)	Time (hour)	Yield % 61
1	TFA	DCM	RT	72	Not expected product
2	$BF_3.OEt_2$	$CDCl_3$-1,4-Dioxane (2:1)	78	5	Not expected product
3	$BF_3.OEt_2$	$CDCl_3$	RT	28	No reaction
4	AgOTf-DBU	DMF-DCM	55	overnight	No reaction

2.12. Coupling reaction of (1*R*,2*R*)-1-(3-chlorophenyl)-2-(4-chlorophenyl)-2-(tritylamino)ethan-1-ol with ethyl (*E*)-5-(benzyloxy)pent-2-enoate

As an alternative approach Michael addition of N-trt protected alcohol to α,β-unsaturated ester (**51**) was tried by using iodine (Table 2.7) However, no reaction was observed between compounds **34** and **51** according to the H-NMR of the crude reaction mixture.

Table 2.7. Attempts for the preparation of 5-(benzyloxy)-3-((1*R*,2*R*)-1-(3-chlorophenyl)-2-(4-chlorophenyl)-2-(tritylamino)ethoxy)pentanoic acid

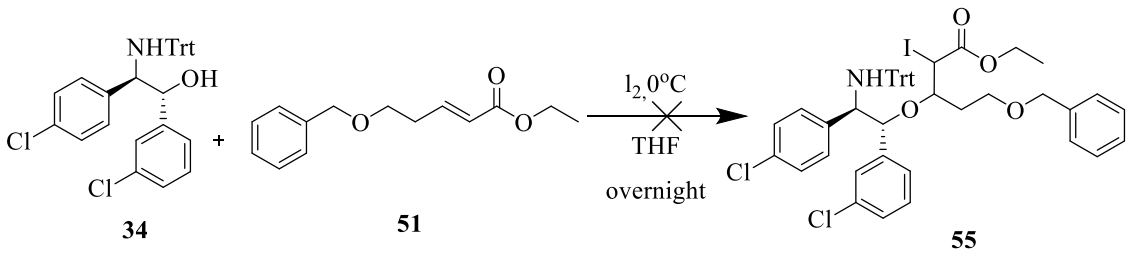

34 **51** **55**

Entry	I_2 (Eq.)	Yield % 55
1	3	No reaction
2	1,5	No reaction

2.13. Reaction of (*1R,2R*)-2-amino-1-(3-chlorophenyl)-2-(4-chlorophenyl)ethan-1-ol with (*S*)-2-(benzyloxy)-1-phenylethyl benzenesulfonate

As an another alternative methadology, introducing a side chain to nitrogen before adding α,β-unsaturated ester to eliminate the acidic NH proton during cyclization reactions. For this purpose compound **56** and **40** was reacted in the presence NaH to produce compound **57** with 27% yield. (Table 2.8.) Then 4-bromobenzenesulfonyl chloride was used to convert alcohol into a good leaving group in compound **57** shown in Table 2.10. Then compound **58** reacted with amino alcohol. (Table 2.8.) However all attempts again was failed to produce compound **59** (Figure 2.11).

Table 2.8. Substitution reaction (*R*)-styrene oxide and benzyl alcohol by using NaH

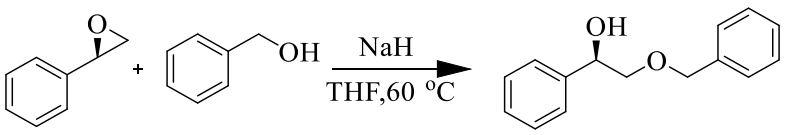

56 **40** **57**

Entry	Epoxide (eq.)	NaH (Eq.)	Time (h)	Yield % 57
1	2	1	Overnight	30
2	2	2	Overnight	32
3	2	2	48	55

Table 2.9. Conversion of alcohol to a good leaving group by using BsCl

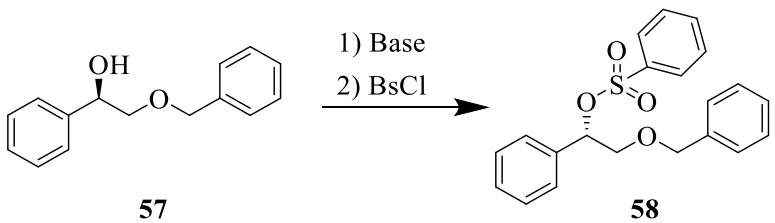

57 **58**

Entry	Solvent	BsCl (Eq.)	Et_3N (Eq.)	DMAP (Eq.)	Temp. (°C)	Time (h)	Yield % 58
1	Pyridine	1.05	-	-	RT	16	No reaction
2	DCM	2	3	0.1	RT	7	40
3	DCM	2.2	0.33	1	0	4	58

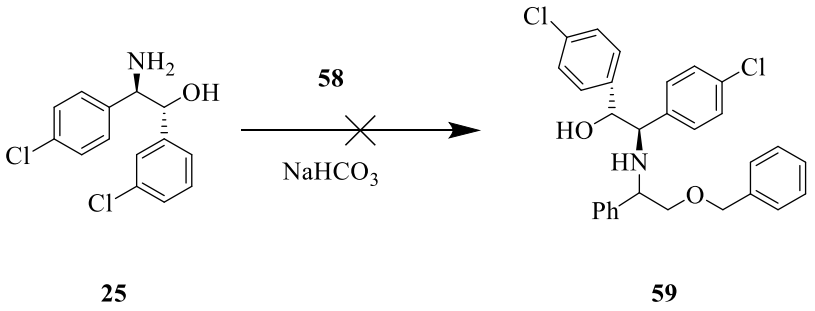

25 **59**

Figure 2.11. Attempts for the synthesis of compound **59**

2.14. Coupling Reaction of (1*R*,2*R*)-1-(3-chlorophenyl)-2-(4-chlorophenyl)-2-((2-hydroxy-1-phenylethyl)amino)ethan-1-ol with 3,3-diethoxypropanoic acid

Another synthetic strategy was started with preparation of compound **60** which can be formed from the reaction of *R*-styrene oxide and compound **25** in methanol however no product was formed. For this reason, *R* styrene oxide was reacted with compound **25** by used lithium perchlorate trihydrate as a catalyst. The compounds **61** and **62** reaction was formed with 39% yield for both. (Figure 2.12.) In the next step coupling reaction was tried between compound **61** and diethoxypropanoic acid (**63**) in the presence of HATU, DIPEA in DMF but the trial was not successful. (Figure 2.13.)

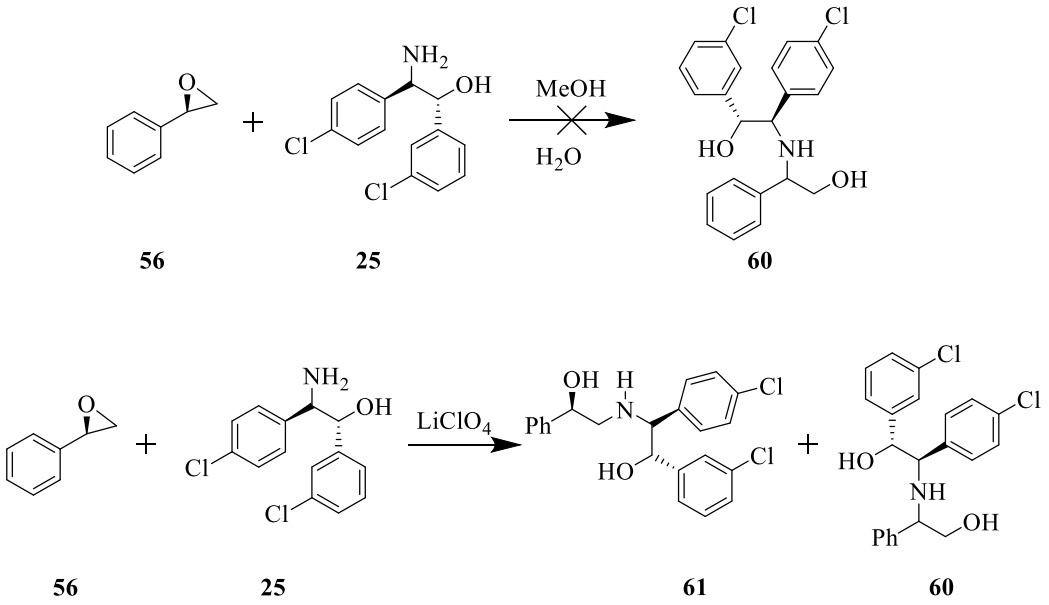

56 **25** **60**

56 **25** **61** **60**

Figure 2.12. Synthesis of compound **60** and **61**

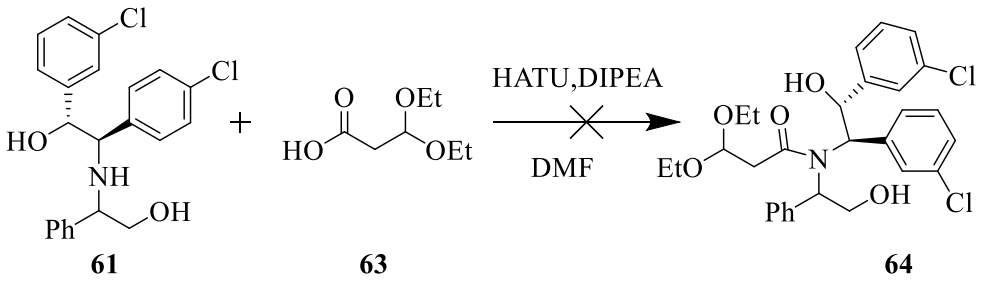

61 **63** **64**

Figure 2.13. Addition of 3,3-diethoxypropanoic acid to chiral secondary amine (**61**)

2.15. Attempts for the cyclization of N-((1*R*,2*R*)-2-(3-chlorophenyl)-1-(4-chlorophenyl)-2-hydroxyethyl)-3-oxopropanamide with using triethylphosphonoacetate

Ethyl 3,3-diethoxypropanoate was hydrolyzed to form corresponding carboxylic acid (**66**) with 100% yield. Compound **25** was reacted with compound **66** with the help of HATU and DIPEA and compound **67** was obtained in 74 % and 82% yield.(Table 2.10.) In next step acetal group of compound **67** was tried to react in acidic solution to form aldehyde. First of all HCl was used as an acid in 1,4-dioxane and formation of a new product was observed on TLC but cannot be isolated in extraction part. Then iodine was used, again formation of a product was observed in crude NMR but after column chromatography aromatic range was too crowded indicating the lack of product. (Figure 2.13) When H_2SO_4 was used crude, H-NMR was acquired and formation of the product was observed but it could not be isolated. (Figure 2.14.) At the end H_3PO_4 was used with THF, experiment was performed at room temperature for 6 hours but no reaction was observed. Thus other trials was performed at 60°C for overnight. The result of these trials aldehyde was produced in small with mostly starting material, crude NMR was checked aldehyde was obtained after column chromatography (100Chloroform:1MeOH) aldehyde was decomposed. (Table 2.11.) In case possibility of the presence small amount of aldehyde it is tried to form cyclization reaction to get compound **69** by using LiCl, H- of the crude product showed no product formation. (Figure 2.15.)

Table 2.10. Coupling Reaction of amino alcohol (**25**) and 3,3-diethoxypropanoic acid

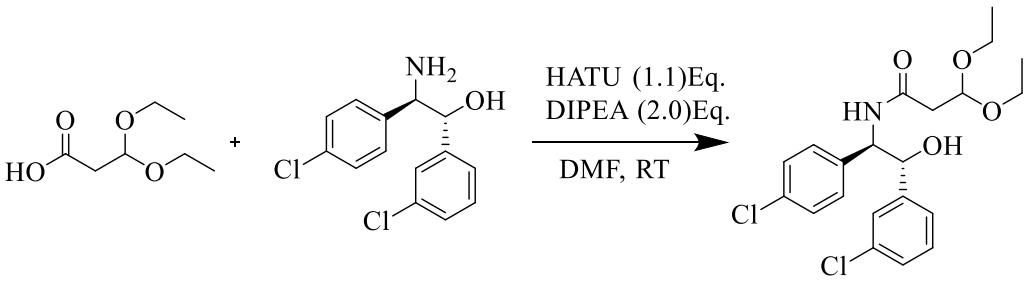

66 **25** **67**

Entry	Compound 66 (Eq)	Time(Hour)	Yield % 67
1	1.1	Overnight	74
2	1.1	36	82

Table 2.11. Acetal group of compound **67** converted to aldehyde with Iodine

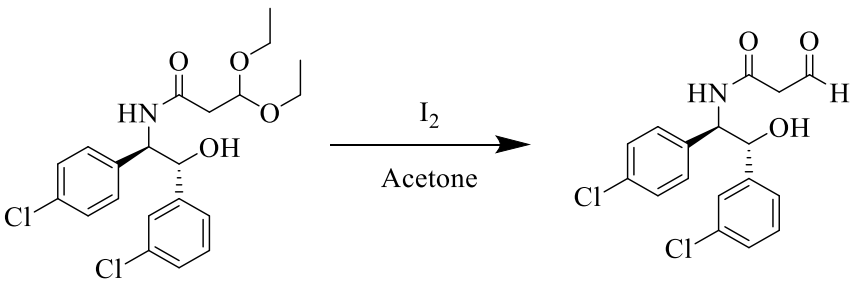

67 **68**

Entry	Time (h)	Yield %
1	1.5	Mostly reactant observed
2	5	Cannot be isolated.

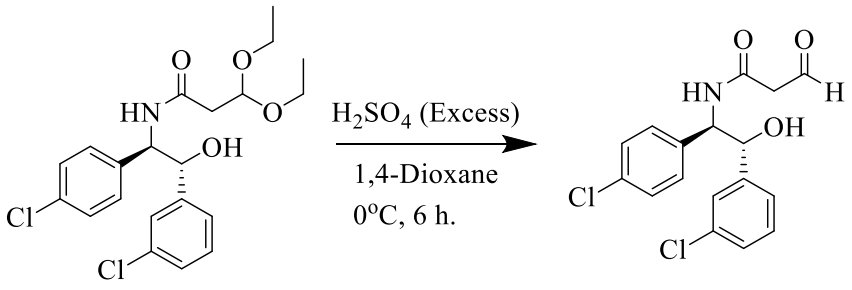

67 **68**

Aldehyde peak observed in NMR

Figure 2.14. Acetal group of compound **67** converted to aldehyde by using H_2SO_4

Table 2.12. Acetal group of compound **67** converted to aldehyde with H_3PO4

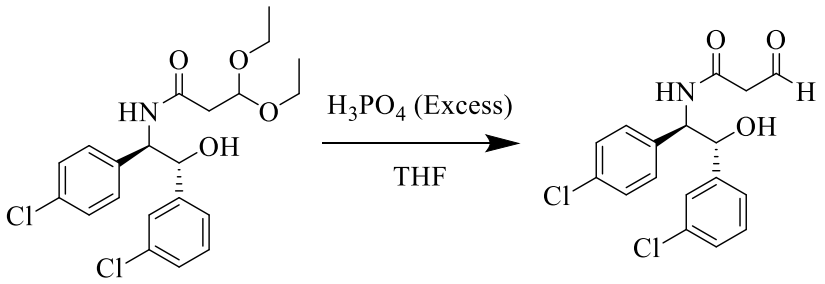

67 **68**

Entry	Temp (°C)	Time (Hour)	Yield % 68
1	RT	6	No reaction
2	60	Overnight	Aldehyde was isolated but it was decomposed.

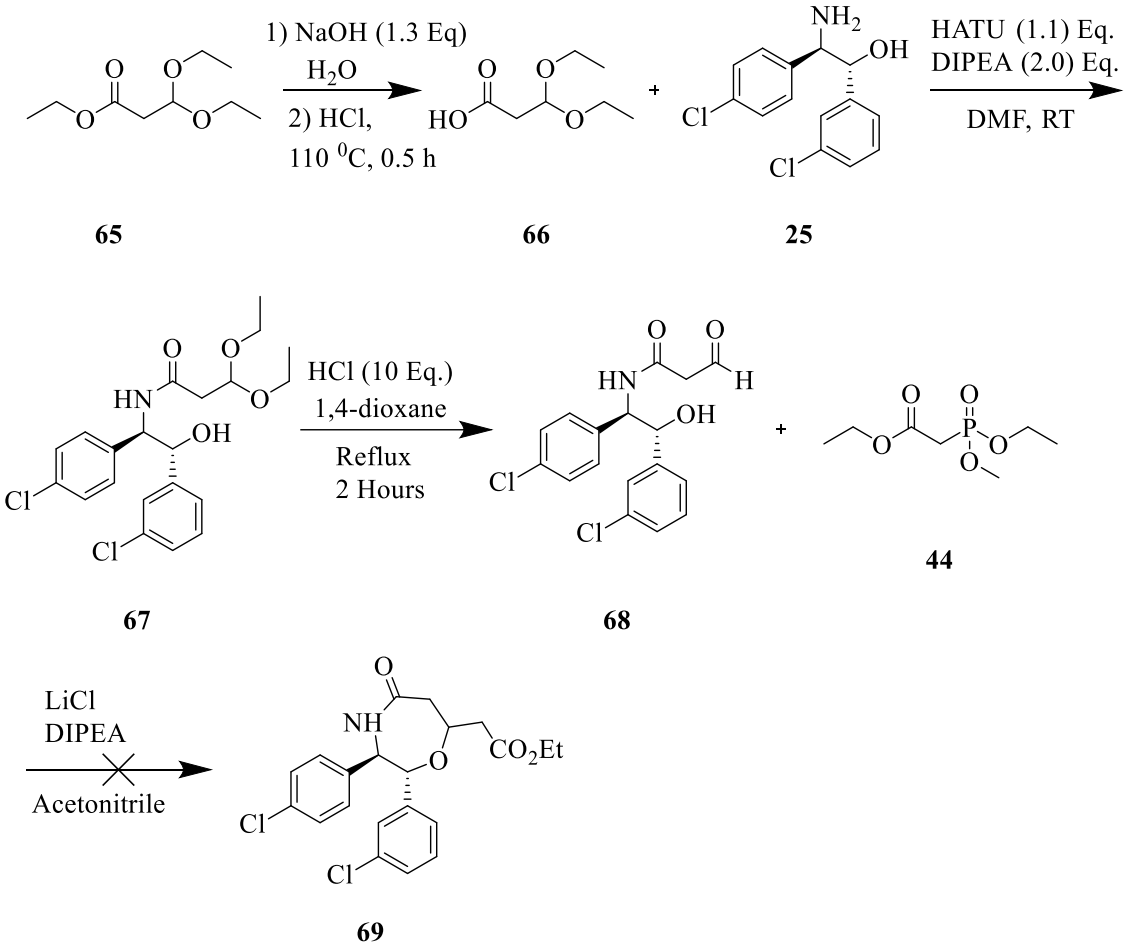

Figure 2.15. Studies toward the synthesis of ethyl (2*R*,3*R*)-2-(3-chlorophenyl)-3-(4-chlorophenyl)-5-oxo-1,4-oxazepane-7-carboxylate

2.16. Strategy toward the cyclization of 3-(((1*R*,2*R*)-2-(3-chlorophenyl)-1-(4-chlorophenyl)-2-hydroxyethyl)amino)-2,2-dimethyl-3-oxopropanoic acid

All of the attempts toward the intramolecular cyclization of α,β-unsaturated modified aminoalcohols were failed. One of the reason can be the higher acidity of the methylene protons between the amide carbonyl and α, β-unsaturated ester groups. Under basic conditions alcohol can be converted to alkoxide which then can be used as base to abstract these protons to form a dienolate instead of making nucleophilic attack to Michael acceptor. Formation of dienolate can cause side reactions and decompositions. (Figure 2.16.)

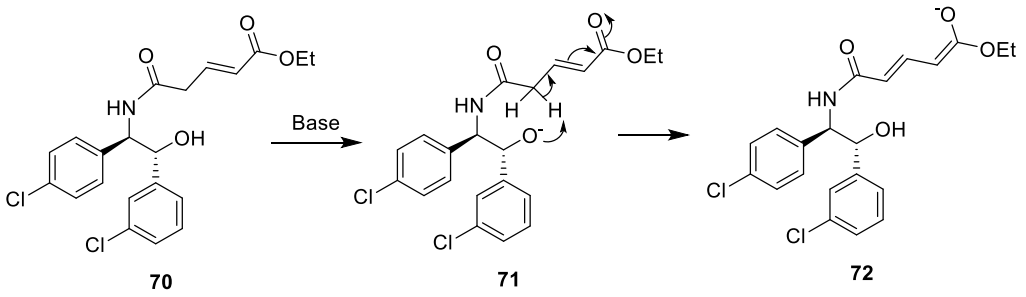

Figure 2.16. Acidity of active methylene protons can the reason for the lack of Michael addition reactions

For this reason a new strategy was proposed and preparation of two methyl substituted α, β-unsaturated ester was aimed in order to eliminate these acid protons. By this way obtained alkoxide can only be used as nucleophile to yield the intramolecular Michael addition reaction. New synthesis plan was started with aminoalcohol reacted with 3-hydroxy-2,2-dimethylpropanoic acid by using HATU and DIPEA in DMF. Reaction stirred overnight at room temperature then compound **74** was with column chromatography (100Chloroform:1MeOH) in 72% and 75% yields. Next step alcohol was oxidized to the aldehyde by using DMP in wet DCM. Compound **75** could not be clearly purified. In the last step, compound **79** was used for cyclization reaction to produce oxazepine by using compound **44,** DIPEA and LiCl in acetonitrile. The reaction stirred overnight at room temperature under nitrogen atmosphere and tried to purify by using column chromatography and H-NMR checked. However, expected signals for the product **76** could not be observed. (Figure 2.17.) Hence, all synthetic approaches were failed to produce 1,4-oxazepine-5-one skeleton.

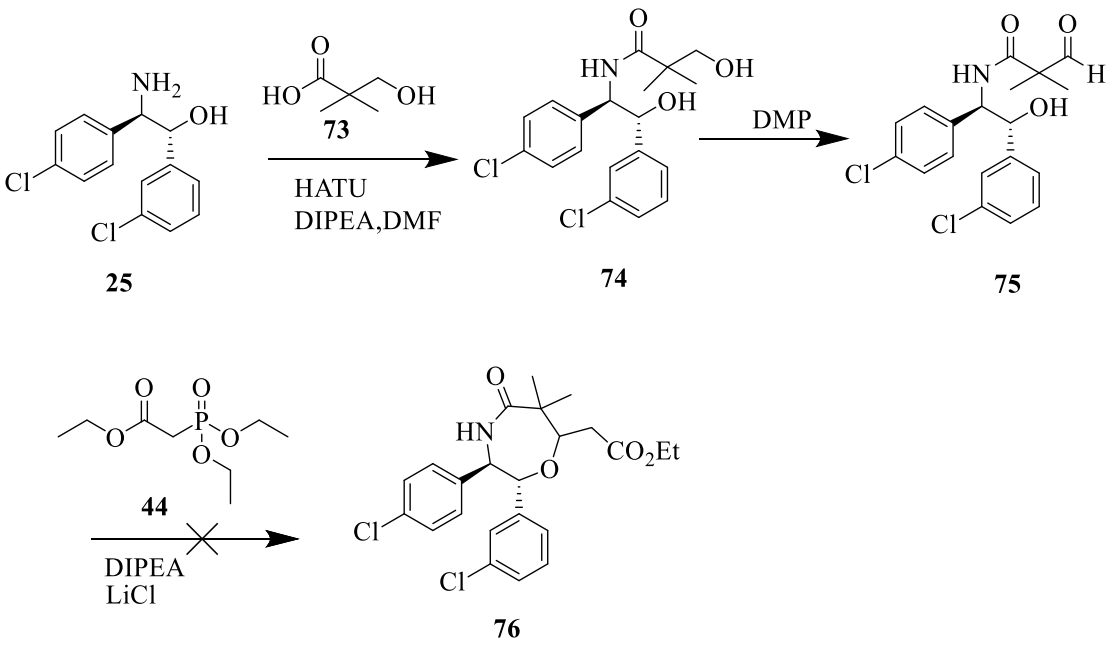

Figure 2.17. Attempts for the synthesis of ethyl 2-((2*R*,3*R*)-2-(3-chlorophenyl)-3-(4-chlorophenyl)-6,6-dimethyl-5-oxo-1,4-oxazepan-7-yl)acetate

CHAPTER 3

EXPERIMENTAL

3.1. General Methods

Reagents were used as supplied and purchased from Sigma-Aldrich and Riedel (Extra pure grade). Reactions were monitored by thin layer chromatography by using Merck TLC plates (Silica gel 60 F254). Chromatographic separations and isolations of compounds were performed by column chromatography. 70-230 mesh silica gel was used for column chromatography. Solvents were also commercial grade and were used as supplied. ^{1}H NMR and ^{13}C NMR data were recorded on Varian 400-MR (400 MHz) spectrometer. Chemical shifts for ^{1}H-NMR and ^{13}C-NMR are reported in δ (ppm). $CDCl_3$ peaks were used as reference in ^{1}H-NMR (7.26 ppm), and ^{13}C-NMR (77.36 ppm) respectively.

3.1.1. (*R*)-2-(4-chlorophenyl)-2-(tritylamino)acetic acid

Into a two necked flask 400 mg (R)-2-amino-2-(4-chlorophenyl) acetic acid (2.16 mmol, 1eq.) was dissolved in 4 mL of dry DMF under nitrogen and 286 μL trimethylsilyl chloride (245.5 mg, 2.26 mmol, 1.05 eq.) was added to the solution. The mixture was stirred for about 10 minutes until a clear solution was obtained. Then, 660 mg trityl chloride (2.37 mmol, 1.1 eq) was added followed by 600 μL triethylamine (435.1 mg, 4.32 mmol, 2 eq.). The reaction mixture was stirred under nitrogen atmosphere for 2 hours, diluted with 20.0 mL of diethyl ether and 20.0 mL of water. The reaction mixture was acidified to pH 3 with 0.01 M HCl. The reaction mixture was extracted with diethyl ether (3×30 mL), then the combined organic phase was dried over anhydrous $MgSO_4$ and filtered. The resulting product was used in the next step without purification.

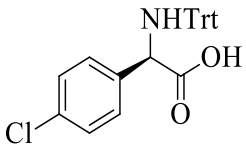

$C_{27}H_{22}ClNO_2$

Rf: 0.22 (EtOAc:Hexane, 1:4)

^{1}H NMR (400 MHz, CDCl3) δ 7.56 – 6.97 (m, 19H),4.30 (s, 1H), 1.30 (s, 1H)

^{13}C NMR (101 MHz, CDCl3) δ 178.47, 145.55, 138.09,
133.84, 128.90, 128.84, 128.61, 128.02, 126.78, 72.09, 59.84.

3.1.2. (*R*)-2-(4-chlorophenyl)-2-(tritylamino)ethane-1-ol

Into a two necked flask 1.01 g of (R)-2-(4-chlorophenyl)-2-(tritylamino)acetic acid (2.36 mmol 1.0 eq) was placed and solved in 3 mL of dry THF under nitrogen atmosphere and stirred under reflux. Afterwards a solution of 175 mg of $LiAlH_4$ (0.67 mmol, 1.5 eq.) in 2 mL dry THF was added drop wise into mixture which was cooled down to 0 ºC. The reaction was quenched with water (10 mL) followed by 20 mL of diethyl ether. 0.01 M sulfuric acid was added until the mixture's pH = 5 and extracted with diethyl ether (3 x 30 mL). The organic phase is washed with saturated NaOH and saturated brine solution. The organic phase was dried with $MgSO_4$. Organic layer was filtered and concentrated under reduced pressure to yield crude product. Purification by column chromatography (EtOAc/Hex; 1:12 to 1:4) resulted desired 489 mg of product with 55% yield.

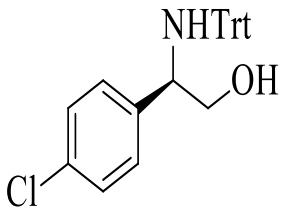

$C_{27}H_{24}ClNO$

R_f: 0.47 (EtOAc:Hexane, 1: 4)

^{1}H NMR (400 MHz, $CDCl_3$) δ 7.50 – 7.47 (m, 4H), 7.31 – 7.13 (m, 15H), 3.72 (t, J = 4.7 Hz, 1H), 3.20 (dd, J = 10.9, 4.4 Hz, 1H), 2.77 (dd, J = 10.9, 5.1 Hz, 1H)

^{13}C NMR (101 MHz, $CDCl_3$) δ 146.19, 142.04, 132.14, 128.80, 128.75, 128.40, 128.25, 127.80, 126.44, 71.72, 66.78, 57.92.

$[\alpha]_D^{20}$= -315º (c= 1.00, CH_2Cl_2)

3.1.3. (*R*)-2-(4-chlorophenyl)-2-(tritylamino)acetaldehyde

In a two necked flask 645 mg Dess-Martin periodinane (1.6 mmol, 2 eq.), was added at room temperature to a solution of 330 mg (R)-2-(4-chlorophenyl)-2 -

(tritylamino)-ethane-1-ol (0.8 mmol, 1 eq.) dissolved in wet dichloromethane (4.0 mL of dichloromethane / 4.0 μL water) under nitrogen atmosphere. The mixture was stirred for 1 hour, diluted with diethyl ether (50.0 mL) and quenched by the addition of a solution of $Na_2S_2O_3$ (7 eq.) dissolved in saturated aqueous $NaHCO_3$ solution (25 mL) at room temperature. The mixture is stirred for 5 minutes and the phases were separated. The water phase was extracted with diethylether (3×30 mL). The combined organic phase was then extracted with saturated aqueous $NaHCO_3$ solution followed by brine solution and the organic phase was dried over anhydrous $MgSO_4$ and filtered. After removal of the solvent under vacuum. The product was used in the next step without further purification and resulted (314 mg crude product with 95% yield).

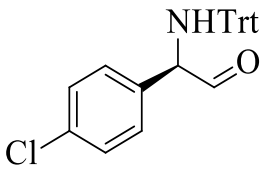

$C_{27}H_{22}ClNO$

Rf: 0.72 (Hexane:EtOAc, 4:1)

^{1}H NMR (400 MHz, $CDCl_3$) δ 9.04 (d, J = 1,0 Hz, 1H), 7.46 – 7.40 (m, 5H), 7.35 – 7.14 (m, 14H), 4.41 (s, 1H), 3.69 (bs, 1H).

3.1.4. (1*R*,2*R*)-1-(3-chlorophenyl)-2-(4-chlorophenyl)-2-(tritylamino)ethane-1-ol

Into a two necked flask 290 mg (R)-2-(4-chlorophenyl)-2-(tritylamino)-acetaldehyde (0.71 mmol, 1 eq.) was dissolved in 4 mL of dry THF under nitrogen atmosphere at -40 °C and 3.56 mL 0.5 M 3-chlorophenylmagnesium bromide (1.78 mmol, 2.5 eq.) was added dropwise. The mixture was stirred at -40 °C under nitrogen for 2 hours. The mixture was poured into 0.01 M H_2SO_4 solution Ph=5-6 and extracted with ethyl acetate (3 x 30 mL). The combined organic phases was dried over anhydrous $MgSO_4$ and filtered. After removal of solvent of the crude product, purification by column chromatography (EtOAc/Hex; 1:16) resulted of 140 mg desired product with 38% yield.

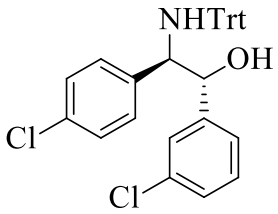

$C_{33}H_{27}Cl_2NO$

R_f: 0.50 (EtOAc: Hexzane, 1:4)

^{1}H NMR (400 MHz, $CDCl_3$) δ 7.41 – 7.35 (m, 6H), 7.20 – 7.09 (m, 10H), 7.08 – 7.02 (m, 2H), 6.85 (d, J = 8.5 Hz, 2H), 6.71 (d, J = 7.6 Hz, 1H), 6.41 (d, J = 8.3 Hz, 2H), 4.42 (d, J = 7.8 Hz, 1H), 3.93 (d, J = 7.9 Hz, 1H).

^{13}C NMR (101 MHz, $CDCl_3$) δ 145.63, 142.84, 139.34, 133.97, 131.99, 129.16, 128.96, 127.93, 127.57, 127.29, 126.74, 125.60, 78.35, 71.52, 63.94.

$[\alpha]_D^{20}$= -416° (c= 1.00, CH_2Cl_2)**.**

3.1.5. (1*R*,2*R*)-2-amino-1-(3-chlorophenyl)-2-(4-chlorophenyl)ethan-1-ol

In a two necked flask 300 mg N-Trt protected amino alcohol (0.57 mmol, 1 eq.) was dissolved in dichloromethane (4 mL) with excess TFA at room temperature 2 Hours later the solvent was evaporated. Then reaction mixtures was extracted with dichloromethane (3x30 mL) and organic phases washed with saturated $NaHCO_3$ solution. Organic phase was dried over anhydrous $MgSO_4$ and filtered. After removal of solvent of the crude product, purification by column chromatography (Chloroform/Methanol; 100:8) resulted desired 100 mg product with 62% yield.

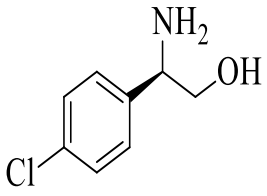

$C_8H_{10}ClNO$

R_f: 0.09 (MeOH:CH_2Cl_2, 12:1)

^{1}H NMR (400 MHz, $CDCl_3$) δ 7.29 (d, J = 8.6 Hz, 2H), 7.23 (d, J = 8.4 Hz, 2H), 3.99 (dd, J = 8.1, 4.2 Hz, 1H), 3.66 (dd, J = 10.9, 4.2 Hz, 1H), 3.48 (dd, J = 10.9, 8.2 Hz, 1H), 2.74 (bs, 2H), 1.44 (s, 1H).

3.1.6. Monomethylglutaconate

In a two necked flask 100 mg of compound 36 (0.76 mmol) and 125 µL of methanol (3.07 mmol) are dissolved in 5.0 mL of dry DCM under nitrogen atmosphere and 370 µL of diethyl azodicarboxylate (DEAD) (0.84 mmol) and 283 mg of resin

bound triphenylphosphine (0.84 mmol) were added. The reaction mixture is stirred for 16 hours under nitrogen atmosphere. After the reaction mixture is filtered with dichloromethane, the solvent is removed in vacuo. The substance is purified by SiO_2 column chromatography eluting with 1:1 EtOAc: Hexane solvent system then 1:1 EtOAc:Hexane 1% acetic acid and 2% methanol with to 28% yield of product.

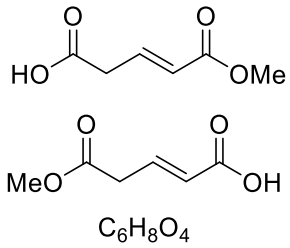

$C_6H_8O_4$

Rf: 0.40 (1% HOAc ve 2% MeOH containing 1:1 EtOAc: Hexane);
^{1}H NMR (400 MHz, $CDCl_3$) δ 7.18 – 6.95 (m, 2H, carbonyl β-protons), 5.96 (dd, J = 15.6 ve 8.7 Hz, 2H, β-protons), 5.96 (dd, J = 15.6 ve 8.7 Hz, 2H, α-protons), 3.75 (s, 3H), 3.73 (s, 3H), 3.29 (d, J = 7.0 Hz, 4H).

3.1.7. 3-((tert-butyldimethylsilyl)oxy)propanal

In a two necked flask 194 mg of sodium acetate (2.37 mmol) is dissolved in 4mL of dry DCM under nitrogen atmosphere, at room temperature 560 µL of 3-((tert-butyldimethylsilyl)oxy)propan-ol (2.63 mmol) and at 0 ºC 625mg PCC (2.9 mmol)are added onto the solution. After the reaction mixture is stirred under nitrogen atmosphere at room temperature for 2 hours, it is diluted with 100 mL of diethyl ether and stirred for an additional 10 minutes. It is filtered through the column prepared with magnesium sulfate silica mixture by using 300 mL of diethyl ether. The obtained organic phase is washed with 10% NaOH solution and brine solution. The combined organic layer is dried with $MgSO_4$, filtered and then the solvent is removed under vacuum. Since the product obtained is volatile, it is used without purification

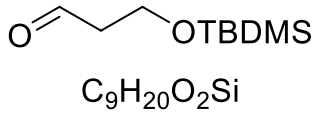

$C_9H_{20}O_2Si$

Rf: 0.6 (1:4 EtOAc:Hexane);
^{1}H NMR (400 MHz, $CDCl_3$) δ 9.78 (t, J = 2.1 Hz, 1H), 3.97 (t, J = 6.0 Hz, 2H), 2.58 (td, J = 6.0 ve 2.1 Hz, 2H), 0.86 (s, 9H), 0.05 (s, 6H).[66]

3.1.8. Ethyl (*E*)-5-((tert-butyldimethylsilyl)oxy)pent-2-enoate

In a two necked flask 158.0 mg of sodium hydride (3.9 mmol) is dissolved in 6 mL of dry THF under nitrogen gas at 0 ºC and 783.0 µL of triethyl phosphonoacetate

(3.9 mmol) is slowly added to the solution over 20 minutes. The reaction mixture was stirred at 0 ºC for 40 minutes, then the temperature of the mixture was reduced to -78 ºC and the solution of 3-((tert-butyldimethylsilyl)oxy)propanal (in 20 mL diethyl ether) was slowly added to the reaction mixture over 30 minutes. The reaction temperature was slowly heated to 0 ºC and stirred at 0 ºC for 30 minutes. The TLC-controlled reaction is terminated and extracted with ammonium chloride. The combined organic layer is washed with water (4x20 mL) and combined organic phase washed with brine. Then, after the organic layer is dried with $MgSO_4$ and filtered, the solvent is removed under vacuum. Compound is purified by SiO_2 column chromatography using a 1:20 EtOAc:Hexane solvent system with 28% yield

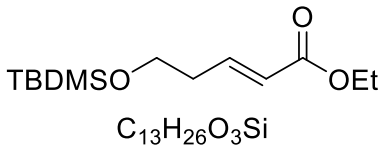

$C_{13}H_{26}O_3Si$

Rf: 0,70 (1:4 EtOAc:Hexan);
^{1}H NMR (400 MHz, $CDCl_3$) δ 6.93 (dt, *J* = 15.7, 7.1 Hz, 1H), 5.84 (dt, *J* = 15.7, 1.5 Hz, 1H), 4.15 (q, *J* = 7.2 Hz, 2H), 3.69 (t, *J* = 6.5 Hz, 2H), 2.38 (ddd, *J* = 13.6, 6.5, 1.5 Hz, 2H), 1.25 (t, *J* = 7.1 Hz, 3H), 0.86 (s, 9H), 0.02 (s, 6H).[66]

3.1.9. (*E*)-5-((tert-butyldimethylsilyl)oxy)pent-2-enoic acid

In a two necked flask 115 mg of ethyl (E)-5-((tert-butyldimethylsilyl)oxy)pent-2-enoate (1.08 mmol) is dissolved in 2.1 mL of 1,4-dioxane under nitrogen atmosphere at room temperature and 1.8 mL of 1.0 M K2CO3 solution (1.8 mmol) is added. The reaction mixture is stirred under nitrogen atmosphere with TLC control for four hours. The reaction is terminated by addition of 100 mL of water and extracted with EtOAc (3x30 mL). The water phase is acidified with 0.5 M H_2SO_4 solution and extracted with EtOAc (3x30 mL). The organic layers obtained from the acidic water phase are dried with $MgSO_4$, filtered, the solvent is removed under vacuum to obtain acid with 3% yield.

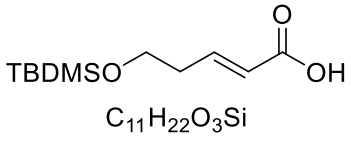

$C_{11}H_{22}O_3Si$

Rf: 0,20 (1:4 EtOAc:Hexane)
^{1}H NMR (400 MHz, $CDCl_3$) δ 7.10 – 7.01 (m, 1H), 5.86 (d, *J* = 15.7 Hz, 1H), 3.72 (t, *J* = 6.3 Hz, 2H), 2.42 (q, *J* = 6.3 Hz, 2H), 0.86 (s, 9H), 0.03 (s, 6H).

3.1.10. Dibenzyl (*E*)-pent-2-enedioate

25 ml round bottom flask equipped with Dean-Stark trap, 500 mg glutaconic acid (3.84 mmol), 830 mg benzyl alcohol (783.0 µL,7.68 mmol) and and TsOH added as a catalyst in toluene (215 mL). Reaction was heated to 110 °C and refluxed for 7 hours. Reaction was cooled the room temperature and solvent was removed under vacuo by using azeotrope (MeOH 71%,Toluene 29%). Compound is purified by SiO_2 column chromatography using a gradient elution with 1:12 EtOAc: Hexane to 1:9 EtOAc:Hexane solvent system to 28% yield product.

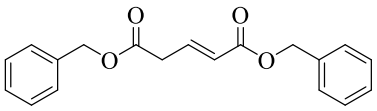

$C_{19}H_{18}O_4$

Rf: 0,25 (1:4 EtOAc:Hexane)
^{1}H NMR (400 MHz, $CDCl_3$) δ 7.41 – 7.31 (m, 1H), 6.00 (dt, *J* = 15.7, 1.6 Hz, 1H), 5.20 (d, *J* = 1.5 Hz, 1H), 5.16 (d, *J* = 2.3 Hz, 1H), 3.27 (ddd, *J* = 15.7, 7.2, 1.6 Hz, 1H).

3.1.11. 3-(Benzyloxy)propan-1-ol

In a two necked flask sodium hydride (1156.0 mg, 28.91 mmol) was dissolved in 6 mL of dry THF under nitrogen atmosphere at 0 °C and 1,3-propanediol (950.0 µL, 13.14 mmol) was added slowly to the solution. The reaction mixture was stirred at 0 °C for 10 minutes and benzyl bromide (950.0 µL, 13.14 mmol) was added to the solution over 10 minutes. The reaction mixture was warmed to room temperature and stirred for 18 hours and extracted with water and EtOAc (3x50 mL) the organic phase was washed with water (4x20 mL). The combined organic layer was dried with $MgSO_4$, filtered, and the filtrate was concentrated under reduced pressure. The residue was purified with SiO_2 column chromatography with 34% yield.

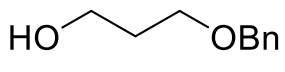

$C_{10}H_{14}O_2$

Rf: 0,22 (1:3 EtOAc:Hexane)
^{1}H NMR (400 MHz, $CDCl_3$) δ 7.31 (s, 5H), 4.48 (s, 2H), 3.71 (t, *J* = 5.8 Hz, 2H), 3.61 (t, *J* = 5.9 Hz, 2H), 2.84 (s, 1H), 1.86 – 1.78 (m, 2H). [67]

3.1.12. 3-(Benzyloxy)propanal

In a two necked flask Sodium acetate (350 mg, 4.67 mmol) was dissolved in 4 mL dry DCM under nitrogen atmosphere 3-(benzyloxy)propan-1-ol (788 mg, 4.74 mmol) was added on it. PCC (1121 mg, 5.2 mmol) was added in two portions at 0º C. The reaction mixture was stirred for 2 hours under nitrogen atmosphere at room temperature and diluted with 100 mL diethyl ether and stirred for a further 5 minutes. The reaction mixture was filtered through a (silica-magnesium sulfate) mixture column with 300 mL diethyl ether. The resulting organic phase was extracted with 10% NaOH solution and brine solution. Combined organic phase was dried with $MgSO_4$ filtered and evaporated under reduced pressure until left about 20 mL diethl ether. Product was used without purification.

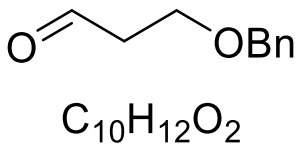

$C_{10}H_{12}O_2$

Rf: 0,57 (1:4 EtOAc:Hexane)

3.1.13. Ethyl (*E*)-5-(benzyloxy)pent-2-enoate

In a two necked flask sodium hydride (245 mg, 6.14 mmol) was dissolved in 6 mL of dry THF under nitrogen atmosphere at 0 °C and triethyl phosphonoacetate (1210 µL, 6.14 mmol) was added over 20 minutes to the solution. The reaction mixture was stirred at 0°C for 40 minutes and the mixture was cooled to -78°C and 3-(benzyloxy)propanal mixture in diethyl ether was added to the reaction mixture over 30 minutes. The reaction was slowly heated to 0 °C and the mixture in THF stirred at 0 °C for 30 minutes. It was extracted with ammonium chloride solution the organic phase was washed with water (4x20mL) and brine solution. The combined organic layer was dried with $MgSO_4$, filtered, and the filtrate was concentrated under reduced pressure. The residue was purified with SiO_2 column chromatography with 28% yield

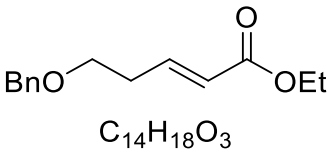

$C_{14}H_{18}O_3$

Rf: 0,54 (1:4 EtOAc:Hexane)
^{1}H NMR (400 MHz, $CDCl_3$) δ 7.36 – 7.21 (m, 5H), 6.97 (dt, J = 15.7, 6.9 Hz, 1H), 5.88 (dt, J = 15.7, 1.6 Hz, 1H), 4.50 (s, 2H), 4.16 (q, J = 7.1 Hz, 2H), 3.56 (t, J = 6.5 Hz, 2H), 2.49 (qd, J = 6.5, 1.6 Hz, 2H), 1.26 (t, J = 7.1 Hz, 3H).[67]

3.1.14. (*E*)-5-(benzyloxy)pent-2-enoic acid

In a two necked flask ethyl (E)-5-(benzyloxy)pent-2-enoate (254 mg, 1.08 mmol) was dissolved in 2 mL of dioxane under nitrogen atmosphere and 1 M NaOH solution (2.16 mL, 2.16 mmol) was added to the solution at room temperature. The reaction mixture was stirred under nitrogen atmosphere for 3 hours at room temperature. The reaction mixture was concentrated under reduced pressure and extracted with water and diethyl ether (2 x 50 mL). Water layer was acidified to pH 5 then extracted with diethyl ether (2 x 50 mL). Both organic phases was washed with water and brine dried with $MgSO_4$, filtered, and the filtrate was concentrated under reduced pressure to product with 66% yield.

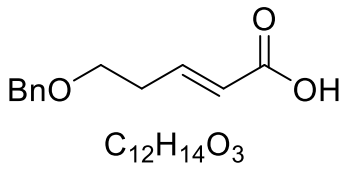

$C_{12}H_{14}O_3$

Rf: 0,23 (%1 HOAc containing 1:4 EtOAc:Hexane)
^{1}H NMR (400 MHz, $CDCl_3$) δ 11.59 (s, 1H), 7.38 – 7.26 (m, 5H), 7.10 (dt, *J* = 15.7, 6.9 Hz, 1H), 5.90 (dt, *J* = 15.7, 1.5 Hz, 1H), 4.52 (s, 2H), 3.59 (t, *J* = 6.4 Hz, 2H), 2.54 (qd, *J* = 6.5, 1.5 Hz, 2H).

3.1.15. (*E*)-5-(benzyloxy)-N-((1*R*,2*R*)-2-(3-chlorophenyl)-1-(4-chlorophenyl)-2-hydroxyethyl)pent-2-enamide (*E*)-5-(benzyloxy)pent-2-enoic acid

In a two necked flask 88 mg of (1*R*, 2*R*)-2-amino-1-(3-chlorophenyl)-2-(4-chlorophenyl)ethan-1-ol (0.31 mmol) is dissolved in 2 mL of dry DMF at room temperature. In another flask, 64 mg of (E)-5-(benzyloxy)pent-2-enoic acid (0.31 mmol), 130 mg of HATU (0.34 mmol) and 107 µL of diisopropylethylamine (0.62 mmol) were dissolved in 2 mL of dry DMF added on the reaction mixture is stirred at room temperature overnight and then controlled by TLC, terminated by adjusting the pH to 5 using 0.5 M H_2SO_4 and extracted with EtOAc (3x50 mL). The combined organic phases then washed with water (5x50 mL). The substance is purified by SiO_2 column chromatography using 1:2 EtOAc: Hexane and 100:4 chloroform: methanol solvent systems to obtain product with 45% yield

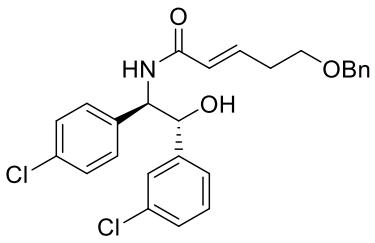

$C_{26}H_{25}Cl_2NO_3$

Rf: 0,14 (100:4 $CDCl_3$:MeOH); $[\alpha]_D^{20}$= +2,0º (c: 0,5, CH_2Cl_2)

^{1}H NMR (400 MHz, $CDCl_3$) δ 7.35 – 7.03 (m, 13H), 6.75 (dt, *J* = 14.0, 6.8 Hz, 1H), 6.28 (d, *J* = 7.5 Hz, 1H), 5.82 (dd, *J* = 15.4, 1.1 Hz, 1H), 5.13 (dd, *J* = 7.4, 4.6 Hz, 1H), 4.89 (d, *J* = 4.5 Hz, 1H), 4.47 (s, 2H), 3.52 (t, *J* = 6.4 Hz, 2H), 2.44 (q, *J* = 6.5 Hz, 2H).

^{13}C NMR (400 MHz, $CDCl_3$) δ 166.1, 142.7, 142.5, 138.0, 137.7, 134.3, 133.6, 129.6, 128.8, 128.4, 128.4, 128.0, 127.7, 127.7, 126.3, 124.3, 124.2, 76.3, 73.0, 68.2, 59.1, 32.4.

3.1.16. (*R*)-2-(benzyloxy)-1-phenylethan-1-ol

Benzyl alcohol (1.29 mL, 12.48 mmol) is dissolved in 3mL of dry DMF under nitrogen atmosphere and sodium hydride (520 mg, 12.48 mmol) is added to the solution in portions. After the reaction is stirred at room temperature for 10 minutes, it is cooled to 0 ºC and (475 µL, 4.16 mmol) (*R*)-styrene oxide is added dropwise to the reaction and the reaction temperature is increased to 60 ºC and stirred under nitrogen gas for 2 days. The reaction mixture is diluted with water and the mixture is extracted with ethyl acetate (3x30 mL). The combined organic layer is dried with $MgSO_4$, filtered, and the solvent is removed under vacuum. The product is purified by SiO_2 column chromatography (1:10 EtoAC: Hexane) with 27% yield.

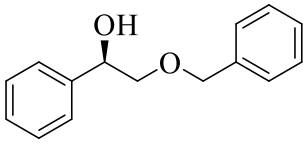

$C_{15}H_{16}O_2$

Rf:0,25 (1:8 EtOAc:Hexane) $[\alpha]^{26.8}D$ = - 80 (c: 1.0, CH_2Cl_2)**^{1}H NMR** (400 MHz, CDCl3) δ 7.39 – 7.22 (m, 9H), 4.92 (dd, J = 9.0, 3.2 Hz, 1H), 4.63 – 4.55 (m, 2H), 3.64 (dd, J = 9.7, 3.2 Hz, 1H), 3.50 (t, J = 9.4 Hz, 1H).

3.1.17. (1*R*,2*R*)-1-(3-chlorophenyl)-2-(4-chlorophenyl)-2-((2-hydroxy-1-phenylethyl)amino)ethanol

Lithium perchlorate, $LiClO_4$ (27 mg, 0.25 mmol) and (*R*)-styrene oxide (28 µL, 0.25 mmol) are dissolved in 2 mL of acetonitrile under nitrogen atmosphere and added on amino alcohol (70 mg, 0.25 mmol). The reaction mixture was stirred at 80 °C overnight, then cooled to room temperature and stirred for 5 hours at room temperature. The reaction mixture is diluted with water and the mixture is extracted with ethyl

acetate (3x30 mL). The combined organic layer is dried with $MgSO_4$, filtered, and the solvent is removed in vacuo. The product is purified by SiO_2 column chromatography (EtOAc:Hexane, 1:6) (Hexane: EtOAc: MeOH, 4: 1: 4%) with 39% yield.

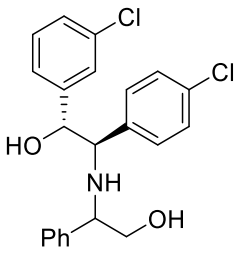

$C_{22}H_{21}Cl_2NO_2$

Rf = 0.34 (Chloroform:MeOH, 100:3)

^{1}H NMR (400 MHz, $CDCl_3$) δ 7.31 – 7.12 (m, 1H), 7.09 – 7.01 (m, 1H), 6.91 (d, J = 8.4 Hz, 1H), 6.83 (d, J = 8.4 Hz, 1H), 6.78 (s, 1H), 4.80 (dd, J = 8.4, 4.1 Hz, 1H), 4.55 (t, J = 7.6 Hz, 1H), 3.77 – 3.72 (m, 1H), 3.67 (dd, J = 7.8, 4.9 Hz, 1H), 2.64 (dd, J = 11.9, 3.7 Hz, 1H)

3.1.18. N-((1*R*,2*R*)-2-(3-chlorophenyl)-1-(4-chlorophenyl)-2-hydroxyethyl)-3,3-diethoxypropanamide

3,3-diethoxypropanoic acid (31 mg, 0.195 mmol), HATU (74 mg, 0.195 mmol) and DIPEA (61 µL, 0.36 mmol) are weighed, orderly dissolved in 1 mL of dry DMF and then under nitrogen atmosphere (1*R*,2*R*)-2-amino-1-(3-chlorophenyl)-2-(4-chlorophenyl)ethan-1-ol is dissolved added to mixture. The solution is stirred at room temperature for 1 night, diluted with distilled water and acidified to pH 5 using 0.05M H_2SO_4 solution, and the mixture is extracted with ethyl acetate (3x30 mL). The combined organic layer is washed with water, dried with $MgSO_4$, filtered, and the solvent is removed under vacuo The product is purified by SiO_2 column chromatography (100 Chloroform:3 MeOH) with 33% yield.

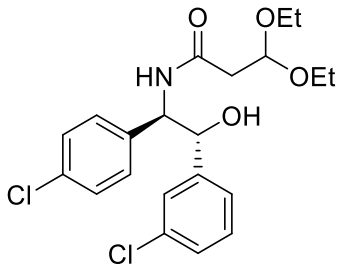

$C_{21}H_{25}Cl_2NO_4$

Rf = 0.74 (Chloroform:MeOH, 100:4)

[α]$^{22.9}_D$ = 64,(c: 1.0,CH_2Cl_2)

^{1}H NMR (400 MHz, $CDCl_3$) δ 7.40 (d, J = 8.2 Hz, 1H), 7.32 (d, J = 1.9 Hz, 1H), 7.27 – 7.24 (m, 3H), 7.21 – 7.15 (m, 5H), 7.12 – 7.08 (m, 1H), 5.10 (dd, J = 8.2, 4.2 Hz, 1H), 4.87 (t, *J* = 3.9 Hz, 1H), 4.65 (t, J = 4.9 Hz, 1H), 3.66 (ddd, J = 8.7, 5.4, 1.6 Hz, 3H), 3.48 (ddd, *J* = 13.2, 9.3, 7.0 Hz, 2H), 2.50 (dd, *J* = 4.9, 0.7 Hz, 2H), 1.19 (dt, J = 13.4, 7.0 Hz, 7H).

3.1.19. N-((1*R*,2*R*)-2-(3-chlorophenyl)-1-(4-chlorophenyl)-2-hydroxyethyl)-3-hydroxy-2,2-dimethylpropanamide

(1*R*,2*R*)-2-amino-1-(3-chlorophenyl)-2-(4-chlorophenyl)ethan-1-ol (90.0 mg, 0.32 mmol) is dissolved in 2 mL of dry DMF at room temperature. In another flask, 3 hydroxy-2,2-dimethylpropanoic acid (41.61 mg, 0.35 mmol), 2-(7-Aza-1H-benzotriazol-1-yl)-1,1,3,3 tetramethyluronium hexafluorophosphate (HATU) (133 mg, 0.35 mmol) and diisopropylethylamine (109 µL, 0.64 mmol) dissolved in 2 mL of dry DMF and this mixture added to the amino alcohol solution. The reaction mixture was stirred at room temperature for 1 night then extracted with DCM (3x20 mL) and $NaHCO_3$. The organic layer was washed with 0.05 M H_2SO_4 solution, then the organic layer was dried with $MgSO_4$ and filtered. The organic layer was tried to be purified by SiO_2 column chromatography (100ch:1 MeOH) with 72% yield.

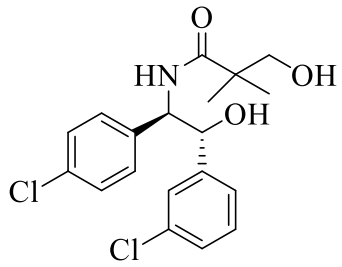

$C_{19}H_{21}Cl_2NO_3$

Rf = 0.59 (Chloroform:MeOH, 100:4)

^{1}H NMR (400 MHz, $CDCl_3$) δ 7.56 – 6.68 (m, 8H), 5.17 (dd, J = 8.0, 3.9 Hz, 1H), 5.06 (dd, J = 8.0, 4.0 Hz, 1H), 4.95 (d, J = 3.8 Hz, 1H), 4.86 (d, J = 3.9 Hz, 1H), 3.51 – 3.47 (m, 1H), 3.41 (s, 1H), 1.07 (s, 3H), 1.03 (s, 3H).

CHAPTER 4

CONCLUSION

Studies in recent year show that MDM2 inhibitors are widely attract the attentions of scientist in the literature. In particular, morpholinone-derived MDM2 inhibitors show the most potent inhibitory activity in in vivo and in vitro studies. Therefore, they are attractive structures that can be modified to develop novel promising MDM2 inhibitors.

For this purpose preparation of amino alcohol which is (1*R*,2*R*)-2-amino-1-(3-chlorophenyl)-2-(4-chlorophenyl)ethan-1-ol was an important intermediate. In this study preparation of this compound was performed in five steps similar procedure reported by Amgen's scientists starting from (*R)*-4-chlorophenylglycine. Firstly, amine group was protected with tritly group by addition of tritylchloride under basic condition. Then protected glycine was reduced to N-Trt protected amino alcohol by using $LiAlH_4$. Formed alcohol was successfully oxidized to aldehyde by Dess-Martin periodinane, then addition of Grignard reagent gave the target aminoalcohol product. This step produces the mixture of the diastereomers, which are difficult to purify. The next step Trt protected group was removed by using TFA. Finally deprotected amino alcohol was obtained.

To develop 1,4-oxazepine-5-one derivatives coupling of deprotected amino alcohol with several α,β-unsaturated acids or esters by using HATU and DIPEA were attempted, and 3 of these trials were succeeded. First trial was using (*E*)-5-(benzyloxy)pent-2-enoic acid second one was using 3,3-diethoxypropanoic acid and the last one was using 3-hydroxy-2,2-dimethylpropanoic acid. In the last step, the cyclization experiments were studied in the presence of bases such as K_2CO_3, DBU and some oter catalysts. Last trial was studied thruogh with the LiCl, DIPEA and triethyl phosphonacetate and the desired molecule was not obtained. Unfortunately, all of these approaches were failed to produce the target 1,4-oxazepine-5-one derivatives.

REFERENCES

(1) Sudhakar, A. History of Cancer, Ancient and Modern Treatment Methods. *Cit. Sudhakar A* **2009**, *1* (2), i–iv. https://doi.org/10.4172/1948-5956.100000e2.

(2) Lane, D. P.; Madhumalar, A.; Lee, A. P.; Tay, B.-H.; Verma, C.; Brenner, S.; Venkatesh, B. Conservation of All Three P53 Family Members and Mdm2 and Mdm4 in the Cartilaginous Fish. *Cell Cycle* **2011**, *10* (24), 4272–4279. https://doi.org/10.4161/cc.10.24.18567.

(3) Lamb, P.; Crawford, L. Characterization of the Human P53 Gene. *Mol. Cell. Biol.* **1986**, *6* (5), 1379–1385. https://doi.org/10.1128/mcb.6.5.1379.

(4) Isobe, M.; Emanuel, B. S.; Givol, D.; Oren, M.; Croce, C. M. Localization of Gene for Human P53 Tumour Antigen to Band 17p13. *Nature* **1986**, *320* (6057), 84–85. https://doi.org/10.1038/320084a0.

(5) Gupta, A.; Shah, K.; Oza, M. J.; Behl, T. Reactivation of P53 Gene by MDM2 Inhibitors: A Novel Therapy for Cancer Treatment. *Biomed. Pharmacother.* **2019**, *109* (October 2018), 484–492. https://doi.org/10.1016/j.biopha.2018.10.155.

(6) Vousden, K. H.; Prives, C. Blinded by the Light: The Growing Complexity of P53. *Cell* **2009**, *137* (3), 413–431. https://doi.org/10.1016/j.cell.2009.04.037.

(7) Kopnin, B. P. Targets of Oncogenes and Tumor Suppressors: Key for Understanding Basic Mechanisms of Carcinogenesis. *Biochem.* **2000**, *65* (1), 2–27.

(8) Kern, S.; Pietenpol, J.; Thiagalingam, S.; Seymour, A.; Kinzler, K.; Vogelstein, B. Oncogenic Forms of P53 Inhibit P53-Regulated Gene Expression. *Science (80-.).* **1992**, *256* (5058), 827–830. https://doi.org/10.1126/science.1589764.

(9) Levine, A. J. The P53 Tumor-Suppressor Gene. *N. Engl. J. Med.* **1992**, *326* (20), 1350–1352. https://doi.org/10.1056/nejm199205143262008.

(10) Hartwell, L.; Weinert, T. Checkpoints: Controls That Ensure the Order of Cell

Cycle Events. *Science (80-.).* **1989**, *246* (4930), 629–634. https://doi.org/10.1126/science.2683079.

(11) Kastan, M. B. Commentary on "Participation of P53 Protein in the Cellular Response to DNA Damage." *Cancer Res.* **2016**, *76* (13), 3663–3665. https://doi.org/10.1158/0008-5472.can-16-1560.

(12) Agarwal, M. L.; Agarwal, A.; Taylor, W. R.; Stark, G. R. P53 Controls Both the G2/M and the G1 Cell Cycle Checkpoints and Mediates Reversible Growth Arrest in Human Fibroblasts. *Proc. Natl. Acad. Sci. U. S. A.* **1995**, *92* (18), 8493–8497. https://doi.org/10.1073/pnas.92.18.8493.

(13) Kastenhuber, E. R.; Lowe, S. W. Putting P53 in Context. *Cell*. 2017. https://doi.org/10.1016/j.cell.2017.08.028.

(14) Haupt, S. Apoptosis - the P53 Network. *J. Cell Sci.* **2003**, *116* (20), 4077–4085. https://doi.org/10.1242/jcs.00739.

(15) Levine, A. J.; Oren, M. The First 30 Years of P53: Growing Ever More Complex. *Nat. Rev. Cancer* **2009**, *9* (10), 749–758. https://doi.org/10.1038/nrc2723.

(16) Michael, D.; Oren, M. The P53–Mdm2 Module and the Ubiquitin System. *Semin. Cancer Biol.* **2003**, *13* (1), 49–58. https://doi.org/10.1016/s1044-579x(02)00099-8.

(17) Fakharzadeh, S. S.; Trusko, S. P.; George, D. L. Tumorigenic Potential Associated with Enhanced Expression of a Gene That Is Amplified in a Mouse Tumor Cell Line. *EMBO J.* **1991**, *10* (6), 1565–1569. https://doi.org/10.1002/j.1460-2075.1991.tb07676.x.

(18) Chen, J.; Wu, X.; Lin, J.; Levine, A. J. Mdm-2 Inhibits the G1 Arrest and Apoptosis Functions of the P53 Tumor Suppressor Protein. *Mol. Cell. Biol.* **1996**, *16* (5), 2445–2452. https://doi.org/10.1128/mcb.16.5.2445.

(19) Peng, Y.; Chen, L.; Li, C.; Lu, W.; Agrawal, S.; Chen, J. Stabilization of the MDM2 Oncoprotein by Mutant P53. *J. Biol. Chem.* **2001**, *276* (9), 6874–6878. https://doi.org/10.1074/jbc.c000781200.

(20) Freedman, D. A.; Wu, L.; Levine, A. J. Functions of the MDM2 Oncoprotein. *Cell. Mol. Life Sci. C.* **1999**, *55* (1), 96–107. https://doi.org/10.1007/s000180050273.

(21) Chen, J.; Marechal, V.; Levine, A. J.; Momand, J.; Zambetti, G. P.; Olson, D. C.; George, D.; Levine, A. J. *Mapping of the P53 and Mdm-2 Interaction Domains The 90-KDa Cellular Protein Encoded by the Mouse Mdm-2 Oncogene Binds to the P53 Protein in Vivo and Inhibits Its Transactivation Function (*; 1993.

(22) Oliner, J. D.; Pietenpol, J. A.; Thiagalingam, S.; Gyuris, J.; Kinzler, K. W.; Vogelstein, B. Oncoprotein MDM2 Conceals the Activation Domain of Tumour Suppressor P53. *Nature* **1993**, *362* (6423), 857–860. https://doi.org/10.1038/362857a0.

(23) Honda, R.; Tanaka, H.; Yasuda, H. Oncoprotein MDM2 Is a Ubiquitin Ligase E3 for Tumor Suppressor P53. *FEBS Lett.* **1997**, *420* (1), 25–27. https://doi.org/10.1016/s0014-5793(97)01480-4.

(24) Li, M. Mono- Versus Polyubiquitination: Differential Control of P53 Fate by Mdm2. *Science (80-.).* **2003**, *302* (5652), 1972–1975. https://doi.org/10.1126/science.1091362.

(25) Giaccia, A. J.; Kastan, M. B. The Complexity of P53 Modulation: Emerging Patterns from Divergent Signals. *Genes Dev.* **1998**, *12* (19), 2973–2983. https://doi.org/10.1101/gad.12.19.2973.

(26) Singh, R. K.; Iyappan, S.; Scheffner, M. Hetero-Oligomerization with MdmX Rescues the Ubiquitin/Nedd8 Ligase Activity of RING Finger Mutants of Mdm2*. *J. Biol. Chem.* **2007**, *282* (15), 10901–10907. https://doi.org/10.1074/jbc.m610879200.

(27) Itahana, K.; Mao, H.; Jin, A.; Itahana, Y.; Clegg, H. V; Lindström, M. S.; Bhat, K. P.; Godfrey, V. L.; Evan, G. I.; Zhang, Y. Targeted Inactivation of Mdm2 RING Finger E3 Ubiquitin Ligase Activity in the Mouse Reveals Mechanistic Insights into P53 Regulation. *Cancer Cell* **2007**, *12* (4), 355–366. https://doi.org/10.1016/j.ccr.2007.09.007.

(28) Li, J.; Kurokawa, M. Regulation of MDM2 Stability After DNA Damage. *J. Cell. Physiol.* **2015**, *230* (10), 2318–2327. https://doi.org/10.1002/jcp.24994.

(29) Liu, Y.; He, Y.; Jin, A.; Tikunov, A. P.; Zhou, L.; Tollini, L. A.; Leslie, P.; Kim, T.-H.; Li, L. O.; Coleman, R. A.; Gu, Z.; Chen, Y. Q.; Macdonald, J. M.; Graves, L. M.; Zhang, Y. Ribosomal Protein-Mdm2-P53 Pathway Coordinates Nutrient Stress with Lipid Metabolism by Regulating MCD and Promoting Fatty Acid Oxidation. *Proc. Natl. Acad. Sci. U. S. A.* **2014**, *111* (23), E2414–E2422. https://doi.org/10.1073/pnas.1315605111.

(30) Riley, M. F.; Lozano, G. The Many Faces of MDM2 Binding Partners. *Genes Cancer* **2012**, *3* (3–4), 226–239. https://doi.org/10.1177/1947601912455322.

(31) Kussie, P. H.; Gorina, S.; Marechal, V.; Elenbaas, B.; Moreau, J.; Levine, A. J.; Pavletich, N. P. Structure of the MDM2 Oncoprotein Bound to the P53 Tumor Suppressor Transactivation Domain. *Science (80-.).* **1996**, *274* (5289), 948–953. https://doi.org/10.1126/science.274.5289.948.

(32) Grasberger, B. L.; Lu, T.; Schubert, C.; Parks, D. J.; Carver, T. E.; Koblish, H. K.; Cummings, M. D.; LaFrance, L. V; Milkiewicz, K. L.; Calvo, R. R.; Maguire, D.; Lattanze, J.; Franks, C. F.; Zhao, S.; Ramachandren, K.; Bylebyl, G. R.; Zhang, M.; Manthey, C. L.; Petrella, E. C.; Pantoliano, M. W.; Deckman, I. C.; Spurlino, J. C.; Maroney, A. C.; Tomczuk, B. E.; Molloy, C. J.; Bone, R. F. Discovery and Cocrystal Structure of Benzodiazepinedione HDM2 Antagonists That Activate P53 in Cells. *J. Med. Chem.* **2005**, *48* (4), 909–912. https://doi.org/10.1021/jm049137g.

(33) Vassilev, L. T.; Vu, B. T.; Graves, B.; Carvajal, D.; Podlaski, F.; Filipovic, Z.; Kong, N.; Kammlott, U.; Lukacs, C.; Klein, C.; Fotouhi, N.; Liu, E. A. In Vivo Activation of the P53 Pathway by Small-Molecule Antagonists of MDM2. *Science (80-.).* **2004**, *303* (5659), 844–848. https://doi.org/10.1126/science.1092472.

(34) Zhang, X.-P.; Liu, F.; Wang, W. Two-Phase Dynamics of P53 in the DNA Damage Response. *Proc. Natl. Acad. Sci. U. S. A.* **2011**, *108* (22), 8990–8995. https://doi.org/10.1073/pnas.1100600108.

(35) Bálint E, E.; Vousden, K. H. Activation and Activities of the P53 Tumour Suppressor Protein. *Br. J. Cancer* **2001**, *85* (12), 1813–1823. https://doi.org/10.1054/bjoc.2001.2128.

(36) Harris, C. C.; Hollstein, M. Clinical Implications of the P53 Tumor-Suppressor Gene. *N. Engl. J. Med.* **1993**, *329* (18), 1318–1327. https://doi.org/10.1056/nejm199310283291807.

(37) Prives, C. How Loops, β Sheets, and α Helices Help Us to Understand P53. *Cell* **1994**, *78* (4), 543–546. https://doi.org/10.1016/0092-8674(94)90519-3.

(38) Lawrence, M. S.; Stojanov, P.; Mermel, C. H.; Robinson, J. T.; Garraway, L. A.; Golub, T. R.; Meyerson, M.; Gabriel, S. B.; Lander, E. S.; Getz, G. Discovery and Saturation Analysis of Cancer Genes across 21 Tumour Types. *Nature* **2014**, *505* (7484), 495–501. https://doi.org/10.1038/nature12912.

(39) Bouaoun, L.; Sonkin, D.; Ardin, M.; Hollstein, M.; Byrnes, G.; Zavadil, J.; Olivier, M. TP53Variations in Human Cancers: New Lessons from the IARC TP53 Database and Genomics Data. *Hum. Mutat.* **2016**, *37* (9), 865–876. https://doi.org/10.1002/humu.23035.

(40) Srivastava, S.; Zou, Z.; Pirollo, K.; Blattner, W.; Chang, E. H. Germ-Line Transmission of a Mutated P53 Gene in a Cancer-Prone Family with Li–Fraumeni Syndrome. *Nature* **1990**, *348* (6303), 747–749. https://doi.org/10.1038/348747a0.

(41) Joerger, A. C.; Fersht, A. R. Structure–Function–Rescue: The Diverse Nature of Common P53 Cancer Mutants. *Oncogene* **2007**, *26* (15), 2226–2242. https://doi.org/10.1038/sj.onc.1210291.

(42) Freed-Pastor, W. A.; Prives, C. Mutant P53: One Name, Many Proteins. *Genes Dev.* **2012**, *26* (12), 1268–1286. https://doi.org/10.1101/gad.190678.112.

(43) Vousden, K. H.; Lu, X. Live or Let Die: The Cell's Response to P53. *Nat. Rev. Cancer* **2002**, *2* (8), 594–604. https://doi.org/10.1038/nrc864.

(44) Harris, S. L.; Levine, A. J. The P53 Pathway: Positive and Negative Feedback Loops. *Oncogene*. April 18, 2005, pp 2899–2908.

https://doi.org/10.1038/sj.onc.1208615.

(45) Shangary, S.; Wang, S. Small-Molecule Inhibitors of the MDM2-P53 Protein-Protein Interaction to Reactivate P53 Function: A Novel Approach for Cancer Therapy. *Annual Review of Pharmacology and Toxicology*. 2009, pp 223–241. https://doi.org/10.1146/annurev.pharmtox.48.113006.094723.

(46) Cordon-Cardo, C.; Latres, E.; Drobnjak, M.; Oliva, M. R.; Pollack, D.; Woodruff, J. M.; Marechal, V.; Chen, J.; Brennan, M. F.; Levine, A. J. Molecular Abnormalities of Mdm2 and P53 Genes in Adult Soft Tissue Sarcomas. *Cancer Res.* **1994**, *54* (3), 794–799.

(47) Clackson, T.; Wells, J. A Hot Spot of Binding Energy in a Hormone-Receptor Interface. *Science (80-.).* **1995**, *267* (5196), 383–386. https://doi.org/10.1126/science.7529940.

(48) Capoulade, C.; Paillerets, B. B.; Lefrère, I.; Ronsin, M.; Feunteun, J.; Tursz, T.; Wiels, J. Overexpression of MDM2, Due to Enhanced Translation, Results in Inactivation of Wild-Type P53 in Burkitt's Lymphoma Cells. *Oncogene* **1998**, *16* (12), 1603–1610. https://doi.org/10.1038/sj.onc.1201702.

(49) Vassilev, L. T.; Vu, B. T.; Graves, B.; Carvajal, D.; Podlaski, F.; Filipovic, Z.; Kong, N.; Kammlott, U.; Lukacs, C.; Klein, C.; Fotouhi, N.; Liu, E. A. In Vivo Activation of the P53 Pathway by Small-Molecule Antagonists of MDM2. *Science (80-.).* **2004**, *303* (5659), 844–848. https://doi.org/10.1126/science.1092472.

(50) Westwell, A. D. Inhibitors of the Hdm2:P53 Complex as Antitumour Agents. *Drug Discov. Today* **2006**, *11* (7–8), 371. https://doi.org/10.1016/j.drudis.2006.02.013.

(51) LaRusch, G. A.; Jackson, M. W.; Dunbar, J. D.; Warren, R. S.; Donner, D. B.; Mayo, L. D. Nutlin3 Blocks Vascular Endothelial Growth Factor Induction by Preventing the Interaction between Hypoxia Inducible Factor 1α and Hdm2. *Cancer Res.* **2007**, *67* (2), 450–454. https://doi.org/10.1158/0008-5472.can-06-2710.

(52) Wang, Z.; Jonca, M.; Lambros, T.; Ferguson, S.; Goodnow, R. Exploration of Liquid and Supercritical Fluid Chromatographic Chiral Separation and Purification of Nutlin-3—A Small Molecule Antagonist of MDM2. *J. Pharm. Biomed. Anal.* **2007**, *45* (5), 720–729. https://doi.org/10.1016/j.jpba.2007.08.013.

(53) Joerger, A. C.; Fersht, A. R. The P53 Pathway: Origins, Inactivation in Cancer, and Emerging Therapeutic Approaches. *Annu. Rev. Biochem.* **2016**, *85* (1), 375–404. https://doi.org/10.1146/annurev-biochem-060815-014710.

(54) Antonchick, A. P.; Gerding-Reimers, C.; Catarinella, M.; Schürmann, M.; Preut, H.; Ziegler, S.; Rauh, D.; Waldmann, H. Highly Enantioselective Synthesis and Cellular Evaluation of Spirooxindoles Inspired by Natural Products. *Nat. Chem.* **2010**, *2* (9), 735–740. https://doi.org/10.1038/nchem.730.

(55) Banholzer, A. Wo 2008/034736 A2 (74). **2008**, *2008* (March).

(56) Ding, K.; Lu, Y.; Nikolovska-Coleska, Z.; Wang, G.; Qiu, S.; Shangary, S.; Gao, W.; Qin, D.; Stuckey, J.; Krajewski, K.; Roller, P. P.; Wang, S. Structure-Based Design of Spiro-Oxindoles as Potent, Specific Small-Molecule Inhibitors of the MDM2−p53 Interaction. *J. Med. Chem.* **2006**, *49* (12), 3432–3435. https://doi.org/10.1021/jm051122a.

(57) Design, synthesis, and evaluation of novel boronic-chalcone derivatives as antitumor agents - PubMed https://pubmed.ncbi.nlm.nih.gov/12825923/ (accessed Apr 12, 2021).

(58) Cummings, M. D.; Schubert, C.; Parks, D. J.; Calvo, R. R.; LaFrance, L. V; Lattanze, J.; Milkiewicz, K. L.; Lu, T. Substituted 1,4-Benzodiazepine-2,5-Diones as Alpha-Helix Mimetic Antagonists of the HDM2-P53 Protein-Protein Interaction. *Chem. Biol. <html_ent glyph="@amp;" ascii="&"/> Drug Des.* **2006**, *67* (3), 201–205. https://doi.org/10.1111/j.1747-0285.2006.00365.x.

(59) Raboisson, P.; Marugán, J. J.; Schubert, C.; Koblish, H. K.; Lu, T.; Zhao, S.; Player, M. R.; Maroney, A. C.; Reed, R. L.; Huebert, N. D.; Lattanze, J.; Parks, D. J.; Cummings, M. D. Structure-Based Design, Synthesis, and Biological Evaluation of Novel 1,4-Diazepines as HDM2 Antagonists. *Bioorg. Med. Chem. Lett.* **2005**, *15* (7), 1857–1861. https://doi.org/10.1016/j.bmcl.2005.02.018.

(60) Galatin, P. S.; Abraham, D. J. A Nonpeptidic Sulfonamide Inhibits the P53-Mdm2 Interaction and Activates P53-Dependent Transcription in Mdm2-Overexpressing Cells. *J. Med. Chem.* **2004**, *47* (17), 4163–4165. https://doi.org/10.1021/jm034182u.

(61) Sun, D.; Li, Z.; Rew, Y.; Gribble, M.; Bartberger, M. D.; Beck, H. P.; Canon, J.; Chen, A.; Chen, X.; Chow, D.; Deignan, J.; Duquette, J.; Eksterowicz, J.; Fisher, B.; Fox, B. M.; Fu, J.; Gonzalez, A. Z.; Gonzalez-Lopez De Turiso, F.; Houze, J. B.; Huang, X.; Jiang, M.; Jin, L.; Kayser, F.; Liu, J.; Lo, M. C.; Long, A. M.; Lucas, B.; McGee, L. R.; McIntosh, J.; Mihalic, J.; Oliner, J. D.; Osgood, T.; Peterson, M. L.; Roveto, P.; Saiki, A. Y.; Shaffer, P.; Toteva, M.; Wang, Y.; Wang, Y. C.; Wortman, S.; Yakowec, P.; Yan, X.; Ye, Q.; Yu, D.; Yu, M.; Zhao, X.; Zhou, J.; Zhu, J.; Olson, S. H.; Medina, J. C. Discovery of AMG 232, a Potent, Selective, and Orally Bioavailable MDM2-P53 Inhibitor in Clinical Development. *J. Med. Chem.* **2014**, *57* (4), 1454–1472. https://doi.org/10.1021/jm401753e.

(62) Gonzalez-Lopez de Turiso, F.; Sun, D.; Rew, Y.; Bartberger, M. D.; Beck, H. P.; Canon, J.; Chen, A.; Chow, D.; Correll, T. L.; Huang, X.; Julian, L. D.; Kayser, F.; Lo, M.-C.; Long, A. M.; McMinn, D.; Oliner, J. D.; Osgood, T.; Powers, J. P.; Saiki, A. Y.; Schneider, S.; Shaffer, P.; Xiao, S.-H.; Yakowec, P.; Yan, X.; Ye, Q.; Yu, D.; Zhao, X.; Zhou, J.; Medina, J. C.; Olson, S. H. Rational Design and Binding Mode Duality of MDM2–P53 Inhibitors. *J. Med. Chem.* **2013**, *56* (10), 4053–4070. https://doi.org/10.1021/jm400293z.

(63) Gonzalez, A. Z.; Eksterowicz, J.; Bartberger, M. D.; Beck, H. P.; Canon, J.; Chen, A.; Chow, D.; Duquette, J.; Fox, B. M.; Fu, J.; Huang, X.; Houze, J. B.; Jin, L.; Li, Y.; Li, Z.; Ling, Y.; Lo, M. C.; Long, A. M.; McGee, L. R.; McIntosh, J.; McMinn, D. L.; Oliner, J. D.; Osgood, T.; Rew, Y.; Saiki, A. Y.; Shaffer, P.; Wortman, S.; Yakowec, P.; Yan, X.; Ye, Q.; Yu, D.; Zhao, X.; Zhou, J.; Olson, S. H.; Medina, J. C.; Sun, D. Selective and Potent Morpholinone Inhibitors of the MDM2-P53 Protein-Protein Interaction. *J. Med. Chem.* **2014**, *57* (6), 2472–2488. https://doi.org/10.1021/jm401767k.

(64) Rew, Y.; Sun, D.; Gonzalez-Lopez De Turiso, F.; Bartberger, M. D.; Beck, H. P.;

Canon, J.; Chen, A.; Chow, D.; Deignan, J.; Fox, B. M.; Gustin, D.; Huang, X.; Jiang, M.; Jiao, X.; Jin, L.; Kayser, F.; Kopecky, D. J.; Li, Y.; Lo, M. C.; Long, A. M.; Michelsen, K.; Oliner, J. D.; Osgood, T.; Ragains, M.; Saiki, A. Y.; Schneider, S.; Toteva, M.; Yakowec, P.; Yan, X.; Ye, Q.; Yu, D.; Zhao, X.; Zhou, J.; Medina, J. C.; Olson, S. H. Structure-Based Design of Novel Inhibitors of the MDM2-P53 Interaction. *J. Med. Chem.* **2012**, *55* (11), 4936–4954. https://doi.org/10.1021/jm300354j.

(65) Gonzalez, A. Z.; Eksterowicz, J.; Bartberger, M. D.; Beck, H. P.; Canon, J.; Chen, A.; Chow, D.; Duquette, J.; Fox, B. M.; Fu, J.; Huang, X.; Houze, J. B.; Jin, L.; Li, Y.; Li, Z.; Ling, Y.; Lo, M. C.; Long, A. M.; McGee, L. R.; McIntosh, J.; McMinn, D. L.; Oliner, J. D.; Osgood, T.; Rew, Y.; Saiki, A. Y.; Shaffer, P.; Wortman, S.; Yakowec, P.; Yan, X.; Ye, Q.; Yu, D.; Zhao, X.; Zhou, J.; Olson, S. H.; Medina, J. C.; Sun, D. Selective and Potent Morpholinone Inhibitors of the MDM2-P53 Protein-Protein Interaction. *J. Med. Chem.* **2014**, *57* (6), 2472–2488. https://doi.org/10.1021/jm401767k.

(66) Subject Index for Volumes 1 and 2. *Handbooks of Management Accounting Research*. Elsevier 2006, pp 1185–1204. https://doi.org/10.1016/s1751-3243(06)02029-3.

(67) Pattenden, G. Professor Gerald Pattenden. *J. Chem. Soc. Perkin Trans. 1* **2000**, No. 6, ix–x. https://doi.org/10.1039/b001289k.

.

APPENDIX A

^{1}H NMR AND ^{13}C NMR SPECTRUM OF THE COMPOUNDS

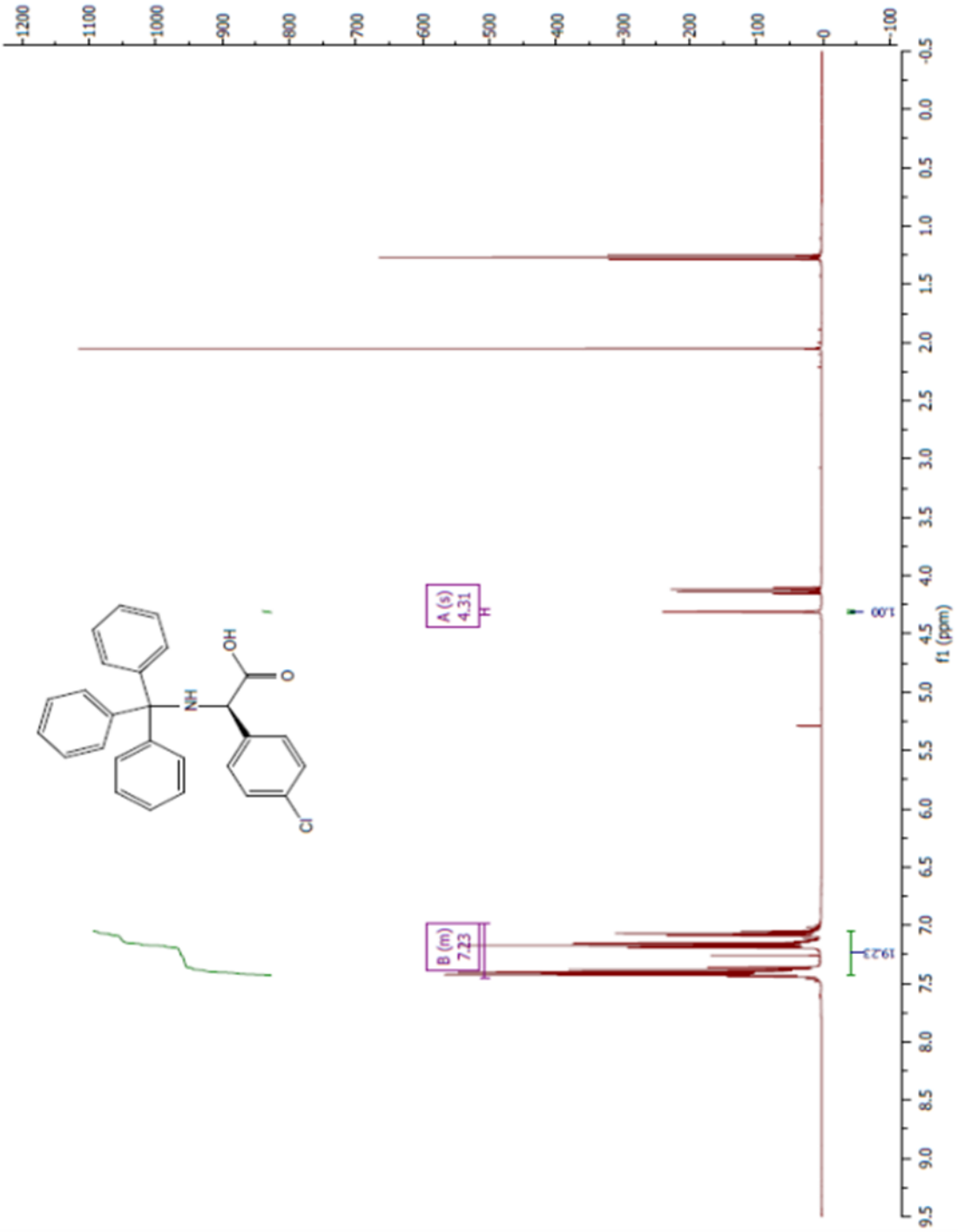

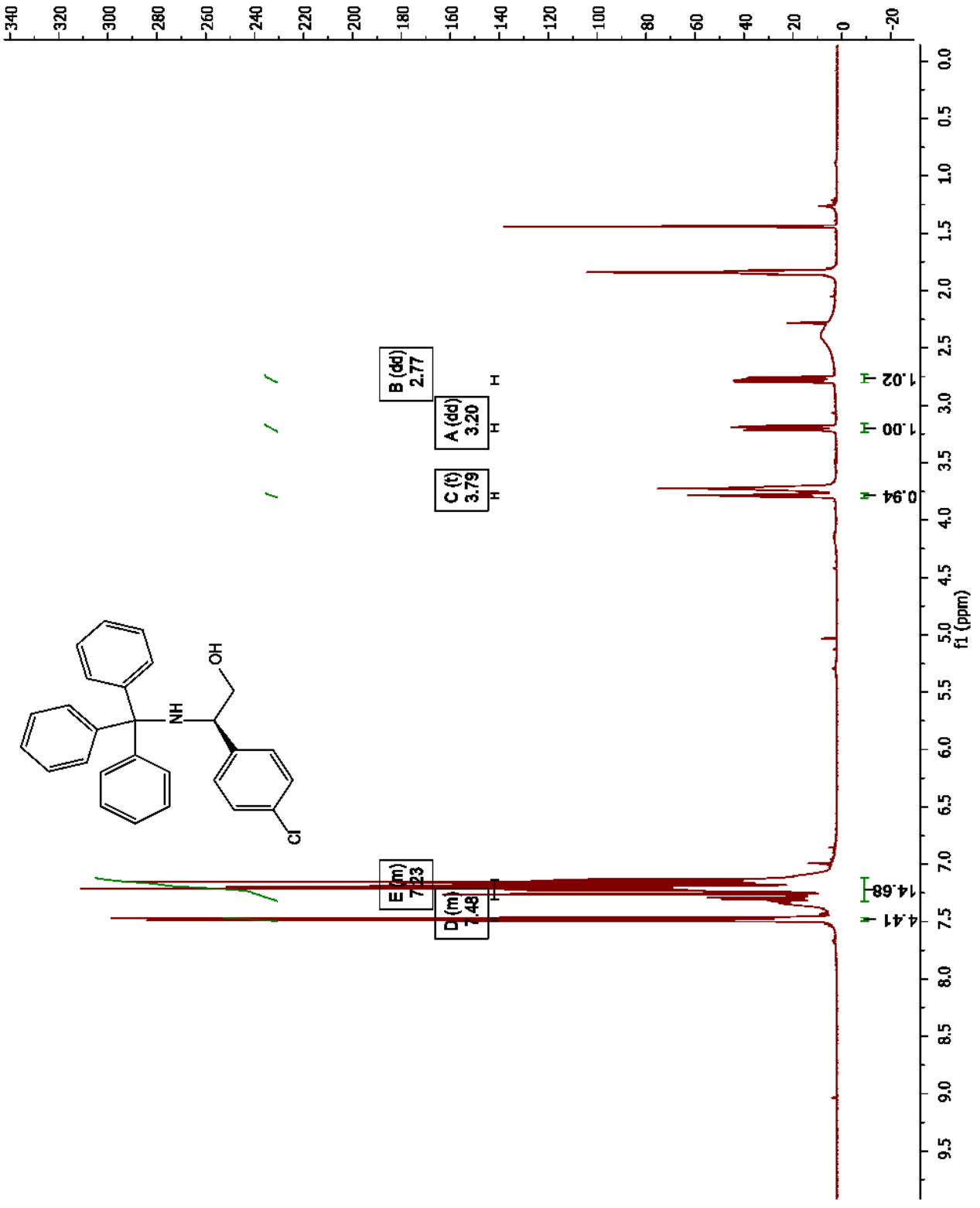
B (dd)
2.77
A (dd)
3.20
C (t)
3.79
E (m)
7.23
D (m)
7.48
1.02
1.00
0.94
14.68
4.41
NH
OH
Cl
f1 (ppm)

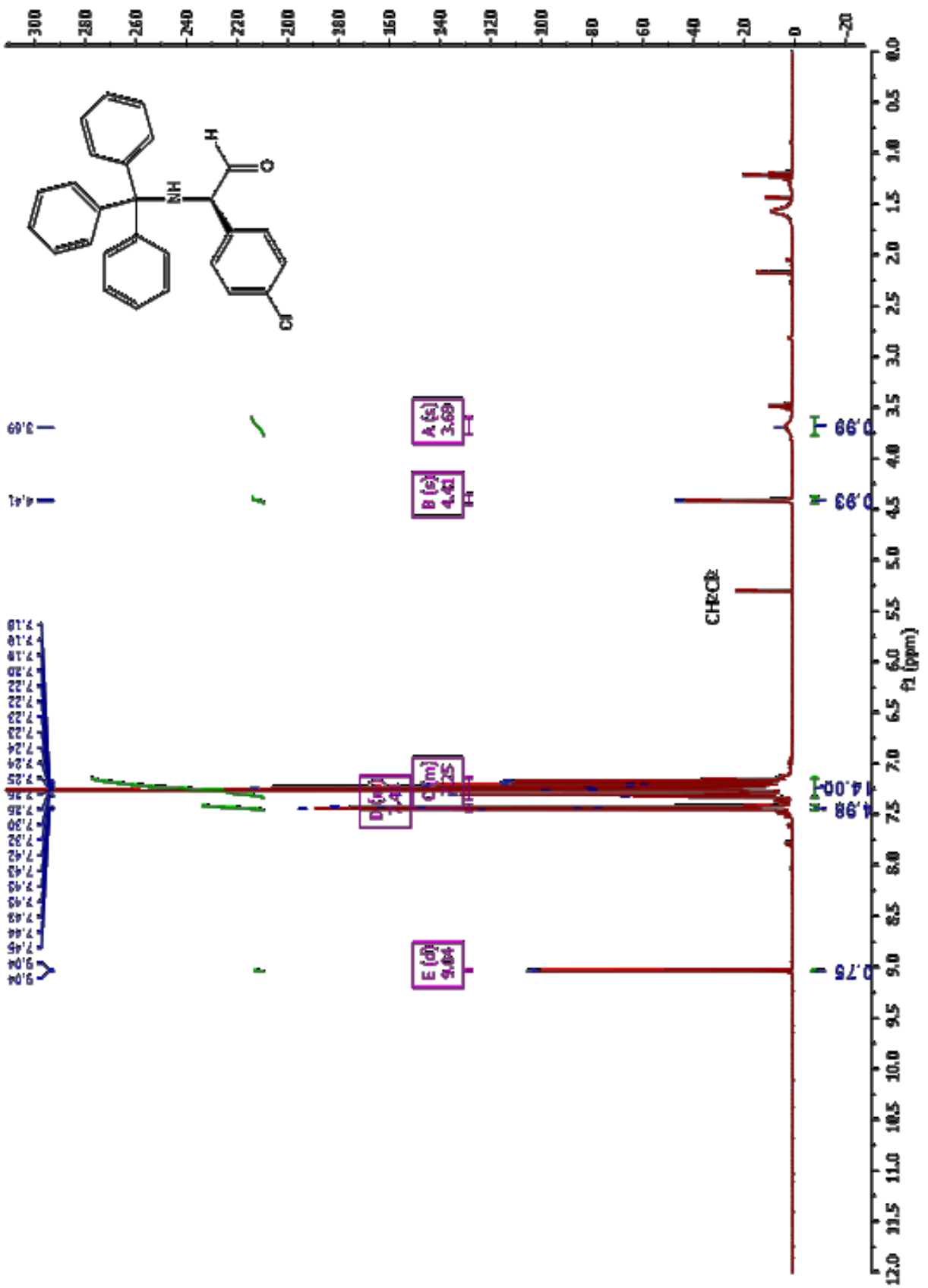
CH2Cl2
f1 (ppm)

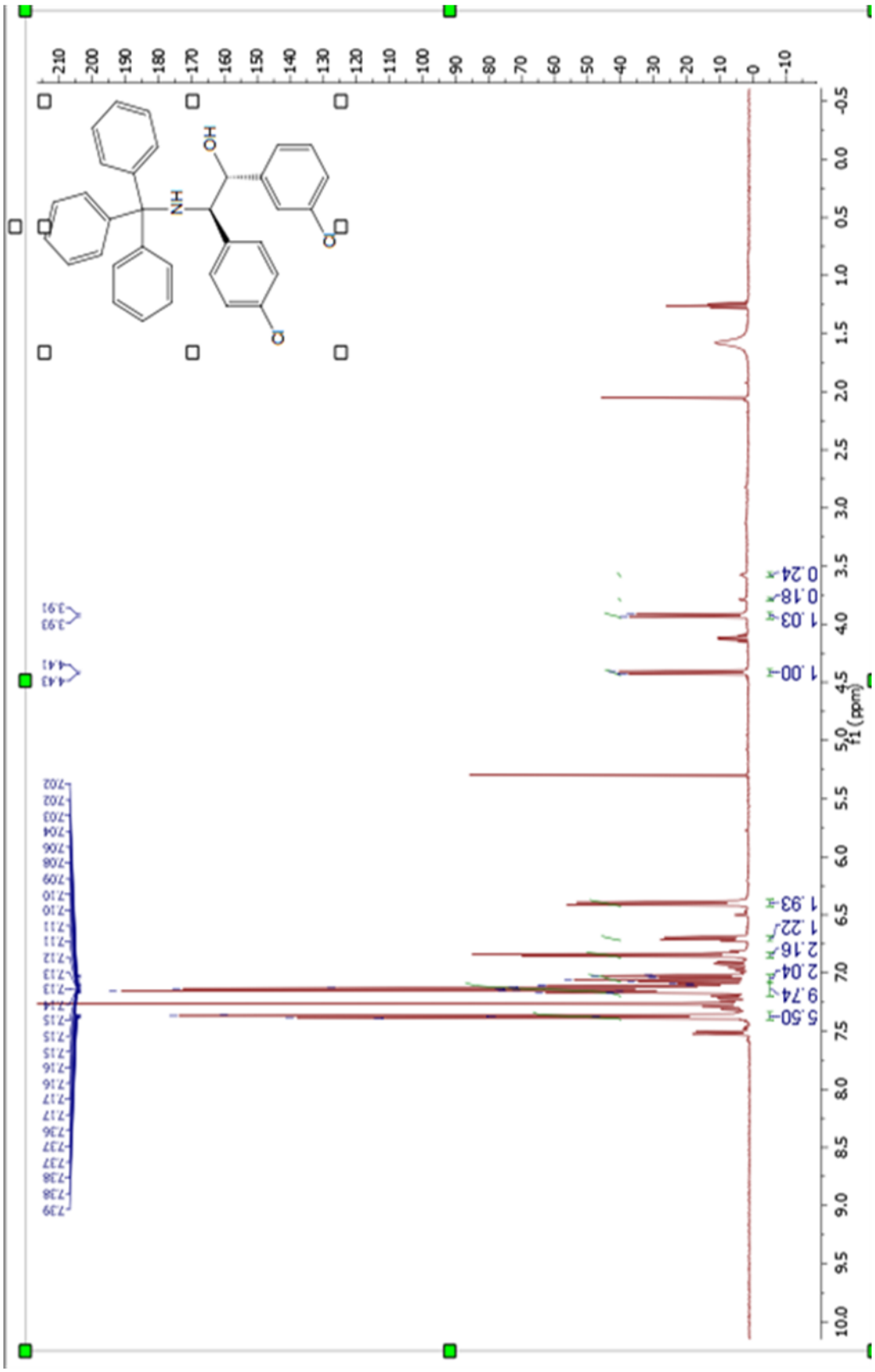
OH
NH
Cl
Cl
f1 (ppm)
5.50
9.74
2.04
2.16
1.22
1.93
1.00
1.03
0.18
0.24

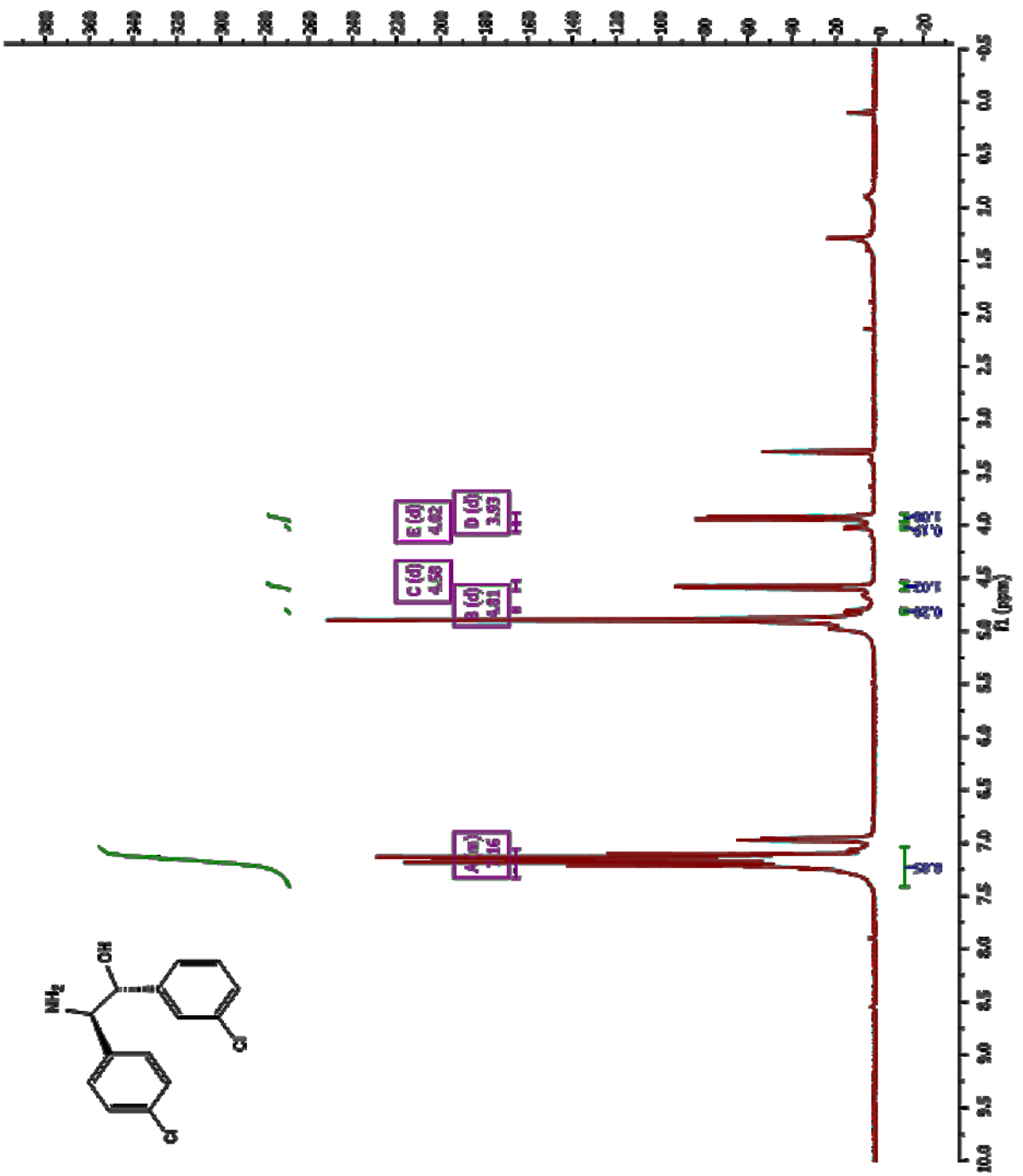
E (d) 4.82
D (d) 3.93
C (d) 4.58
B (d) 4.81
A (m) 7.15
f1 (ppm)

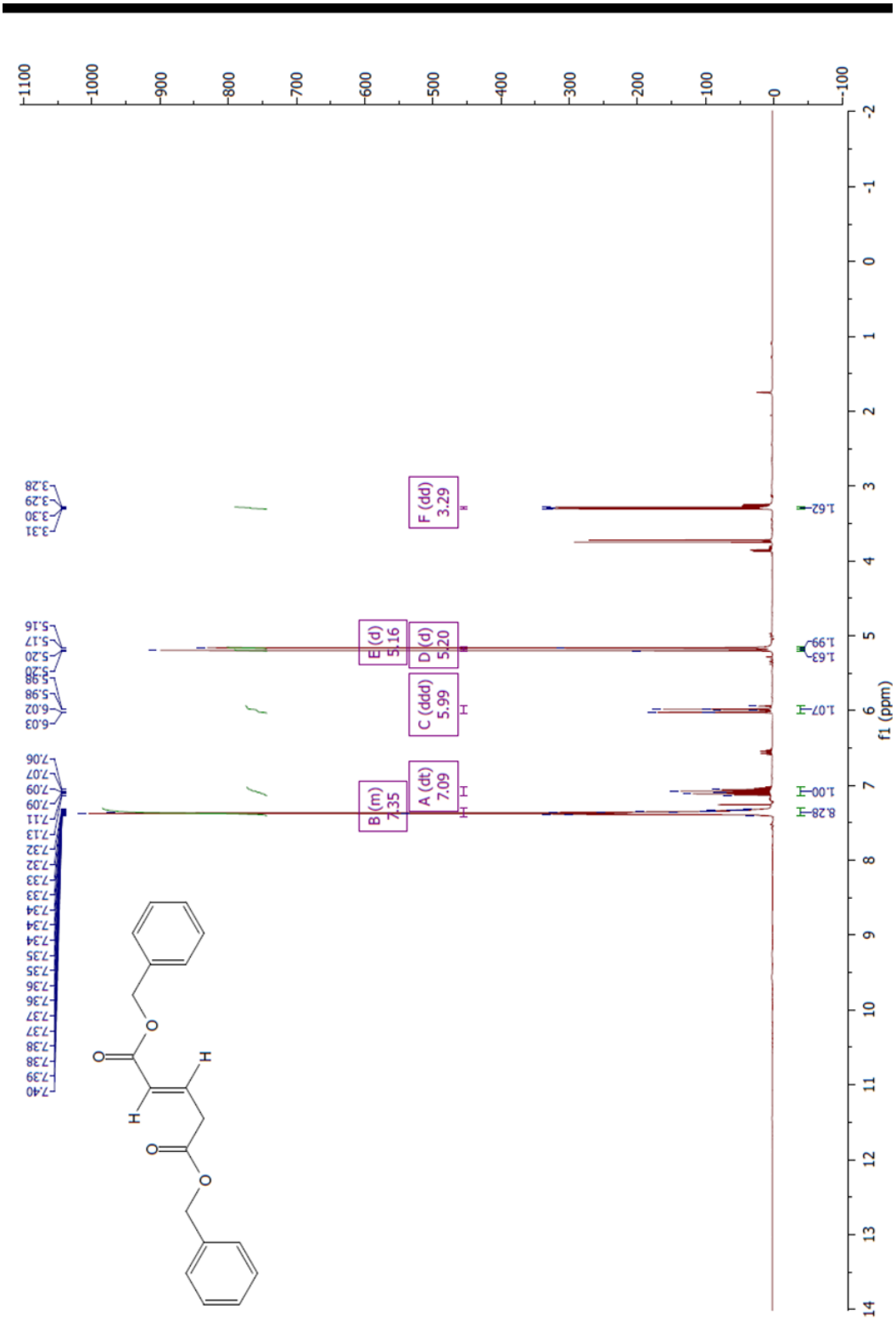
F (dd) 3.29
E (d) 5.16
D (d) 5.20
C (ddd) 5.99
A (dt) 7.09
B (m) 7.35
f1 (ppm)

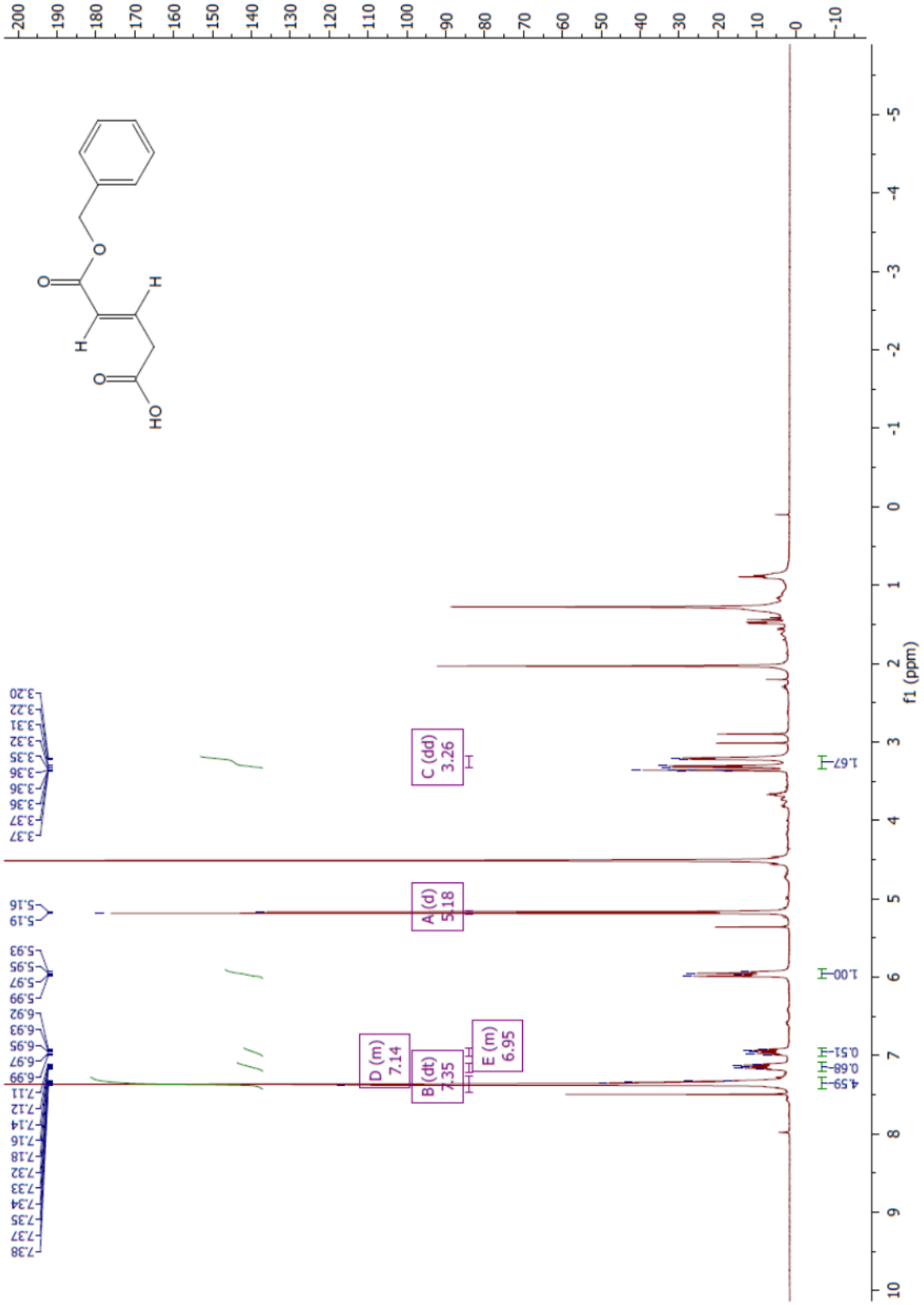
O
O
H
H
O
HO
C (dd)
3.26
A (d)
5.18
D (m)
7.14
B (dt)
7.35
E (m)
6.95
1.67
1.00
0.51
0.68
4.59
f1 (ppm)

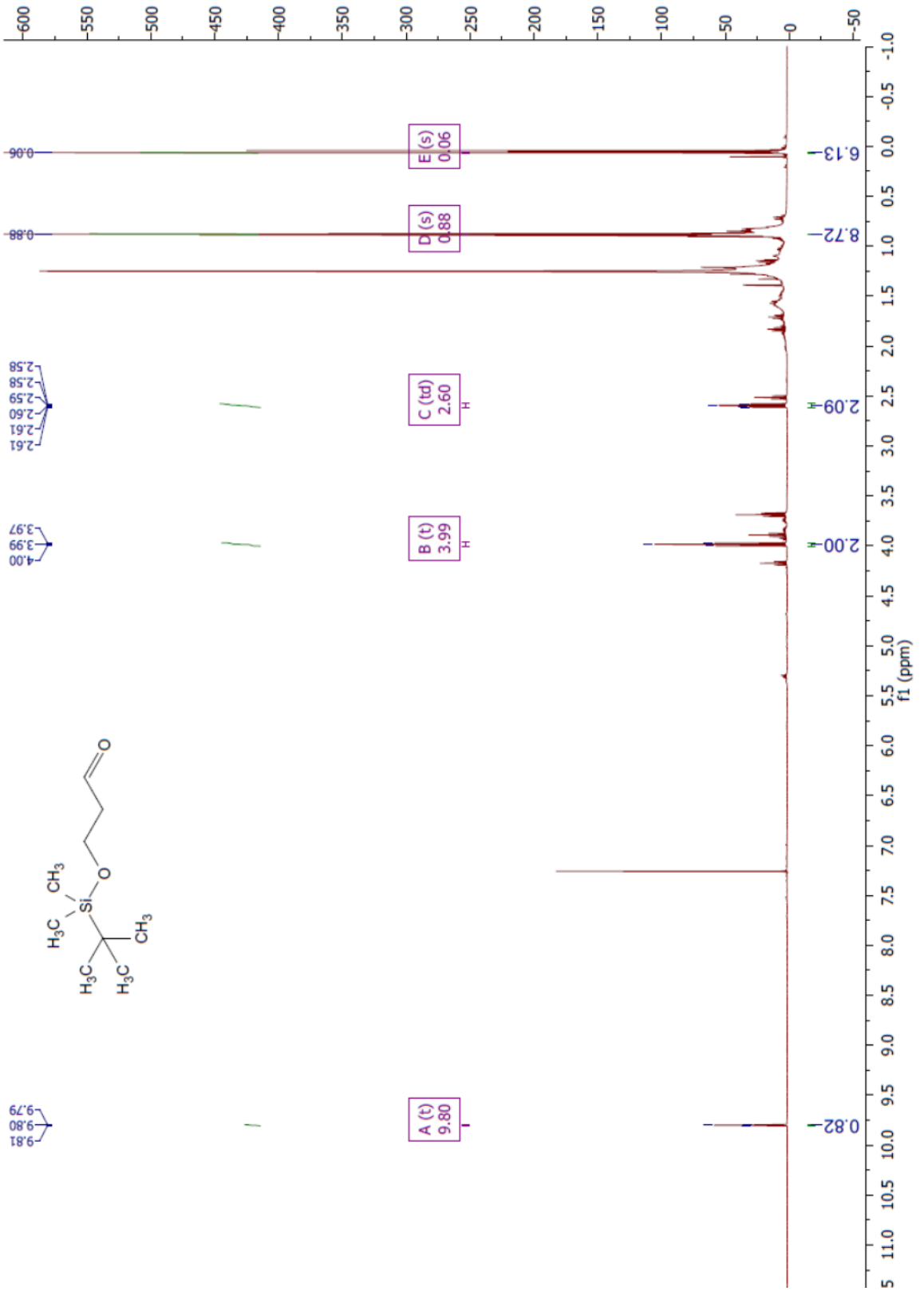
A (t) 9.80 1
B (t) 3.99 H
C (td) 2.60 H
D (s) 0.88
E (s) 0.06
f1 (ppm)

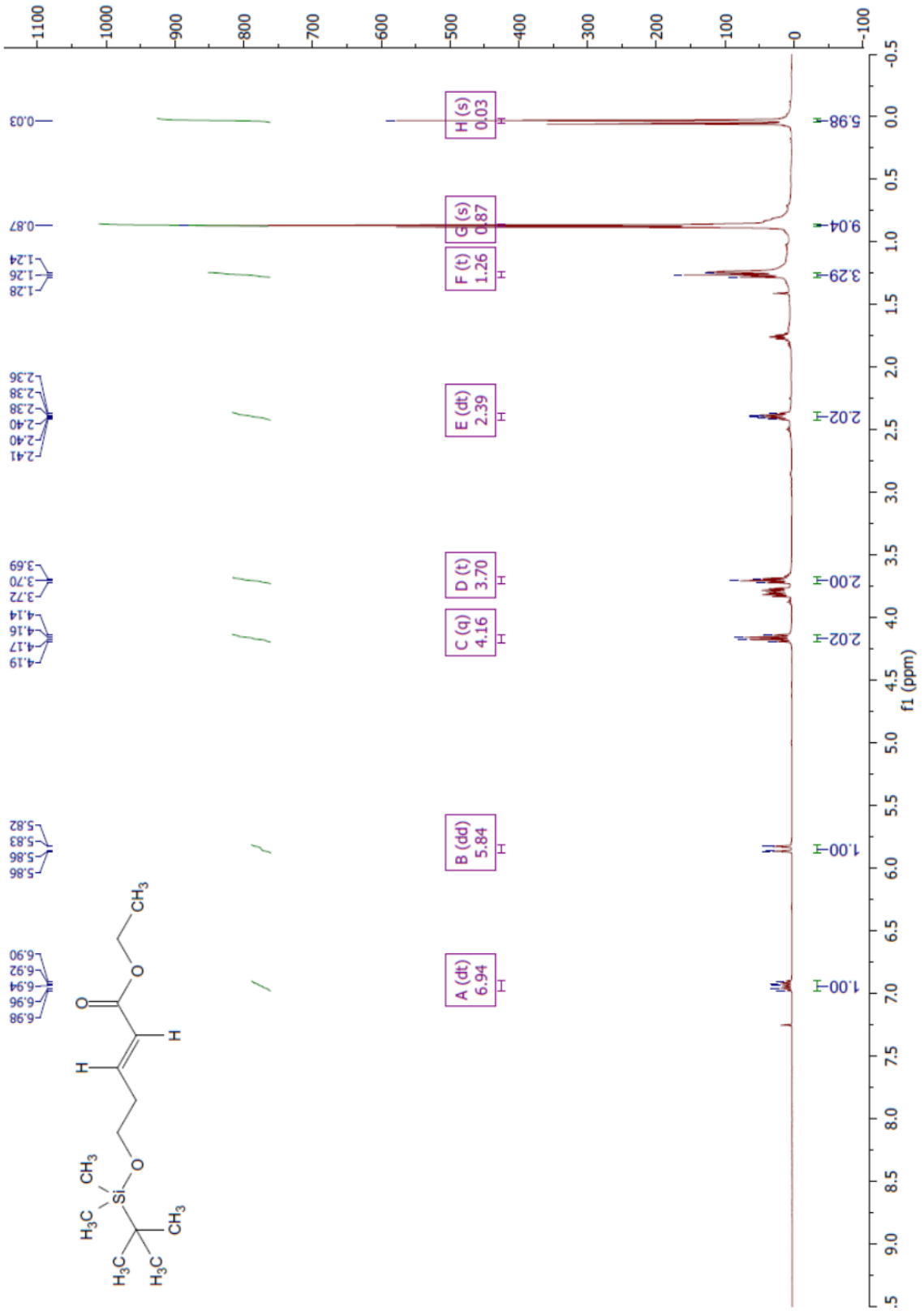
A (dt) 6.94
B (dd) 5.84
C (q) 4.16
D (t) 3.70
E (dt) 2.39
F (t) 1.26
G (s) 0.87
H (s) 0.03
f1 (ppm)

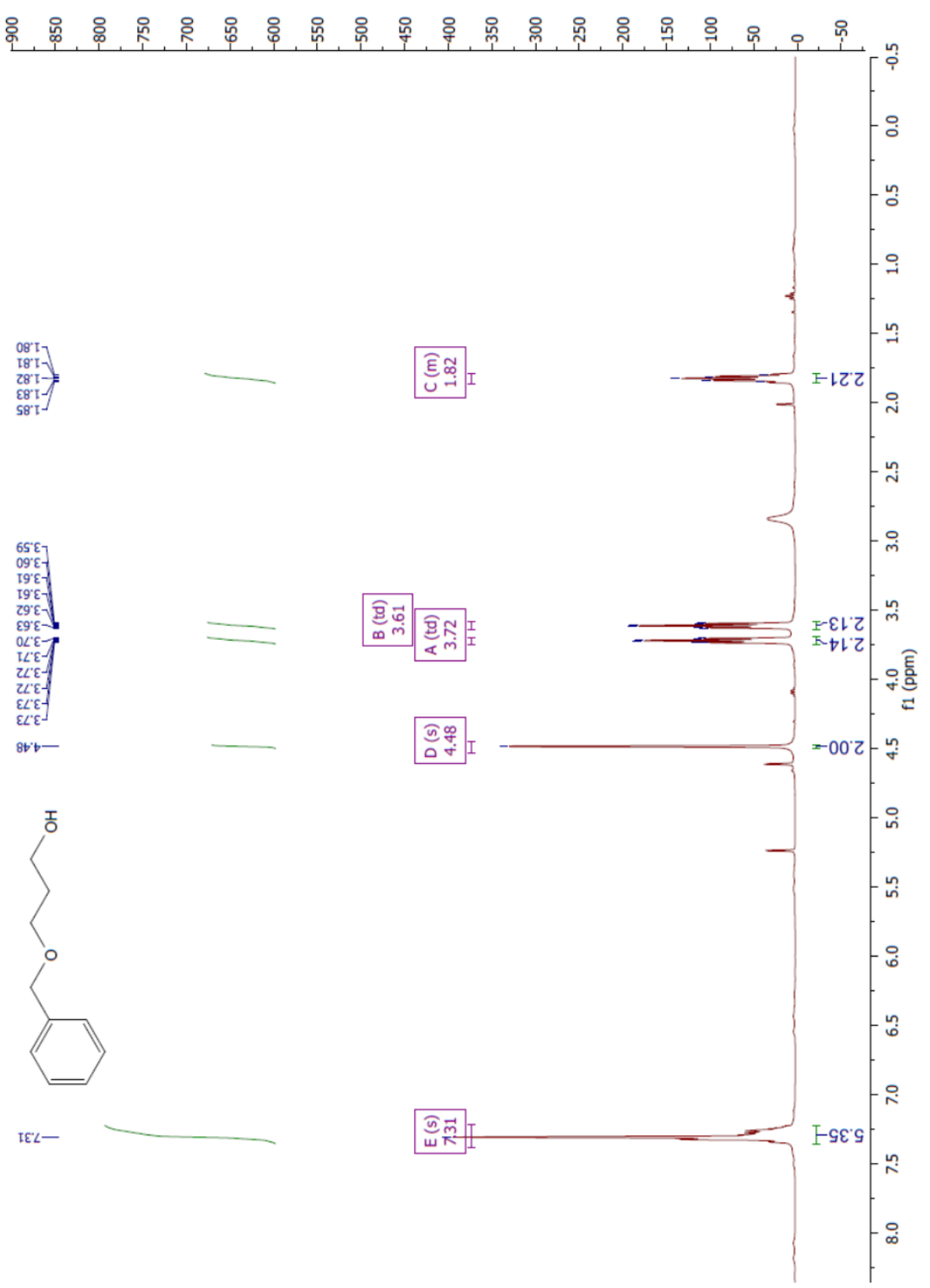
OH
O
7.31
4.48
3.73
3.72
3.72
3.72
3.71
3.70
3.63
3.62
3.61
3.61
3.60
3.59
1.85
1.83
1.82
1.81
1.80
E (s) 7.31
D (s) 4.48
B (td) 3.61
A (td) 3.72
C (m) 1.82
5.35
2.00
2.13
2.14
2.21
f1 (ppm)

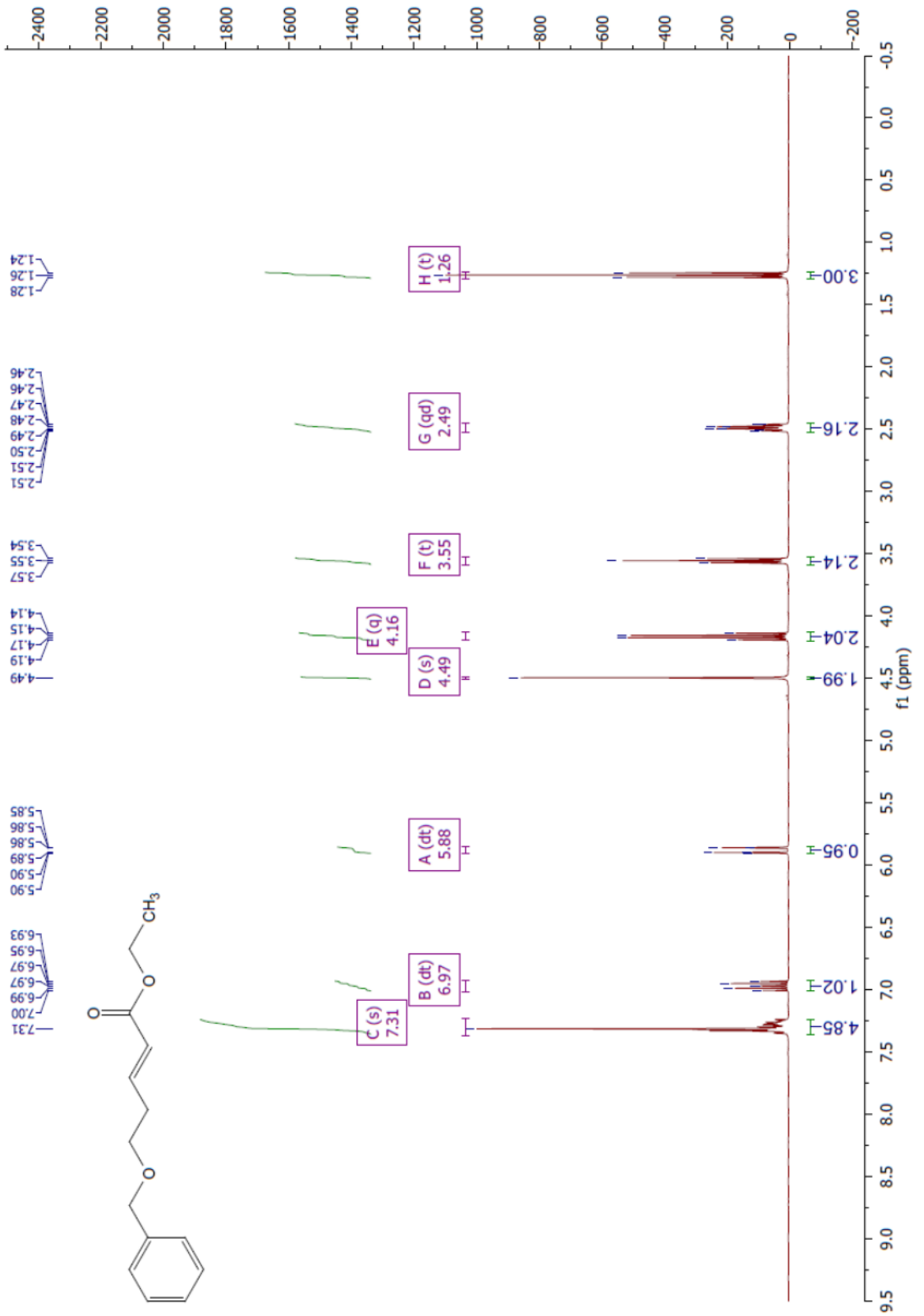
H (t) 1.26
G (qd) 2.49
F (t) 3.55
E (q) 4.16
D (s) 4.49
C (s) 7.31
B (dt) 6.97
A (dt) 5.88
3.00
2.16
2.14
2.04
1.99
0.95
1.02
4.85
f1 (ppm)

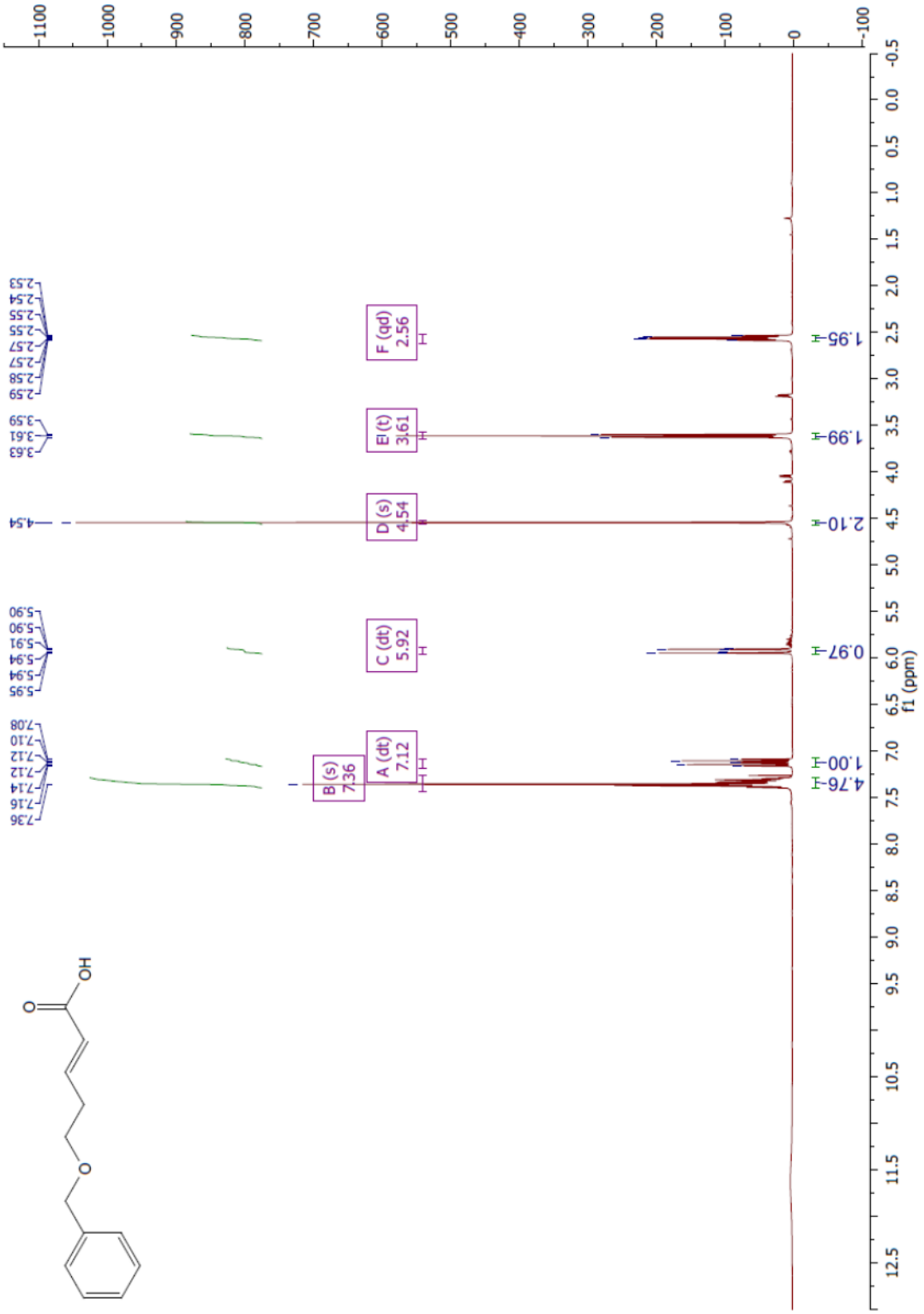
F (qd) 2.56
El (t) 3.61
D (s) 4.54
C (dt) 5.92
B (s) 7.36
A (dt) 7.12
1.95
1.99
2.10
0.97
1.00
4.76
f1 (ppm)
O
OH
O

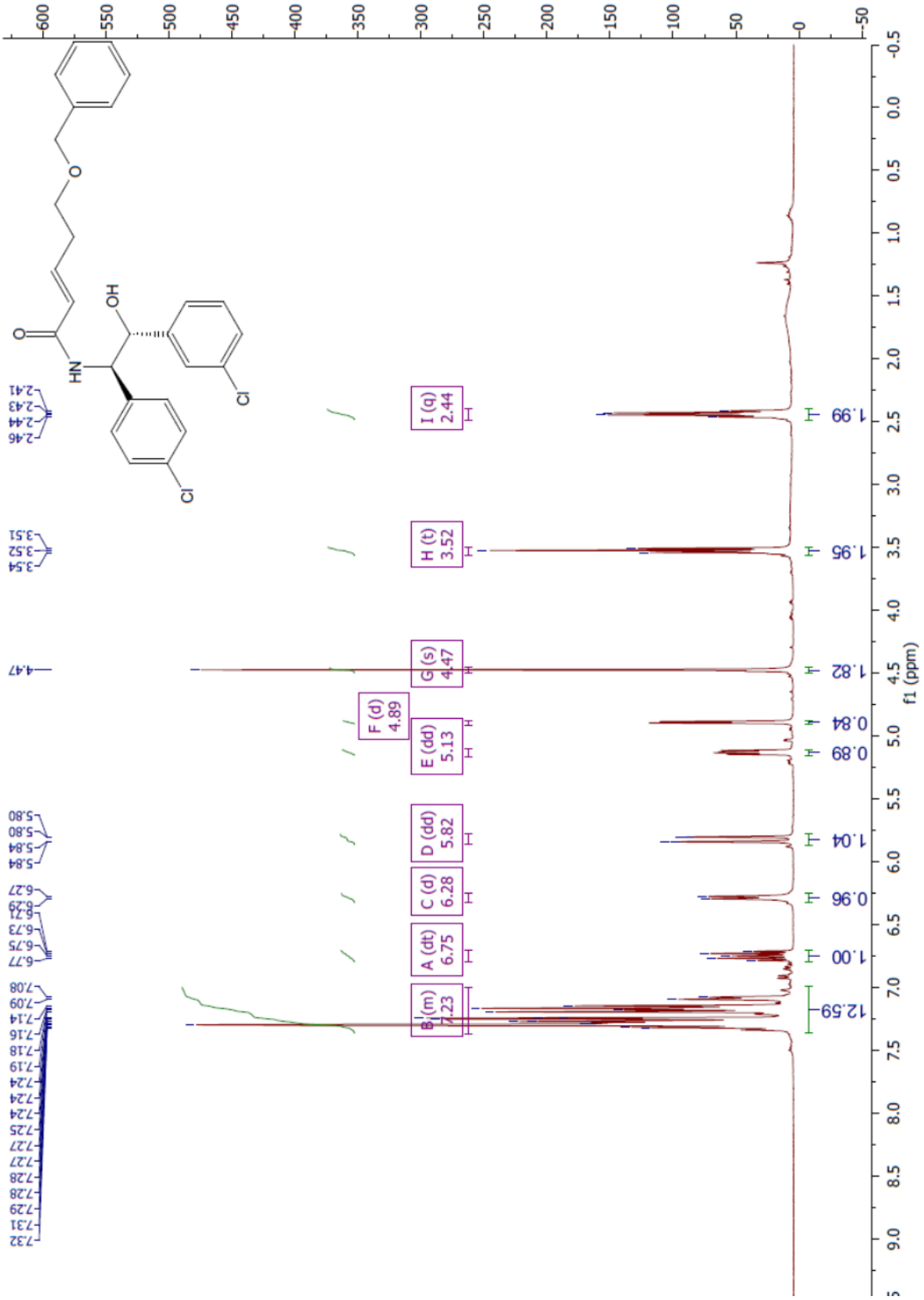
O
HN
OH
Cl
Cl
B (m) 7.23
A (dt) 6.75
C (d) 6.28
D (dd) 5.82
E (dd) 5.13
F (d) 4.89
G (s) 4.47
H (t) 3.52
I (q) 2.44
12.59
1.00
0.96
1.04
0.84
0.89
1.82
1.95
1.99
f1 (ppm)

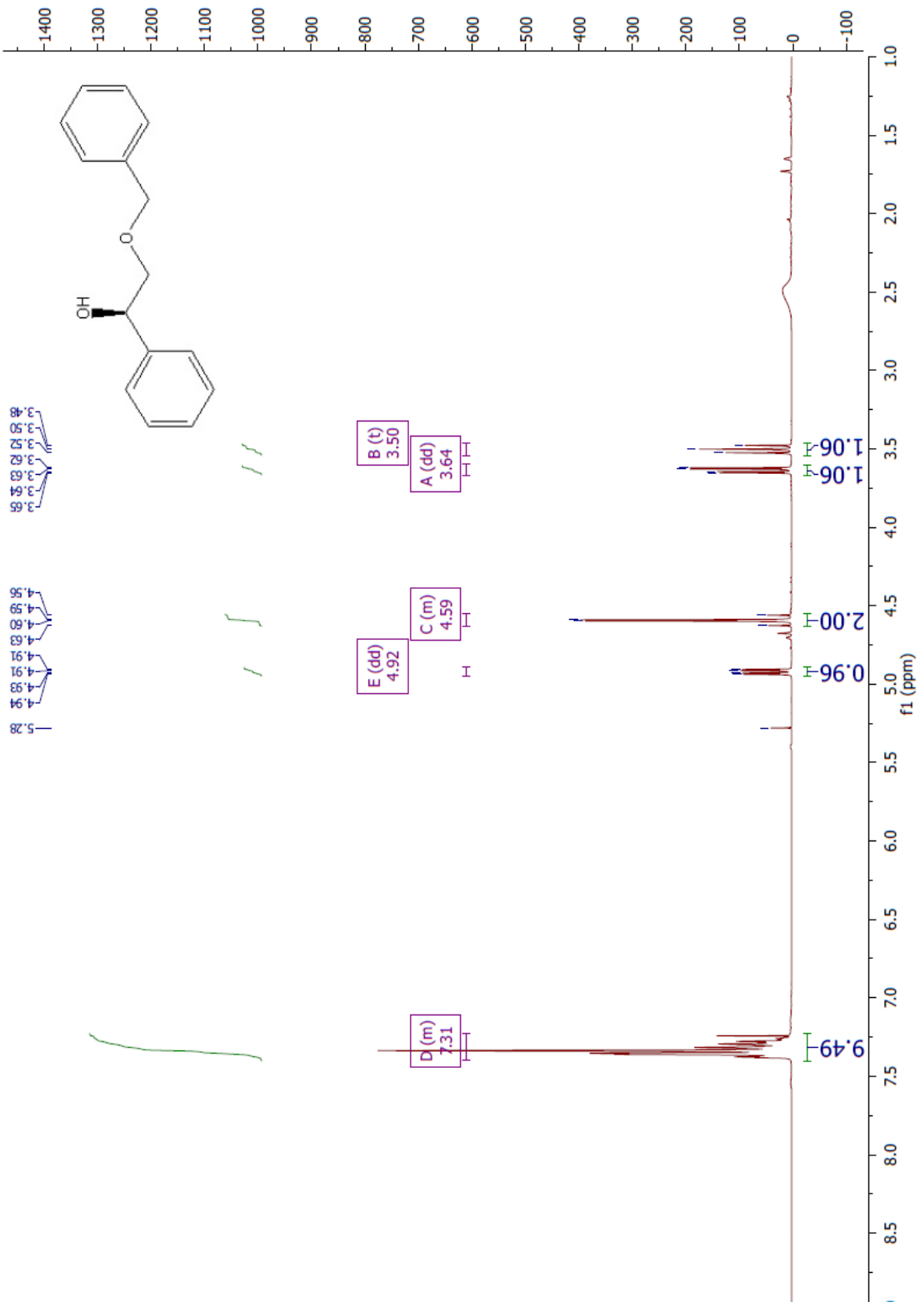
D (m)
7.31
E (dd)
4.92
C (m)
4.59
B (t)
3.50
A (dd)
3.64
9.49
2.00
0.96
1.06
1.06
f1 (ppm)

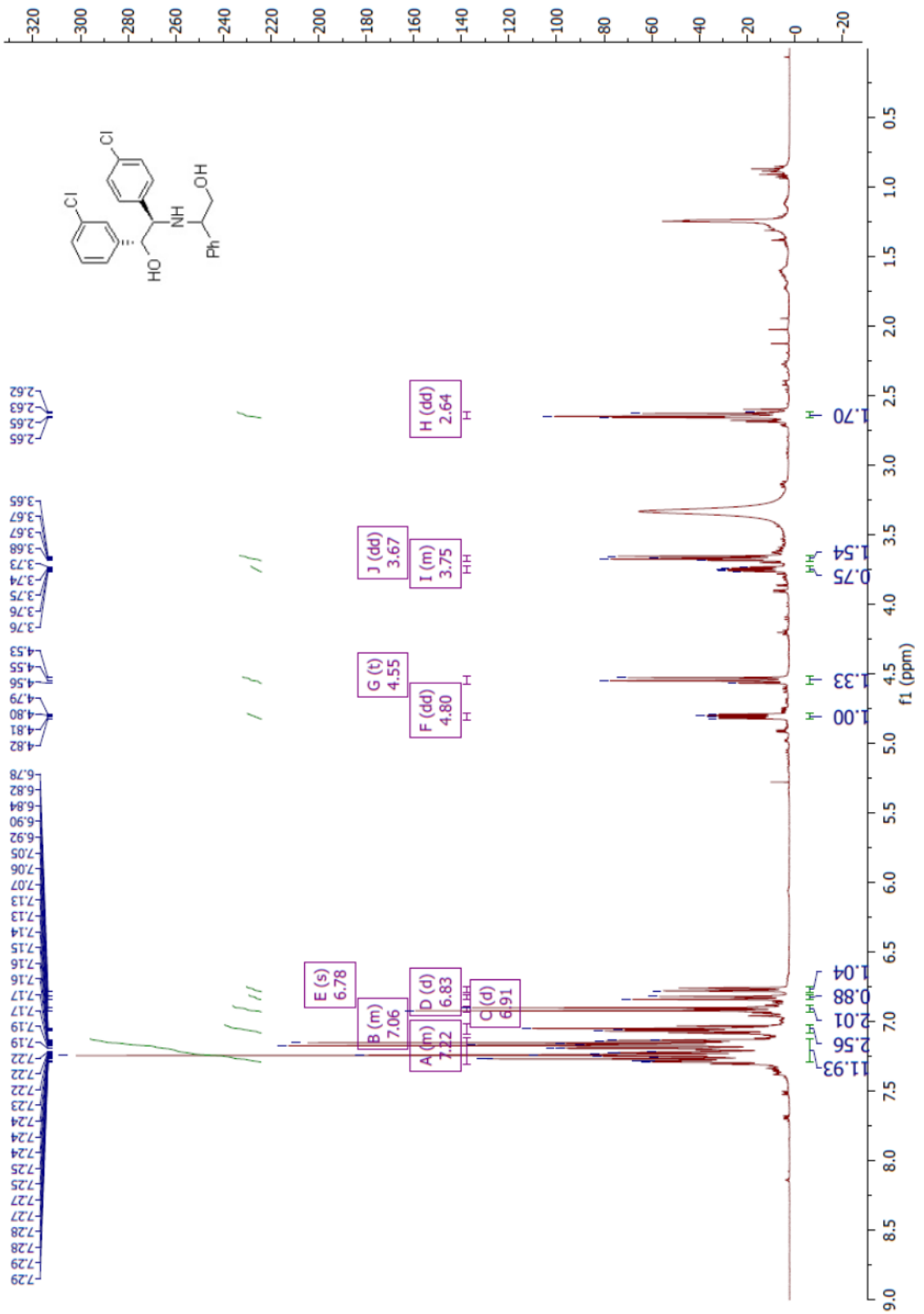
Cl
Cl
OH
NH
Ph
HO
A (m) 7.22
B (m) 7.06
C (d) 6.91
D (d) 6.83
E (s) 6.78
F (dd) 4.80
G (t) 4.55
H (dd) 2.64
I (m) 3.75
J (dd) 3.67
11.93
2.56
2.01
0.88
1.04
1.00
1.33
0.75
1.54
1.70
f1 (ppm)

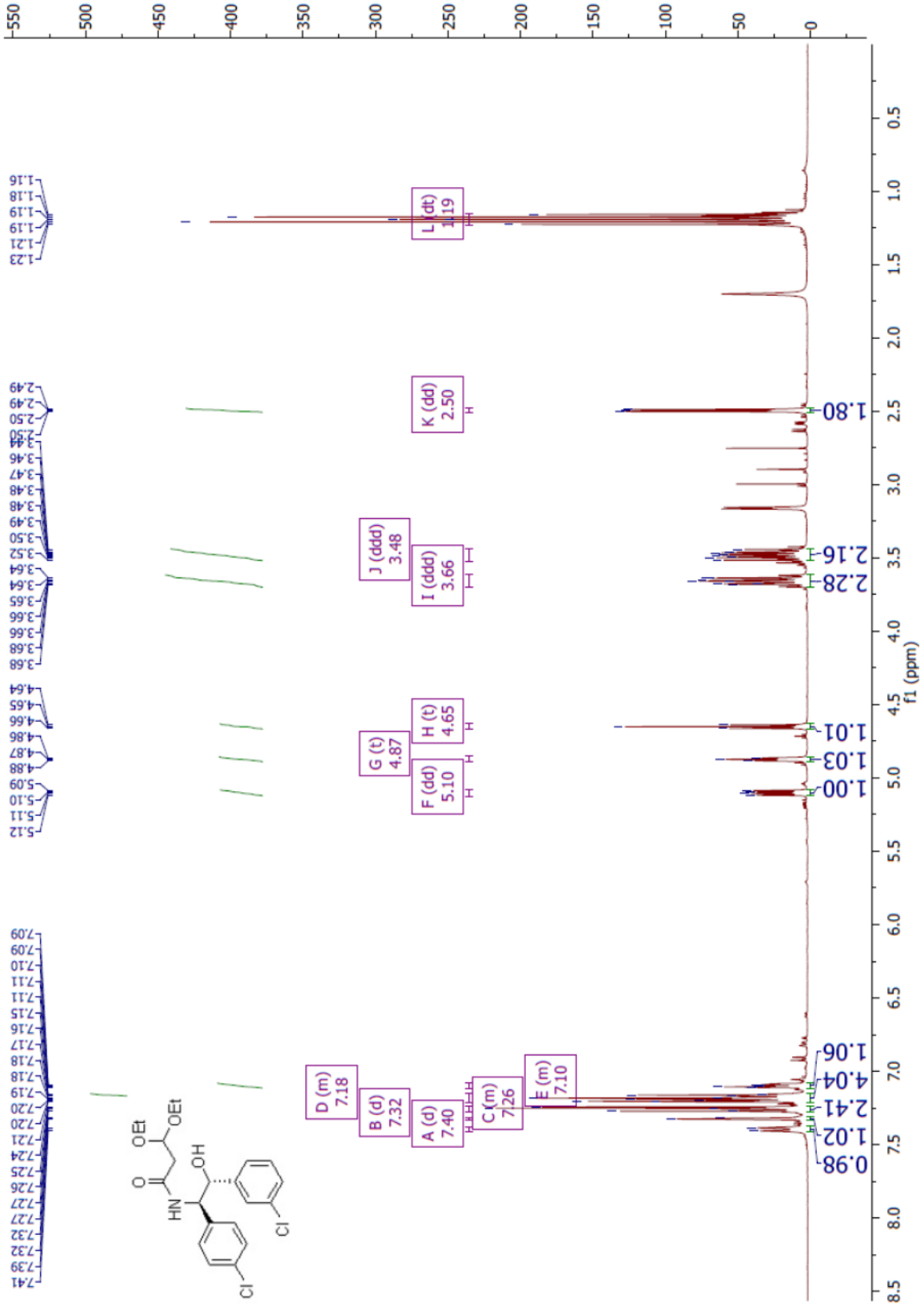
L (dt) 1.19
K (dd) 2.50
J (ddd) 3.48
I (ddd) 3.66
H (t) 4.65
G (t) 4.87
F (dd) 5.10
D (m) 7.18
B (d) 7.32
A (d) 7.40
C (m) 7.26
E (m) 7.10
1.80
2.16
2.28
1.01
1.03
1.00
1.06
4.04
2.41
1.02
0.98
f1 (ppm)

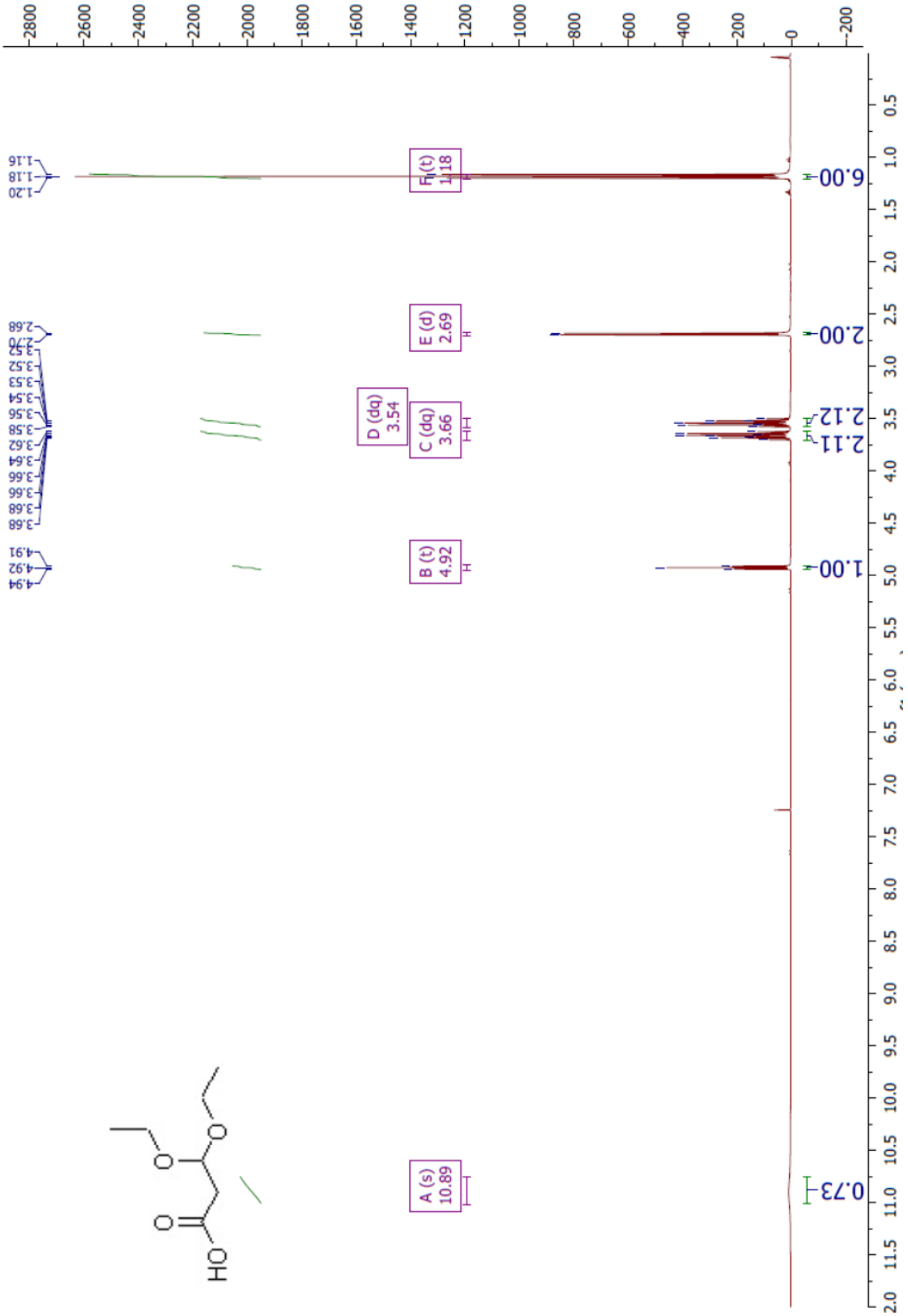
A (s) 10.89
B (t) 4.92
C (dq) 3.66
D (dq) 3.54
E (d) 2.69
F (t) 1.18
6.00
2.00
2.12
2.11
1.00
0.73
HO
O
O
O
O